

Pharmacokinetics and Metabolism in Drug Design
Edited by D. A. Smith, H. van de Waterbeemd, D. K. Walker, R. Mannhold, H. Kubinyi, H. Timmerman
Copyright © 2001 Wiley-VCH Verlag GmbH
ISBNs: 3-527-30197-6 (Hardcover); 3-527-60021-3 (Electronic)

**Pharmacokinetics and Metabolism
in Drug Design**

*by Dennis A. Smith,
Han van de Waterbeemd and
Don K. Walker*

Pharmacokinetics and Metabolism in Drug Design
Edited by D. A. Smith, H. van de Waterbeemd, D. K. Walker,
R. Mannhold, H. Kubinyi, H. Timmerman
Copyright © 2001 Wiley-VCH Verlag GmbH
ISBNs: 3-527-30197-6 (Hardcover); 3-527-60021-3 (Electronic)

Methods and Principles in Medicinal Chemistry

Edited by
R. Mannhold
H. Kubinyi
H. Timmerman

Editorial Board
G. Folkers, H.-D. Höltje, J. Vacca,
H. van de Waterbeemd, T. Wieland

Pharmacokinetics and Metabolism in Drug Design

Edited by D. A. Smith, H. van de Waterbeemd, D. K. Walker, R. Mannhold, H. Kubinyi, H. Timmerman

Copyright © 2001 Wiley-VCH Verlag GmbH

ISBNs: 3-527-30197-6 (Hardcover); 3-527-60021-3 (Electronic)

Pharmacokinetics and Metabolism in Drug Design

*by Dennis A. Smith,
Han van de Waterbeemd
and Don K. Walker*

 **WILEY-VCH**

Weinheim – New-York – Chichester – Brisbane – Singapore – Toronto

Series Editors:

Prof. Dr. Raimund Mannhold
Biomedical Research Center
Molecular Drug Research Group
Heinrich-Heine-Universität
Universitätsstraße 1
D-40225 Düsseldorf
Germany

Prof. Dr. Hugo Kubinyi
BASF AG Ludwigshafen
c/o Donnersbergstraße 9
D-67256 Weisenheim am Sand
Germany

Prof. Dr. Hendrik Timmerman
Faculty of Chemistry
Dept. of Pharmacochimistry
Free University of Amsterdam
De Boelelaan 1083
NL-1081 HV Amsterdam
The Netherlands

Dr. Dennis A. Smith
Dr. Han van de Waterbeemd
Don K. Walker
Pfizer Global Research and Development
Sandwich Laboratories
Department of Drug Metabolism
Sandwich, Kent CT13 9NJ
UK

■ This book was carefully produced. Nevertheless, authors, editors and publisher do not warrant the information contained therein to be free of errors. Readers are advised to keep in mind that statements, data, illustrations, procedural details or other items may inadvertently be inaccurate.

Library of Congress Card No.:
applied for

British Library Cataloguing-in-Publication Data
A catalogue record for this book is available from the British Library.

Die Deutsche Bibliothek – CIP Cataloguing-in-Publication Data
A catalogue record for this publication is available from Die Deutsche Bibliothek

© Wiley-VCH Verlag GmbH, Weinheim; 2001

All rights reserved (including those of translation into other languages).
No part of this book may be reproduced in any form – by photoprinting, microfilm, or any other means – nor transmitted or translated into a machine language without written permission from the publishers.

Printed in the Federal Republic of Germany

Printed on acid-free paper

Cover Design Gunther Schulz,
Fußgönheim
Typesetting TypoDesign Hecker GmbH,
Leimen
Printing Strauss Offsetdruck,
Mörlenbach
Binding Osswald & Co.,
Neustadt (Weinstraße)

ISBN 3-527-30197-6

Contents

Preface IX

A Personal Foreword XI

1 Physicochemistry 1

- 1.1 Physicochemistry and Pharmacokinetics 2
- 1.2 Partition and Distribution Coefficient as Measures of Lipophilicity 2
- 1.3 Limitations in the Use of 1-Octanol 5
- 1.4 Further Understanding of log P 6
 - 1.4.1 Unravelling the Principal Contributions to log P 6
 - 1.4.2 Hydrogen Bonding 6
 - 1.4.3 Molecular Size and Shape 8
- 1.5 Alternative Lipophilicity Scales 8
- 1.6 Computational Approaches to Lipophilicity 9
- 1.7 Membrane Systems to Study Drug Behaviour 10
- References 12

2 Pharmacokinetics 15

- 2.1 Setting the Scene 16
- 2.2 Intravenous Administration: Volume of Distribution 17
- 2.3 Intravenous Administration: Clearance 18
- 2.4 Intravenous Administration: Clearance and Half-life 19
- 2.5 Intravenous Administration: Infusion 20
- 2.6 Oral Administration 22
- 2.7 Repeated Doses 23
- 2.8 Development of the Unbound (Free) Drug Model 24
- 2.9 Unbound Drug and Drug Action 25
- 2.10 Unbound Drug Model and Barriers to Equilibrium 27
- 2.11 Slow Offset Compounds 29
- 2.12 Factors Governing Unbound Drug Concentration 31
- References 34

3	Absorption	35
3.1	The Absorption Process	35
3.2	Dissolution	36
3.3	Membrane Transfer	37
3.4	Barriers to Membrane Transfer	41
3.5	Models for Absorption Estimation	44
3.6	Estimation of Absorption Potential	44
3.7	Computational Approaches	45
	References	46
4	Distribution	47
4.1	Membrane Transfer Access to the Target	47
4.2	Brain Penetration	48
4.3	Volume of Distribution and Duration	51
4.4	Distribution and T _{max}	56
	References	57
5	Clearance	59
5.1	The Clearance Processes	59
5.2	Role of Transport Proteins in Drug Clearance	60
5.3	Interplay Between Metabolic and Renal Clearance	62
5.4	Role of Lipophilicity in Drug Clearance	63
	References	66
6	Renal Clearance	67
6.1	Kidney Anatomy and Function	67
6.2	Lipophilicity and Reabsorption by the Kidney	68
6.3	Effect of Charge on Renal Clearance	69
6.4	Plasma Protein Binding and Renal Clearance	69
6.5	Balancing Renal Clearance and Absorption	70
6.6	Renal Clearance and Drug Design	71
	References	73
7	Metabolic (Hepatic) Clearance	75
7.1	Function of Metabolism (Biotransformation)	75
7.2	Cytochrome P450	76
7.2.1	Catalytic Selectivity of CYP2D6	78
7.2.2	Catalytic Selectivity of CYP2C9	80
7.2.3	Catalytic Selectivity of CYP3A4	81
7.3	Oxidative Metabolism and Drug Design	85
7.4	Non-Specific Esterases	86
7.4.1	Function of Esterases	86
7.4.2	Ester Drugs as Intravenous and Topical Agents	88
7.5	Pro-drugs to Aid Membrane Transfer	89
7.6	Enzymes Catalysing Drug Conjugation	90

7.6.1	Glucuronyl- and Sulpho-Transferases	90
7.6.2	Methyl Transferases	92
7.6.3	Glutathione-S-Transferases	93
7.7	Stability to Conjugation Processes	93
7.8	Pharmacodynamics and Conjugation	95
	References	97
8	Toxicity	99
8.1	Toxicity Findings	99
8.1.1	Pharmacophore-induced Toxicity	99
8.1.2	Structure-related Toxicity	101
8.1.3	Metabolism-induced Toxicity	102
8.2	Epoxides	103
8.3	Quinone Imines	104
8.4	Nitrenium Ions	109
8.5	Imminium Ions	110
8.6	Hydroxylamines	111
8.7	Thiophene Rings	112
8.8	Thioureas	114
8.9	Chloroquinolines	114
8.10	Stratification of Toxicity	115
8.11	Toxicity Prediction - Computational Toxicology	115
8.12	Toxicogenomics	116
8.13	Enzyme Induction (CYP3A4) and Drug Design	117
	References	121
9	Inter-Species Scaling	123
9.1	Objectives of Inter-Species Scaling	124
9.2	Allometric Scaling	124
9.2.1	Volume of Distribution	124
9.2.2	Clearance	126
9.3	Species Scaling: Adjusting for Maximum Life Span Potential	128
9.4	Species Scaling: Incorporating Differences in Metabolic Clearance	128
9.5	Inter-Species Scaling for Clearance by Hepatic Uptake	129
9.6	Elimination Half-life	131
	References	132
10	High(er) Throughput ADME Studies	133
10.1	The HTS Trend	133
10.2	Drug Metabolism and Discovery Screening Sequences	134
10.3	Physicochemistry	135
10.3.1	Solubility	136
10.3.2	Lipophilicity	136
10.4	Absorption / Permeability	136
10.5	Pharmacokinetics	137

VIII | *Contents*

10.6	Metabolism	137
10.7	Computational Approaches in PK and Metabolism	138
10.7.1	QSPR and QSMR	138
10.7.2	PK Predictions Using QSAR and Neural Networks	138
10.7.3	Physiologically-Based Pharmacokinetic (PBPK) Modelling	139
10.8	Outlook	139
	References	140

Index	143
--------------	-----

Preface

The present volume of the series *Methods and Principles in Medicinal Chemistry* focuses on the impact of pharmacokinetics and metabolism in Drug Design. Pharmacokinetics is the study of the kinetics of absorption, distribution, metabolism, and excretion of drugs and their pharmacologic, therapeutic, or toxic response in animals and man.

In the last 10 years drug discovery has changed rapidly. Combinatorial chemistry and high-throughput screening have been introduced widely and now form the core of the Discovery organizations of major pharmaceutical and many small biotech companies. However, the hurdles between a hit, a lead, a clinical candidate, and a successful drug can be enormous.

The main reasons for attrition during development include pharmacokinetics and toxicity. Common to both is drug metabolism. The science of drug metabolism has developed over the last 30 years from a purely supporting activity trying to make the best out of a development compound, to a mature partner in drug discovery. Drug metabolism departments are now working closely together with project teams to discover well-balanced clinical candidates with a good chance of survival during development.

The present volume draws on the long career in drug metabolism and experience in the pharmaceutical industry of Dennis Smith. Together with his colleagues Han van de Waterbeemd and Don Walker, all key issues in pharmacokinetics and drug metabolism, including molecular toxicology have been covered, making the medicinal chemist feel at home with this highly important topic.

After a short introduction on physicochemistry, a number of chapters deal with pharmacokinetics, absorption, distribution, and clearance. Metabolism and toxicity are discussed in depth. In a further chapter species differences are compared and inter-species scaling is introduced. The final chapter deals with high(er) throughput ADME studies, the most recent trend to keep pace with similar paradigms in other areas of the industry, such as chemistry.

This book is a reflection of today's knowledge in drug metabolism and pharmacokinetics. However, there is more to come, when in the future the role and function of various transporters is better understood and predictive methods have matured further.

As series editors we would like to thank the authors for their efforts in bringing this book to completion. No doubt the rich experience of the authors expressed in

this volume will be of great value to many medicinal chemists, experienced or junior, and this volume will be a treasure in many laboratories engaged in the synthesis of drugs.

Last, but not least we wish to express our gratitude to Gudrun Walter and Frank Weinreich from Wiley-VCH publishers for the fruitful collaboration.

April 2001

Raimund Mannhold, Düsseldorf

Hugo Kubinyi, Ludwigshafen

Henk Timmerman, Amsterdam

A Personal Foreword

The concept of this book is simple. It represents the distillation of my experiences over 25 years within Drug Discovery and Drug Development and particularly how the science of Drug Metabolism and Pharmacokinetics impacts upon Medicinal Chemistry. Hopefully it will be a source of some knowledge, but more importantly, a stimulus for medicinal chemists to want to understand as much as possible about the chemicals they make. As the work grew I realized it was impossible to fulfil the concept of this book without involving others. I am extremely grateful to my co-authors Don Walker and Han van de Waterbeemd for helping turn a skeleton into a fully clothed body, and in the process contributing a large number of new ideas and directions. Upon completion of the book I realize how little we know and how much there is to do. Medicinal chemists often refer to the 'magic methyl'. This term covers the small synthetic addition, which almost magically solves a Discovery problem, transforming a mere ligand into a potential drug, beyond the scope of existing structure–activity relationships. A single methyl can disrupt crystal lattices, break hydration spheres, modulate metabolism, enhance chemical stability, displace water in a binding site and turns the sometimes weary predictable plod of methyl, ethyl, propyl, futile into methyl, ethyl, another methyl magic! This book has no magical secrets unfortunately, but time and time again the logical search for solutions is eventually rewarded by unexpected gains.

Sandwich, June 2001

Dennis A. Smith

Index

a

absorption 35, 64, 71, 137
 absorption potential 44
 absorption window 38
 accumulation ratio 24
 acetaminophen 105
 acetanilide 107
 acidic drugs 126
 actin 48
 active secretion 67
 active site 77
 topography 77
 active transport 67, 69
 ADME criteria 134
 ADME screens 133
 affinity constant 25
 age 71, 124
 agonist 26
 agranulocytosis 104, 105, 111, 112, 119
 albumin 48
 alcohol 91, 94
 alfentanil 3
 alkylating compounds 93
 allometric exponent 125
 allometric relationship 130
 allometric scaling 124, 129
 allometry 129
 amiodarone 101
 amlodipine 17, 53, 54
 amodiaquine 104
 anilino function 108
 animal models 116
 animal test 99
 antagonist 26
 anti-allergy agents 102
 antiarrhythmic drugs 109
 antiarrhythmic 55
 anticholinergics 89
 anti-diabetic 107
 antihypertensive 95

anti-inflammatory agent 113
 antimalarial 104
 antimuscarinic compounds 87
 antipyrene 128
 aplastic anaemia 103, 111
 aqueous channels 28, 29
 hydrophilic compounds 29
 aqueous pore 47, 64
 aqueous pores (tight junctions) 38
 atenolol 27, 50, 51, 64, 107
 azithromycin 54

b

β 1/ β 2 selectivity 51
 β 2-adrenergic receptor 30
 β -adrenoceptor antagonists 39, 64
 β -adrenoceptor blockers 86
 benzoquinone 104
 benzylic hydroxylation 83
 benzylic positions 83
 beta-adrenoceptor antagonist 42
 betaxolol 42, 79
 biliary cannaliculus 102
 biliary clearance 60
 biliary excretion 60, 130
 bioavailability 22, 23, 41, 42
 bioisosteres 94
 biophase 27
 blood dyscrasias 114
 blood flow 126
 blood-brain barrier 27, 28, 29, 50, 71
 body weight 124
 bosentan 129
 brain weight 128

c

caco-2 44
 caco-2 cells 43
 caco-2 monolayers 3, 137
 calcium channel blockers 54

- candoxatril 89
 - candoxatrilat 89
 - captopril 88
 - carbamazepine 50, 103, 118
 - carboxylic acid 90
 - carbutamide 107
 - carcinogenesis 102
 - carfentanil 30
 - cassette dosing 137
 - catechol methyl transferases 95
 - catechols 92
 - celecoxib 83
 - celiprolol 43
 - cell death 102
 - chloroquinoline 114
 - chlorphentermine 11
 - chlorpropamide 80
 - cholesterol absorption inhibitor 83, 85
 - cholinesterase inhibitor 62
 - chromone 102
 - cimetidine 3, 68, 114
 - cisplatin 116
 - class III antidysrhythmic agents 69
 - clearance 17, 32, 59, 126, 138
 - AUC 19
 - free drug 18
 - high clearance drugs 19
 - intrinsic clearance 18
 - intrinsic clearance 19
 - low clearance drugs 19
 - organs of extraction 18
 - systemic clearance 18
 - unbound clearance 19
 - cloned receptors 134
 - clozapine 109, 119
 - CNS 28, 47, 48, 49, 50
 - CNS uptake 7
 - $\Delta \log D$ 7
 - $\Delta \log P$ 7
 - zwitterions 7
 - co-administered drugs 117
 - cocktail dosing 137
 - codeine 55
 - collecting tubule 67
 - combinatorial chemistry 133
 - co-medications 124
 - computational systems 135
 - creatinine clearance 127
 - creatinine 71
 - cromakalim 86
 - crystal packing 36
 - CSF 49
 - cyclooxygenase inhibitor 83
 - cyclosporin A 41, 81, 82
 - CYP2C9 112, 127
 - CYP2C9 80
 - active site 80
 - substrate-protein interactions 80
 - template 80
 - CYP2D6 32, 78
 - basic nitrogen 78
 - catalytic selectivity 78
 - substrate-protein interaction 78
 - template models 78
 - CYP3A4 41, 44, 81, 117, 119
 - access channel 81
 - active site 81
 - SAR 81
 - selectivity 81
 - cytochrome 61
 - cytochrome P450 32, 41, 62, 75, 76, 77, 104, 110, 112, 114, 117, 138
 - chemistry 76
 - reactive species 77
 - 3 D-structure 77
 - cytotoxic 110
- d**
- danazole 37
 - dealkylation 77
 - deprotonation 91, 92
 - DEREK 116, 138
 - desipramine 49
 - desolvation 39
 - D-glucuronic acid 90
 - diclofenac 81, 105
 - diflunisal 116
 - dihydropyridine 54
 - diltiazem 84
 - disease states 124
 - disease 71
 - disobutamide 55
 - disopyramide 55
 - dissociation constant 26, 29
 - dissolution 36, 65, 136
 - rate of dissolution 36
 - solubility 36
 - surface area 36
 - distal tubule 67
 - distribution coefficient 4, 5
 - degree of ionization 4
 - diprotic molecules 5
 - Henderson-Hasselbalch relationship 4
 - monoprotic organic acids 4
 - monoprotic organic bases 4
 - distribution 47, 65
 - DNA microarrays 116
 - dofetilide 22

dopamine D₂ antagonists 28
 dopamine 91
 dose size 117, 120
 dose-response curve 65, 79
 dosing frequency 31
 dosing interval 24
 drug affinity 26
 drug concentrations 16
 free drug levels 16
 protein binding 16
 total drug levels 16
 drug interactions 70
 drug-like property 134
 duration of action 51, 52, 80

e

ECF 49
 efavirenz 118
 efflux pumps 41
 electron abstraction 84
 elimination half-life 131
 elimination rate constant 20
 endothelin antagonists 40, 41
 environmental factors 124
 enzyme induction 117
 epoxide hydrolase 103
 epoxide metabolites 103
 equilibrium 25
 erythromycin 54
 ester hydrolysis 89
 ester lability 87
 steric effects 87
 esterase activity 89
 esterase 86
 aliesterases 86
 arylesterases 86
 rodent blood 86
 extensive metabolizers 79

f

felodipine 22
 felodopam 92
 fenclofenac 81
 fibrinogen receptor antagonist 43
 filtration 126
 first-pass extraction 56
 first-pass 22
 flavin-containing monooxygenases 114
 flecainide 109
 fluconazole 72, 125, 127
 flufenamic acid 116
 fractional responder 25
 free concentration 27
 free drug 26, 27, 28, 48, 50, 68

free plasma concentration 31
 free radical formation 128
 free radicals 117
 free volume 52

g

γ-glutamylcysteine synthetase 117
 gastrointestinal tract 22, 35, 37, 41, 56
 gem-dimethyl 86
 genetic polymorphism 79
 glomerular filtration rate 67, 127
 glomerular filtration 62
 glomerulus 67
 glucuronic acid 93
 glucuronidation 75, 90, 94
 glucuronyl transferase 62, 90, 91, 93
 glutathione conjugate 113, 115
 glutathione depletion 103
 glutathione transferase 102
 glutathione 93, 102
 glutathione-S-transferases 93
 glycine/NMDA antagonists 3
 G-protein coupled receptors 27, 47
 G-protein-coupled receptor antagonists 71
 griseofulvin 37
 GSTs 93

h

haem iron 77
 haemolysis 112
 haemolytic anaemia 107
 half-life 17, 20, 24, 33
 dosing interval 20
 clearance 20
 volume of distribution 20
 halofantrine 37
 haloperidol 28
 H-bonding 39, 40, 45, 48, 60, 136
 hepatic blood flow 129
 hepatic clearance 60, 130
 hepatic extraction 19, 23
 blood flow 19
 hepatic impairment 56
 hepatic microsomes 128
 hepatic necrosis 103
 hepatic portal vein 22
 hepatic shunts 56
 hepatic uptake 60, 61, 131
 hepatitis 104
 hepatocyte 60, 129, 138
 hepatotoxicity 102, 105
 high throughput permeability
 assessment 137
 high throughput screening 133

high-speed chemistry 134
HT-29 44
human exposure 99
hydrogen abstraction 80
hydrogen bonding 6
hydrophilic compounds 51
hydrophobicity 2
hydroxylamines 91, 111
hyperkeratosis 106
hypersensitivity 112

i

idiosyncratic 118
iminium ion 110, 111
immobilized artificial membranes 136
immune response 102
in silico 135, 137
in vitro 96, 99, 128, 133, 134
indinavir 37
indomethacin 105
interstitial fluid 47
intracellular targets 47
intravenous infusion 20, 88
intrinsic clearance 128
iodine 101
ion-pair interactions 52
isolated perfused rat liver 61
isoprenaline 91

k

ketoconazole 37, 61, 71
kidney 62, 100

l

lidocaine 109
ligandin 48
lipid-bilayer 37
lipophilicity 2, 36, 43, 48, 63, 102, 136, 138
 calculation approaches 136
 fragmental approaches 136
 measured 136
liposome/water partitioning 136
liquid chromatography/mass spectrometry 137
liver 56
local action 89
lofentanil 30
log *D* 4, 39, 45, 48, 49
log *D*_{7,4} 63, 69
log *P* 2, 6
 bonding 6
 hydrogen 6
 molar volume 6
 polarity 6

 size 6
loop diuretics 100
loop of Henle 67
low solubility 37

m

macrolide 54
maximum absorbable dose 45
maximum life span potential 128
MDCK 44
melanin 48
membrane barriers 2
 phospholipid bilayers 2
membrane interactions 48
membrane permeability 136
membrane transfer 65
membrane transport 137
membrane 37
MetabolExpert 138
metabolic clearance 63
metabolic lability 39
metabolism 65, 75, 137, 138
 conjugative 75
 oxidative 75
 phase I 75
 phase II 75
metabolite 138
MetaFore 138
metazosin 127
Meteor 138
methaemoglobinemia 112
methyl transferase 92
metiamide 114
metoprolol 42, 51, 79
mianserin 110
microdialysis 50
microsomal stability 129
midazolam 23, 82, 124
minoxidil 95
molecular lipophilicity potential 10
molecular modelling 138
molecular size 45, 48
molecular surface area 8
 absorption 8
 bile excretion 8
molecular weight 43
moricizine 118
morphine 91, 95
myeloperoxidase 106
myosin 48

n

napsagatran 131
N-dealkylation 82, 111

- N*-demethylation 82, 84
 necrosis 102
 nephron 67
 neural network 115, 136, 138
 nifedipine 53, 54
 nitrenium ion 109, 119
 nitrofurantoin 37
 NMR spectroscopy 137
 no-effect doses 100
 nomifensine 107
 non-linearity 137
 non-steroidal anti-inflammatory drugs 80
 nucleophilicity 91
- o**
- occupancy theory 25
 octanol 5, 8
 alternative lipophilicity scales 8
 H-bonding 5
 model of a biological membrane 5
 olanzapine 119
 opioid analgesic 95
 organic cation transporter 62
 ototoxicity 100
 oxcarbazepine 104
 oxidation 76
 oxidative stress 116
 oxygen rebound 76
- p**
- P450 enzyme inhibition 138
 P450 inhibitor 61
 pafenolol 43
 PAPS 91
 paracellular absorption 38
 paracellular pathway 47, 71
 paracellular route 64
 parallel synthesis 133
 paroxetine 92
 partition coefficient 2, 9, 10
 absence of dissociation or ionization 3
 artificial membranes 9
 basic drugs 11
 calculation 9
 chromatographic techniques 9
 intrinsic lipophilicity 3
 ionic interactions 11
 liposomes 9
 membrane systems 10
 phospholipids 10
 shake-flask 9
 unilamellar vesicles 10
 unionized form 3
 passive diffusion 68, 136
 peak-to-trough variations 56
 peptidic renin inhibitors 8
 permeability 136
 peroxisome proliferator-activated receptor γ 120
 PET scanning 28
 P-glycoprotein 41, 42, 43, 137
 pharmacokinetic modelling 139
 pharmacokinetic phase 26
 phase II conjugation 90
 phenacetin 104
 phenol 90, 91, 94
 phenolate anion 91
 phenytoin 37, 80, 103, 118, 128
 pholcodine 55
 phospholipid 52, 54
 phospholipidosis 102
 physiological models 139
 physiological time 127
 pindolol 51
 pirenzepine 30
 pK_a 136
 plasma protein binding 32, 69, 125, 129
 polar surface area 45, 136
 polyethylene glycol 36
 polypharmacology 100
 poor absorption 23
 poor metabolizers 79
 practionolol 106
 predictive methods 115
 pre-systemic metabolism 22
 procainamide 109
 pro-drug design 43
 pro-drug 89
 pro-moiety 43
 propafenone 79
 propranolol 27, 38, 42, 51, 64, 88
 protein binding 137
 proxicromil 102
 proximal tubule 67
 pulsed ultrafiltration-mass spectrometry 138
- q**
- QSAR 115, 138
 quantitative structure-pharmacokinetic relationships 138
 quantitative structure-metabolism relationships 138
 quinone imine 104, 111
- r**
- radical stability 84
 Raevsky 40
 rash 106

- reabsorption 68
 - reactive metabolite 103, 104, 105, 110, 113
 - real-time SAR 135
 - receptor occupancy 26, 28, 51
 - receptor occupation 25
 - receptor-ligand complex 25
 - relative metabolic stability 129
 - remifentanyl 89
 - remoxipride 28
 - renal clearance 62, 63, 126, 127
 - renal injury 113
 - rifabutin 52
 - rifampicin 52
 - rifamycin SV 52
 - rosiglitazone 119
 - rule-of-five 40
- s**
- salbutamol 30
 - salmeterol 30
 - SAM 92
 - SCH 48461 83, 85
 - screening sequences 134
 - secondary amines 84
 - sensitization period 119
 - serine esterases 87
 - side-effects 56, 88, 89
 - sinusoidal carrier systems 60
 - skin rash 103
 - slow offset 29, 30
 - pharmacodynamic action 30
 - SM-10888 63, 75
 - small intestine 38
 - soft-drug 89
 - solubility 45, 136
 - species-specific differences 127, 129
 - steady state concentration 21
 - clearance 21
 - half-life 21
 - intravenous infusion 21
 - steady state 24, 26, 33, 88
 - steroid receptors 29
 - (S)-warfarin 80
 - Stevens-Johnson syndrome 112
 - structure-activity relationships 26
 - structure-toxicity relationships 115
 - substrate radical 76
 - sulphamethoxazole 111
 - sulphate transferases 91
 - sulphate 93, 95
 - sulphonamide 107
 - sulphotransferases 91, 95
 - phenol-sulphotransferase 91
 - sulpiride 28, 49
 - suprofen 112
- t**
- tacrine 105
 - talinolol 42
 - telenzepine 30
 - tenidap 113
 - teratogenicity 100, 103
 - terfenadine 82
 - tertiary amine 82
 - thalidomide 100
 - thioether adducts 109
 - thiolate anion 93
 - thiophene ring 112
 - thiophene S-oxide 112
 - thiophene 113
 - thioridazine 28
 - thiourea 114
 - thromboxane A₂ receptor antagonists 61
 - thromboxane receptor antagonists 130
 - thromboxane synthase inhibitors 61
 - ticlopidine 112
 - tienilic acid 112, 127
 - tissue half-life 54
 - T_{max} 56
 - tocainide 109
 - tolbutamide 80, 107, 127
 - topical administration 88
 - toxicity 99, 101, 102
 - idiosyncratic 102
 - metabolism 102
 - pharmacology 99
 - physiochemical properties 101
 - structure 101
 - toxicogenomics 116
 - toxicology 118
 - toxicophore 108, 115
 - transcellular diffusion 38
 - transport proteins 41, 67, 69
 - transport systems 60
 - transporter proteins 129, 130, 137
 - transporter 60, 61, 137
 - canalicular 60
 - sinusoid 60
 - triamterene 37
 - triazole 72
 - troglitazone 119
 - tubular carrier systems 62
 - tubular pH 69
 - tubular reabsorption 70, 72, 126
 - tubular secretion 69, 70
 - turbidimetry 136

u

UDP- α -glucuronic acid 90
unbound drug concentration 50
unbound drug 24, 125
 GABA uptake inhibitors 6
 histamine H₁-receptor antagonists 6
 uptake of drugs in the brain 6
urea 42
urine 62, 67

v

variability 124
verapamil 68
vesnarinone 111
volume of distribution 17, 32, 51, 64,
124, 136

apparent free volume 32
extracellular water volume 17
plasma volume 17
tissue affinity 17
total body water volume 17

w

water solubility 37
white blood cell toxicity 113

z

zamifenacin 92, 126

96-well 137

1

Physicochemistry**Abbreviations**

CPC	Centrifugal partition chromatography
CoMFA	Comparative field analysis
3D-QSAR	Three-dimensional quantitative structure–activity relationships
IUPAC	International Union of Pure and Applied Chemistry
MLP	Molecular lipophilicity potential
RP-HPLC	Reversed-phase high performance liquid chromatography
PGDP	Propylene glycol dipelargonate
SF	Shake flask, referring to traditional method to measure $\log P$ or $\log D$

Symbols

$\Delta \log D$	Difference between $\log D$ in octanol/water and $\log D$ in alkane/water
$\Delta \log P$	Difference between $\log P$ in octanol/water and $\log P$ in alkane/water
f	Rekker or Leo/Hansch fragmental constant for $\log P$ contribution
K_a	Ionization constant
Λ	Polarity term, mainly related to hydrogen bonding capability of a solute
$\log P$	Logarithm of the partition coefficient (P) of neutral species
$\log D$	Logarithm of the distribution coefficient (D) at a selected pH, usually assumed to be measured in octanol/water
$\log D_{\text{oct}}$	Logarithm of the distribution coefficient (D) at a selected pH, measured in octanol/water
$\log D_{\text{chex}}$	Logarithm of the distribution coefficient (D) at a selected pH, measured in cyclohexane/water
$\log D_{7.4}$	Logarithm of the distribution coefficient (D) at pH 7.4
MW	Molecular weight
π	Hansch constant; contribution of a substituent to $\log P$
$\text{p}K_a$	Negative logarithm of the ionization constant K_a

1.1

Physicochemistry and Pharmacokinetics

The body can be viewed as primarily composed of a series of membrane barriers dividing aqueous filled compartments. These membrane barriers are comprised principally of the phospholipid bilayers which surround cells and also form intracellular barriers around the organelles present in cells (mitochondria, nucleus, etc.). These are formed with the polar ionized head groups of the phospholipid facing towards the aqueous phases and the lipid chains providing a highly hydrophobic inner core. To cross the hydrophobic inner core a molecule must also be hydrophobic and able to shed its hydration sphere. Many of the processes of drug disposition depend on the ability or inability to cross membranes and hence there is a high correlation with measures of lipophilicity. Moreover, many of the proteins involved in drug disposition have hydrophobic binding sites further adding to the importance of the measures of lipophilicity [1].

At this point it is appropriate to define the terms hydrophobicity and lipophilicity. According to recently published IUPAC recommendations both terms are best described as follows [2]:

Hydrophobicity is the association of non-polar groups or molecules in an aqueous environment which arises from the tendency of water to exclude non-polar molecules

Lipophilicity represents the affinity of a molecule or a moiety for a lipophilic environment. It is commonly measured by its distribution behaviour in a biphasic system, either liquid–liquid (e.g. partition coefficient in 1-octanol/water) or solid–liquid (retention on reversed-phase high-performance liquid chromatography (RP-HPLC) or thin-layer chromatography (TLC) system).

The role of dissolution in the absorption process is further discussed in Section 3.2.

1.2

Partition and Distribution Coefficient as Measures of Lipophilicity

The inner hydrophobic core of a membrane can be modelled by the use of an organic solvent. Similarly a water or aqueous buffer can be used to mimic the aqueous filled compartment. If the organic solvent is not miscible with water then a two-phase system can be used to study the relative preference of a compound for the aqueous (hydrophilic) or organic (hydrophobic, lipophilic) phase.

For an organic compound, lipophilicity can be described in terms of its partition coefficient P (or $\log P$ as it is generally expressed). This is defined as the ratio of concentrations of the compound at equilibrium between the organic and aqueous phases:

$$P = \frac{[\text{drug}]_{\text{organic}}}{[\text{drug}]_{\text{aqueous}}} \quad (1.1)$$

The partition coefficient ($\log P$) describes the *intrinsic lipophilicity* of the collection of functional groups and carbon skeleton, which combine to make up the structure of the compound, *in the absence of dissociation or ionization*. Methods to measure partition and distribution coefficients have been described [3, 4].

Every component of an organic compound has a defined lipophilicity and calculation of partition coefficient can be performed from a designated structure. Likewise, the effect on $\log P$ of the introduction of a substituent group into a compound can be predicted by a number of methods as pioneered by Hansch [5–8] (π values), Rekker [9–10] (f values) and Leo/Hansch [5–7, 11–12] (f' values).

Partitioning of a compound between aqueous and lipid (organic) phases is an equilibrium process. When in addition the compound is partly ionized in the aqueous phase a further (ionization) equilibrium is set up, since it is assumed that under normal conditions only the unionized form of the drug penetrates the organic phase [13]. This traditional view is shown schematically in Figure 1.1 below. However, the nature of the substituents surrounding the charged atom as well as the degree of delocalization of the charge may contribute to the stabilization of the ionic species and thus not fully exclude partitioning into an organic phase or membrane [14]. An example of this is the design of acidic 4-hydroxyquinolones (Figure 1.2) as glycine/NMDA antagonists [15]. Despite a formal negative charge these compounds appear to behave considerable ability to cross the blood–brain barrier.

In a study of the permeability of alfentanil and cimetidine through Caco-2 cells, a model for oral absorption, it was deduced that at pH 5 about 60 % of the cimetidine transport and 17 % of the alfentanil transport across Caco-2 monolayers can be attributed to the ionized form [16] (Figure 1.3). Thus the dogma that only neutral species can cross a membrane has been challenged recently.

The intrinsic lipophilicity (P) of a compound refers only to the equilibrium of the unionized drug between the aqueous phase and the organic phase. It follows that the

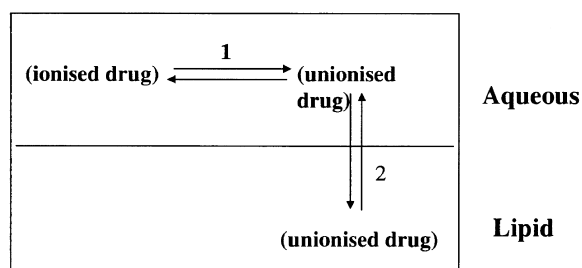
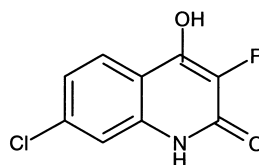


Fig. 1.1 Schematic depicting the relationship between $\log P$ and $\log D$ and pK_a .

1. Is a function of acid/base strength pK_a
2. Is a function of P ($\log P$)

Fig. 1.2 4-Hydroxyquinolines with improved oral absorption and blood–brain barrier permeability [15].



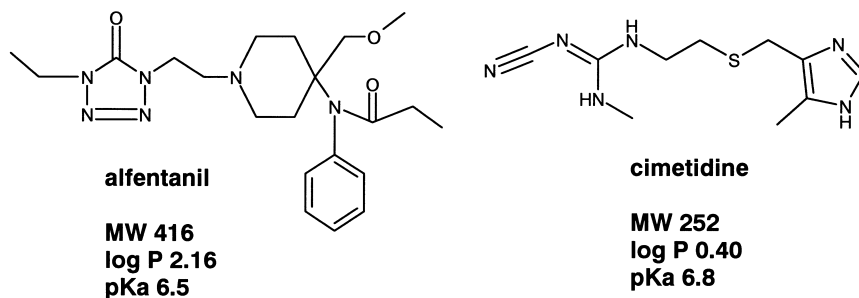


Fig. 1.3 Transportation rate of basic drugs across Caco-2 monolayers: alfentanil, rapid transport; cimetidine, slow transport [16].

remaining part of the overall equilibrium, i.e. the concentration of ionized drug in the aqueous phase, is also of great importance in the overall observed partition ratio. This in turn depends on the pH of the aqueous phase and the acidity or basicity (pK_a) of the charged function. The overall ratio of drug, ionized and unionized, between the phases has been described as the *distribution coefficient* (D), to distinguish it from the intrinsic lipophilicity (P). The term has become widely used in recent years to describe, in a single term the *effective (or net) lipophilicity* of a compound at a given pH taking into account both its intrinsic lipophilicity and its degree of ionization. The distribution coefficient (D) for a monoprotic acid (HA) is defined as:

$$D = [HA]_{\text{organic}} / ([HA]_{\text{aqueous}} + [A^-]_{\text{aqueous}}) \quad (1.2)$$

where [HA] and $[A^-]$ represent the concentrations of the acid in its unionized and dissociated (ionized) states respectively. The ionization of the compound in water is defined by its dissociation constant (K_a) as:

$$K_a = [H^+][A^-] / [HA] \quad (1.3)$$

sometimes referred to as the Henderson–Hasselbach relationship. Combination of Eqs. (1.1)–(1.3) gives the pH-distribution (or ‘pH-partition’) relationship:

$$D = P / (1 + \{K_a / [H^+]\}) \quad (1.4)$$

more commonly expressed for monoprotic organic acids in the form of Eqs. (1.5) and (1.6), below:

$$\log (\{P/D\} - 1) = \text{pH} - \text{p}K_a \quad (1.5)$$

or

$$\log D = \log P - \log(1 + 10^{\text{pH} - \text{p}K_a}) \quad (1.6)$$

For monoprotic organic bases (BH^+ dissociating to B) the corresponding relationships are:

$$\log (\{P/D\} - 1) = \text{p}K_a - \text{pH} \quad (1.7)$$

or

$$\log D = \log P - \log(1 + 10^{\text{pH} - \text{p}K_{\text{a}}}) \quad (1.8)$$

From these equations it is possible to predict the effective lipophilicity ($\log D$) of an acidic or basic compound at any pH value. The data required in order to use the relationship in this way are the intrinsic lipophilicity ($\log P$), the dissociation constant ($\text{p}K_{\text{a}}$), and the pH of the aqueous phase. The overall effect of these relationships is the effective lipophilicity of a compound, at physiological pH, is the $\log P$ value minus one unit of lipophilicity, for every unit of pH the $\text{p}K_{\text{a}}$ value is below (for acids) and above (for bases) pH 7.4. Obviously for compounds with multifunctional ionizable groups the relationship between $\log P$ and $\log D$, as well as $\log D$ as function of pH become more complex [17]. For diprotic molecules there are already 12 different possible shapes of $\log D$ -pH plots.

1.3

Limitations in the Use of 1-Octanol

Octanol is the most widely used model of a biological membrane [18] and $\log D_{7.4}$ values above 0 normally correlate with effective transfer across the lipid core of the membrane, whilst values below 0 suggest an inability to traverse the hydrophobic barrier.

Octanol, however, supports H-bonding. Besides the free hydroxyl group, octanol also contains 4% v/v water at equilibrium. This obviously conflicts with the exclusion of water and H-bonding functionality at the inner hydrocarbon core of the membrane. For compounds that contain functionality capable of forming H-bonds, therefore, the octanol value can over-represent the actual membrane crossing ability. These compounds can be thought of as having a high hydration potential and difficulty in shedding their water sphere.

Use of a hydrocarbon solvent such as cyclohexane can discriminate these compounds either as the only measured value or as a value to be subtracted from the octanol value ($\Delta \log P$) [19–21]. Unfortunately, cyclohexane is a poor solvent for many compounds and does not have the utility of octanol. Groups which hydrogen bond and attenuate actual membrane crossing compared to their predicted ability based on octanol are listed in Figure 1.4. The presence of two or more amide, carboxyl functions in a molecule will significantly impact on membrane crossing ability and will need substantial intrinsic lipophilicity in other functions to provide sufficient hydrophobicity to penetrate the lipid core of the membrane.

1.4

Further Understanding of $\log P$

1.4.1

Unravelling the Principal Contributions to $\log P$

The concept that $\log P$ or $\log D$ is composed of two components [22], that of size and polarity is a useful one. This can be written as Eq. (1.9),

$$\log P \text{ or } \log D = a \cdot V - \Lambda \quad (1.9)$$

where V is the molar volume of the compound, Λ a general polarity descriptor and a is a regression coefficient. Thus the size component will largely reflect the carbon skeleton of the molecule (lipophilicity) whilst the polarity will reflect the hydrogen bonding capacity. The positioning of these properties to the right and left of Figure 1.4 reflects their influence on the overall physicochemical characteristics of a molecule.

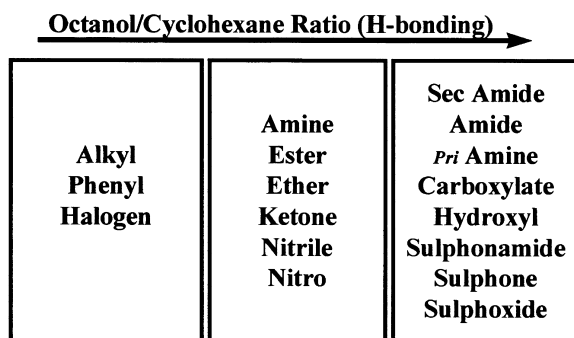


Fig. 1.4 Functionality and H-bonding.

1.4.2

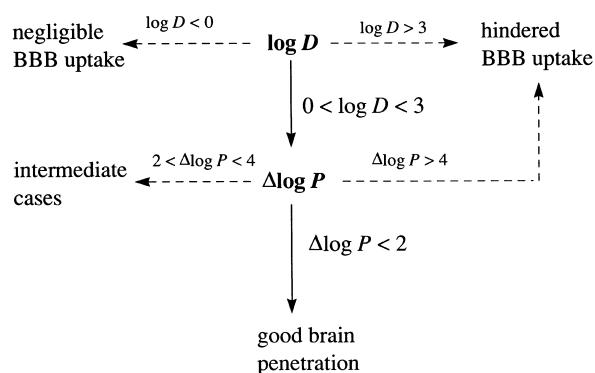
Hydrogen Bonding

Hydrogen bonding is now seen as an important property related to membrane permeation. Various scales have been developed [23]. Some of these scales describe total hydrogen bonding capability of a compound, while others discriminate between donors and acceptors [24]. It has been demonstrated that most of these scales show considerable intercorrelation [25].

Lipophilicity and H-bonding are important parameters for uptake of drugs in the brain [26]. Their role has e.g. been studied in a series of structurally diverse sedating and non-sedating histamine H_1 -receptor antagonists [27]. From these studies a decision tree guideline for the development of non-sedative antihistamines was designed (see Figure 1.5).

GABA (γ -aminobutyric acid) is a major neurotransmitter in mammals and is involved in various CNS disorders. In the design of a series of GABA uptake inhibitors a large difference in *in vivo* activity between two compounds with identical IC_{50} val-

Fig. 1.5 Decision tree for the design of non-sedative H_1 -antihistaminics. $\log D$ is measured at pH 7.4, while $\Delta\log P$ refers to compounds in their neutral state (redrawn from reference [27]).



ues was observed, one compound being devoid of activity [28]. The compounds have also nearly identical pK_a and $\log D_{\text{oct}}$ values (see Figure 1.6) and differ only in their distribution coefficient in cyclohexane/water ($\log D_{\text{chex}}$). This results in a $\Delta\log D$ of 2.71 for the *in vivo* inactive compounds, which is believed to be too large for CNS uptake. The active compound has a $\Delta\log D$ of 1.42, well below the critical limit of approximately 2. Besides this physicochemical explanation further evaluation of metabolic differences should complete this picture. It should be noted that the concept of using the differences between solvent systems was originally developed for compounds in their neutral state ($\Delta\log P$ values, see Section 2.2). In this case two zwitterions are being compared, which are considered at pH 7.4 to have a net zero charge, and thus the $\Delta\log P$ concept seems applicable.

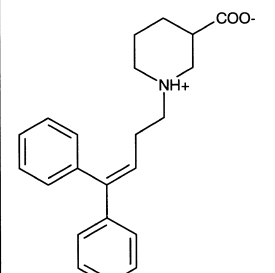
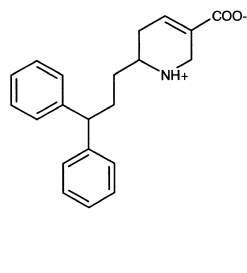
		
IC_{50} <i>in vivo</i>	0.11 mM active	0.1 mM inactive
pK_a	3.57/9.23	3.39/9.25
$\log D_{\text{oct}}$	0.99	0.71
$\log D_{\text{chex}}$	-0.43	-2.00
$\Delta\log D$	1.42	2.71

Fig. 1.6 Properties of GABA-uptake inhibitors [28].

1.4.3

Molecular Size and Shape

Molar volume as used in Eq. (1.9) is one way to express the size of a compound. It is very much related to molecular surface area. For convenience often the molecular weight (MW) is taken as a first estimate of size. It is also useful to realize that size is not identical to shape.

Many companies have tried to develop peptidic renin inhibitors. Unfortunately these are rather large molecules and not unexpectedly poor absorption was often observed. The role of physicochemical properties has been discussed for this class of compounds. One of the conclusions was that compounds with higher lipophilicity were better absorbed from the intestine [29]. Absorption and bile elimination rate are both MW-dependent. Lower MW results in better absorption and less bile excretion. The combined influence of molecular size and lipophilicity on absorption of a series of renin inhibitors can be seen from Figure 1.7. The observed iso-size curves are believed to be part of a general sigmoidal relationship between permeability and lipophilicity [30–31] (for further details see Chapter 3).

1.5

Alternative Lipophilicity Scales

Since 1-octanol has certain limitations (see Section 1.3) many alternative lipophilicity scales have been proposed (see Figure 1.8). A critical quartet of four solvent systems of octanol (amphiprotic), alkane (inert), chloroform (proton donor) and propy-

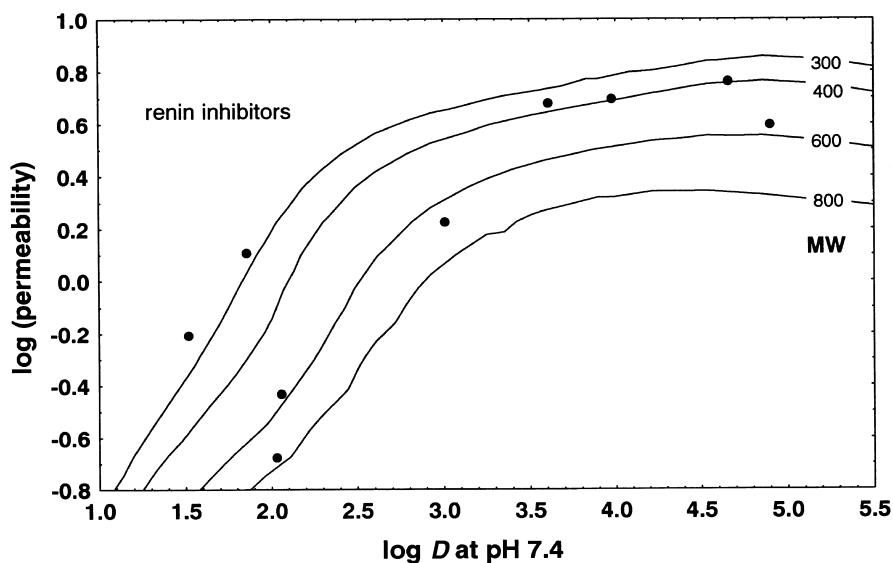


Fig. 1.7 Iso-molecular weight curves showing the influence of molecular size on membrane permeability with increasing lipophilicity [32].

lene glycol dipelargonate (PGDP) has been advocated [33–34]. By measuring distribution in all four, a full coverage of partitioning properties should be obtained. Also non-aqueous systems such as heptane/acetonitrile [35] or heptane/glycol [36] may be of use. This latter system appears to offer a direct measure for hydrogen bonding. In order to increase throughput over the traditional shake-flask and related methods, various chromatographic techniques can be used [1]. Immobilized artificial membranes (IAM) in particular, have been given considerable attention [37, 38]. IAMs consist of phospholipids grafted onto a solid phase HPLC support intended to mimic a membrane. It appears that IAM retention times are highly correlated with shake flask $\log D$ octanol/water coefficients and thus do not really measure anything new. Along the same lines several groups have suggested that studying partitioning into liposomes may produce relevant information related to membrane uptake and absorption [38, 39].

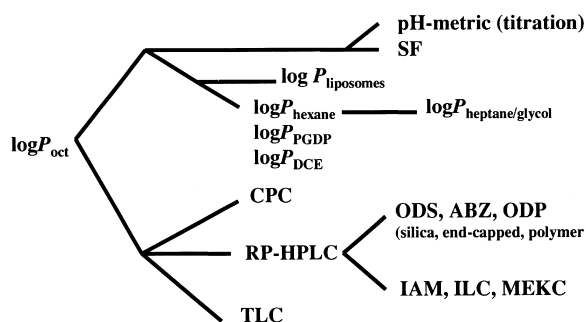


Fig. 1.8 Experimental methods to measure lipophilicity (modified after reference [23]). $\log P_{\text{oct}}$, 1-octanol/water partition coefficient; $\log P_{\text{liposomes}}$, partition coefficient between liposomes and buffer; $\log P_{\text{hexane}}$, 1-hexane/water partition coefficient; $\log P_{\text{PGDP}}$, propyleneglycol dipelargonate/water partition coefficient; $\log P_{\text{heptane/glycol}}$, a non-aqueous partitioning system; SF, shake-flask; pH-metric, $\log P$ determination based on potentiometric titration in water and octanol/water; CPC, centrifugal partition chromatography; RP-HPLC, reversed-phase high performance liquid chromatography; TLC, thin-layer chromatography; ODS, octadecylsilane; ABZ, end-capped silica RP-18 column; ODP, octadecylpolyvinyl packing; IAM, immobilized artificial membrane; ILC, immobilized liposome chromatography; MEKC, micellar electrokinetic capillary chromatography.

1.6

Computational Approaches to Lipophilicity

In the design of new compounds as well as the design of experimental procedures an *a priori* calculation $\log P$ or $\log D$ values may be very useful. Methods may be based on the summation of fragmental [40–42], or atomic contributions [43–45], or a combination [46, 47]. Reviews on various methods can be found in references [40, 48–51]. Further approaches based on the used of structural features have been suggested [48,

52]. Atomic and fragmental methods suffer from the problem that not all contributions may be parameterized. This leads to the observation that for a typical pharmaceutical file about 25 % of the compounds cannot be computed. Recent efforts have tried to improve the “missing value” problem [53].

Molecular lipophilicity potential (MLP) has been developed as a tool in 3D-QSAR, for the visualization of lipophilicity distribution on a molecular surface and as an additional field in CoMFA studies [49]. MLP can also be used to estimate conformation-dependent log *P* values.

1.7

Membrane Systems to Study Drug Behaviour

In order to overcome the limitations of octanol other solvent systems have been suggested. Rather than a simple organic solvent, actual membrane systems have also been utilized. For instance the distribution of molecules has been studied between unilamellar vesicles of dimyristoylphosphatidylcholine and aqueous buffers. These systems allow the interaction of molecules to be studied within the whole membrane which includes the charged polar head group area (hydrated) and the highly lipophilic carbon chain region. Such studies indicate that for amine compounds ionized at physiological pH, partitioning into the membrane is highly favoured and independent of the degree of ionization. This is believed to be due to electrostatic interactions with the charged phospholipid head group. This property is not shared

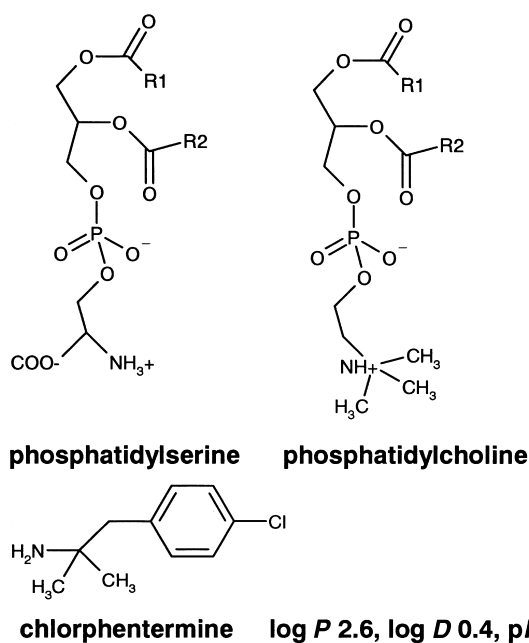


Fig. 1.9 Structures of charge neutral (phosphatidylcholine) and acidic (phosphatidylserine) phospholipids together with the moderately lipophilic and basic drug chlorphentermine. The groupings R1 and R2 refer to the acyl chains of the lipid portions.

with acidic compounds even for the “electronically neutral” phosphatidylcholine [54]. Such ionic interactions between basic drugs are even more favoured for membranes containing “acidic” phospholipids such as phosphatidylserine [55]. The structures of these two phospholipids are shown in Figure 1.9 below together with the structure of the basic drug chlorphentermine.

Table 1.1 shows the preferential binding of chlorphentermine to phosphatidylcholine-containing membranes, the phospholipid with overall acidic charge. These systems predict the actual affinity of the compound for the membrane, rather than its ability to cross the membrane. Membrane affinity, and hence tissue affinity, is particularly important in the persistence of drugs within the body, a topic which will be covered in Section 4.2.

Tab. 1.1: Affinity (k) and capacity (moles drug/moles lipid) of chlorphentermine for liposomes prepared from phosphatidylcholine and phosphatidylserine.

Phospholipid	k (10^{-4}) M	n_{\max}
Phosphatidylserine	2.17	0.67
Phosphatidylcholine	1.26	0.05

References

- 1 Pliska V, Testa B, Van de Waterbeemd H (Eds). *Lipophilicity in Drug Action and Toxicology*. VCH, Weinheim, 1996.
- 2 Van de Waterbeemd H, Carter RE, Grassy G, Kubinyi H, Martin YC, Tute MS, Willett P, *Pure Chem.* 1997, 69, 1137–1152; *Ann. Rep. Med. Chem.* 1998, 33, 397–409.
- 3 Dearden JC, Bresnen GM, *Quant. Struct. Activity Relat.* 1988, 7, 133–144.
- 4 Hersey A, Hill AP, Hyde RM, Livingstone DJ, *Quant. Struct. Activity Relat.* 1989, 8, 288–296.
- 5 Hansch C, Leo A, *Substituent Constants for Correlation Analysis in Chemistry and Biology*. Wiley Interscience, New York, 1979.
- 6 Hansch C, Leo A, Hoekman D, *Exploring QSAR. Hydrophobic, Electronic, and Steric Constants*. ACS, Washington, 1995.
- 7 Hansch C, Leo A, *Exploring QSAR. Fundamentals and Applications in Chemistry and Biology*. ACS, Washington, 1995.
- 8 Fujita T, Iwasa J, Hansch C, *J. Amer. Chem. Soc.* 1964, 86, 5175–5180.
- 9 Rekker RF, De Kort HM, *Eur. J. Med. Chem.* 1979, 14, 479–488.
- 10 Rekker RF, Mannhold R, *Calculation of Drug Lipophilicity*. VCH, Weinheim, 1992.
- 11 Leo A, Abraham DJ, *Proteins: Struct. Funct. Gen.* 1988, 2, 130–152.
- 12 Leo A, Hansch C, Elkins D, *Chem. Rev.* 1971, 71, 525–616.
- 13 Manners CN, Payling DW, Smith DA, *Xenobiotica* 1988, 18, 331–350.
- 14 Kulagowski JJ, Baker R, Curtis NR, Leeson PD, Mawer IM, Moseley AM, Ridgill MP, Rowley M, Stansfield I, Foster AC, Gromwood S, Hill RG, Kemp JA, Marshall GR, Saywell KL, Tricklebank MD, *J. Med. Chem.* 1994, 37, 1402–1405.
- 15 Palm K, Luthman K, Ros J, Grasjo J, Artursson P, *J. Pharmacol. Exp. Ther.* 1999, 291, 435–443.
- 16 Reymond F, Carrupt PA, Testa B, Girault HH, *Chem. Eur. J.* 1999, 5, 39–47.
- 17 Smith RN, Hansch C, Ames MM, *J. Pharm. Sci.* 1975, 64, 599–605.
- 18 Avdeef A, In: *Lipophilicity in Drug Action and Toxicology* (Eds Pliska V, Testa B, Van de Waterbeemd H), pp. 109–139. VCH, Weinheim, 1996.
- 19 Young RC, Mitchell RC, Brown TH, Ganellin CR, Griffiths R, Jones M, Rana KK, Saunders D, Smith IR, Sore NE, Wilks TJ, *J. Med. Chem.* 1988, 31, 656–671.
- 20 El Tayar N, Tsai RS, Testa B, Carrupt PA, Leo A, *J. Pharm. Sci.* 1991, 80, 590–598.
- 21 Abraham MH, Chadha HS, Whiting GS, Mitchell RC, *J. Pharm. Sci.* 1994, 83, 1085–1100.
- 22 Van de Waterbeemd H, Testa B, *Adv. Drug Res.* 1987, 16, 85–225.
- 23 Van de Waterbeemd H, In: *Methods for Assessing Oral Drug Absorption* (Ed. Dressman J), Marcel Dekker, New York, 2000, pp. 31–49.
- 24 Abraham MH, Chadha HS, Martins F, Mitchell RC, *Pestic. Sci.* 1999, 55, 78–99.
- 25 Van de Waterbeemd H, Camenisch G, Folkers G, Raevsky OA, *Quant. Struct. Activity Relat.* 1996, 15, 480–490.
- 26 Van de Waterbeemd H, Camenisch G, Folkers G, Chretien JR, Raevsky OA, *J. Drug Target.* 1998, 6, 151–165.
- 27 Ter Laak AM, Tsai RS, Donné-Op den Kelder GM, Carrupt PA, Testa B, *Eur. J. Pharm. Sci.* 1994, 2, 373–384.
- 28 N'Goka V, Schlewer G, Linget JM, Chambon J-P, Wermuth C-G, *J. Med. Chem.* 1991, 34, 2547–2557.
- 29 Hamilton HW, Steinbaugh BA, Stewart BH, Chan OH, Schmid HL, Schroeder R, Ryan MJ, Keiser J, Taylor MD, Blankley CJ, Kaltenbronn JS, Wright J, Hicks J, *J. Med. Chem.* 1995, 38, 1446–1455.
- 30 Camenisch G, Folkers G, Van de Waterbeemd H, *Pharm. Acta Helv.* 1996, 71, 309–327.
- 31 Camenisch G, Folkers G, Van de Waterbeemd H, *Eur. J. Pharm. Sci.* 1998, 6, 321–329.
- 32 Van de Waterbeemd H, *Eur. J. Pharm. Sci.* 1997, 2 (Suppl.), S26–S27.

- 33 Leahy DE, Taylor PJ, Wait AR, *Quant. Struct. Activity Relat.* **1989**, *8*, 17–31.
- 34 Leahy DE, Morris JJ, Taylor PJ, Wait AR, *J. Chem. Soc. Perkin Trans.* **1992**, *2*, 723–731.
- 35 Suzuki N, Yoshida Y, Watarai H, *Bull. Chem. Soc. Jpn.* **1982**, *55*, 121–125.
- 36 Paterson DA, Conradi RA, Hilgers AR, Vidmar ThJ, Burton PhS, *Quant. Struct. Activity Relat.* **1994**, *13*, 4–10.
- 37 Yang CY, Cai SJ, Liu H, Pidgeon Ch, *Adv. Drug Del. Rev.* **1996**, *23*, 229–256.
- 38 Ottiger C, Wunderli-Allenspach H, *Pharm. Res.* **1999**, *16*, 643–650.
- 39 Balon K, Riebesehl BU, Muller BW, *Pharm. Res.* **1999**, *16*, 882–888.
- 40 Leo A, *Chem. Rev.* **1993**, *93*, 1281–1308.
- 41 Mannhold R, Rekker R.F, Dross K, Bijloo G, De Vries G, *Quant. Struct. Activity Relat.* **1998**, *17*, 517–536.
- 42 Rekker RF, Mannhold R, Bijloo G, De Vries G, Dross K, *Quant. Struct. Activity Relat.* **1998**, *17*, 537–548.
- 43 Kellogg GE, Joshi GS, Abraham DJ, *Med. Chem. Res.* **1992**, *1*, 444–453.
- 44 Viswanadhan VN, Ghose AK, Revankar GR, Robins RK, *J. Chem. Inf. Comput. Sci.* **1989**, *29*, 163–172.
- 45 Ghose AK, Crippen GM, *J. Chem. Inf. Comput. Sci.* **1987**, *27*, 21–35.
- 46 Meylan WM, Howard PH, *J. Pharm. Soc.* **1995**, *84*, 83–92.
- 47 Spessard GO, *J. Chem. Inf. Comput. Sci.* **1998**, *38*, 55–57.
- 48 Buchwald P, Bodor N, *Curr. Med. Chem.* **1998**, *5*, 353–380.
- 49 Carrupt PA, Testa B, Gaillard P, *Rev. Comput. Chem.* **1997**, *11*, 241–315.
- 50 Van de Waterbeemd H, Mannhold R, *Quant. Struct. Activity Relat.* **1996**, *15*, 410–412.
- 51 Mannhold R, Van de Waterbeemd H, *J. Comput-Aid. Mol. Deg.* **2001**, *15*, 337–354.
- 52 Moriguchi I, Hirono S, Nakagome I, Hirano H, *Chem. Pharm. Bull.* **1994**, *42*, 976–978.
- 53 Leo A, ACS Meeting, Anaheim, **1999**.
- 54 Austin RP, Davis AM, Manners CN, *J. Pharm. Sci.* **1995**, *84*, 1180–1183.
- 55 Lullman H, Wehling M, *Biochem. Pharmacol.* **1979**, *28*, 3409–3415.

2**Pharmacokinetics****Abbreviations**

ADME	Absorption, distribution, metabolism and excretion
CNS	Central nervous system
CYP2D6	Cytochrome P450 2D6 enzyme
GIT	Gastrointestinal tract
i.v.	Intravenous
PET	Positive emission tomography

Symbols

A_{av}	Average amount of drug in the body over a dosing interval
A_{max}	Maximum amount of drug in the body over a dosing interval
A_{min}	Minimum amount of drug in the body over a dosing interval
AUC	Area under plasma concentration time curve
C_o	Initial concentration after i. v. dose
$C_{av_{ss}}$	Average plasma concentration at steady state
$C_{p(f)}$	Free (unbound) plasma concentration
$C_{p(f0)}$	Initial free (unbound) plasma concentration
C_{ss}	Steady state concentration
Cl	Clearance
Cl_u	Unbound clearance
Cl_H	Hepatic clearance
Cl_i	Intrinsic clearance
Cl_{iu}	Intrinsic clearance of unbound drug
Cl_o	Oral clearance
Cl_p	Plasma clearance
Cl_R	Renal clearance
Cl_s	Systemic clearance
D	Dose
E	Extraction
E_F	Fractional response
E_M	Maximum response

F	Fraction of dose reaching systemic circulation (bioavailability)
f_u	Fraction of drug unbound
K_A	Affinity constant
K_B	Dissociation constant for a competitive antagonist
K_d	Dissociation constant
k_{el}	Elimination rate constant
K_m	Affinity constant (concentration at 50 % V_{max})
k_o	Infusion rate
k_{+1}	Receptor on rate
k_{-1}	Receptor off rate
L	Ligand
$\log D_{7.4}$	Distribution coefficient (octanol/buffer) at pH 7.4
$\ln 2$	Natural logarithm of 2 (i. e. 0.693)
pA_2	Affinity of antagonist for a receptor ($= -\log_{10}[K_B]$)
Q	Blood flow
R	Receptor
RL	Receptor ligand complex
RO	Receptor occupancy
s	Substrate concentration
t	time after drug administration
T	Dosing interval
$t_{1/2}$	Elimination half-life
V_d	Volume of distribution
$V_{d(f)}$	Apparent volume of distribution of free (unbound) drug
V_{max}	Maximum rate of reaction (Michaelis–Menten enzyme kinetics)
ε	Dosing interval in terms of half-life ($= T/t_{1/2}$)

2.1

Setting the Scene

Pharmacokinetics is the study of the time course of a drug within the body and incorporates the processes of absorption, distribution, metabolism and excretion (ADME). In general, pharmacokinetic parameters are derived from the measurement of drug concentrations in blood or plasma. The simplest pharmacokinetic concept is that based on total drug in plasma. However, drug molecules may be bound to a greater or lesser extent to the proteins present within the plasma, thus free drug levels may be vastly different from those of total drug levels. Blood or plasma are the traditionally sampled matrices due to (a) convenience and (b) to the fact that the concentrations in the circulation will be in some form of equilibrium with the tissues of the body. Because of analytical difficulties (separation, sensitivity) it is usually the total drug that is measured and used in pharmacokinetic evaluation. Such measurements and analysis are adequate for understanding a single drug in a single species in a number of different situations since both protein binding and the resultant unbound fraction are approximately constant under these conditions. When species or

drugs are compared, certain difficulties arise in the use of total drug and unbound (free) drug is a more useful measure (see below).

2.2

Intravenous Administration: Volume of Distribution

When a drug is administered intravenously into the circulation the compound undergoes distribution into tissues etc. and clearance. For a drug that undergoes rapid distribution a simple model can explain the three important pharmacokinetic terms: volume of distribution, clearance and half-life.

Volume of distribution (Vd) is a theoretical concept that connects the administered dose with the actual initial concentration (C_0) present in the circulation. The relationship is shown below:

$$Vd = \text{Dose}/C_0 \quad (2.1)$$

For a drug that is confined solely to the circulation (blood volume is 80 mL kg^{-1}) the volume of distribution will be 0.08 L kg^{-1} . Distribution into total body water (800 mL kg^{-1}) results in a volume of distribution of 0.8 L kg^{-1} . Beyond these values the number has only a mathematical importance. For instance a volume of distribution of 2 L kg^{-1} means only, that less than 5% of the drug is present in the circulation. The drug may be generally distributed to many tissues and organs or concentrated in only a few.

For different molecules, the apparent volume of distribution may range from about 0.04 L kg^{-1} to more than 20 L kg^{-1} . High molecular weight dyes, such as indocyanine green, are restricted to the circulating plasma after intravenous administration and thus exhibit a volume of distribution of about 0.04 L kg^{-1} . For this reason such compounds are used to estimate plasma volume [1] and hepatic blood flow [2]. Certain ions, such as chloride and bromide, rapidly distribute throughout extracellular fluid, but do not readily cross cell membranes and therefore exhibit a volume of distribution of about 0.4 L kg^{-1} which is equivalent to the extracellular water volume [3]. Neutral lipid-soluble substances can distribute rapidly throughout intracellular and extracellular water. For this reason antipyrine has been used as a marker of total body water volume and exhibits a volume of distribution of about 0.7 L kg^{-1} [4]. Compounds which bind more favourably to tissue proteins than to plasma proteins can exhibit apparent volumes of distribution far in excess of the body water volume. This is because the apparent volume is dependent on the ratio of free drug fractions in the plasma and tissue compartments [5]. High tissue affinity is most commonly observed with basic drugs and can lead to apparent volumes of distribution up to 21 L kg^{-1} for the primary amine-containing calcium channel blocker, amlodipine [6].

2.3

Intravenous Administration: Clearance

Clearance of drug occurs by the perfusion of blood to the organs of extraction. Extraction (E) refers to the proportion of drug presented to the organ which is removed irreversibly (excreted) or altered to a different chemical form (metabolism). Clearance (Cl) is therefore related to the flow of blood through the organ (Q) and is expressed by the formula:

$$Cl = Q \cdot E \quad (2.2)$$

The organs of extraction are generally the liver (hepatic clearance – metabolism and biliary excretion; Cl_H) and the kidney (renal excretion, Cl_R) and the values can be summed together to give an overall value for systemic clearance (Cl_S):

$$Cl_S = Cl_H + Cl_R \quad (2.3)$$

Extraction is the ratio of the clearance process compared to the overall disappearance of the compound from the organ. The clearance process is termed intrinsic clearance Cl_i , the other component of disappearance is the blood flow (Q) from the organ. This is shown in Figure 2.1 below.

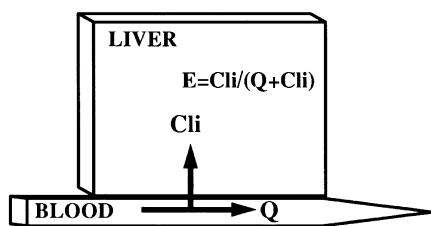


Fig. 2.1 Schematic illustrating hepatic extraction with Q , blood flow and Cl_i , intrinsic clearance (metabolism).

Combining Eqs. (2.2) and (2.3) with the scheme in Figure 2.1 gives the general equation for clearance:

$$Cl = Q \cdot Cl_i / (Q + Cl_i) \quad (2.4)$$

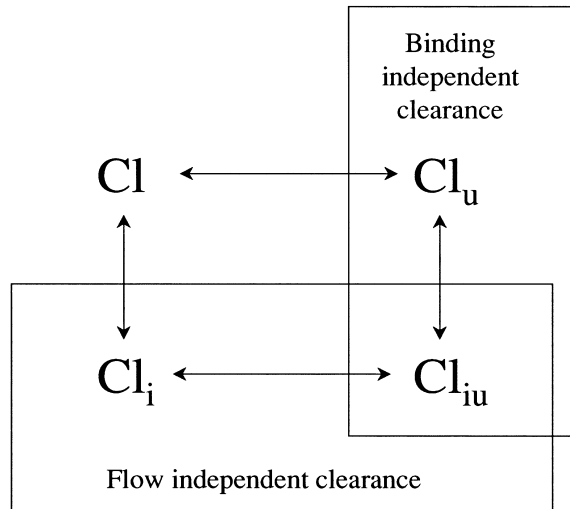
Where $Cl = Cl_S$ if only one organ is involved in drug clearance. Within this equation Cl_i is the intrinsic clearance based on total drug concentrations and therefore includes drug bound to protein. Lipophilic drugs bind to the constituents of plasma (principally albumin) and in some cases to erythrocytes. It is a major assumption, supported by a considerable amount of experimental data, that only the unbound (free) drug can be cleared. The intrinsic clearance (Cl_i) can be further defined as:

$$Cl_i = Cl_{iu} \cdot f_u \quad (2.5)$$

Where Cl_{iu} is the intrinsic clearance of free drug, i. e. unrestricted by either flow or binding, and f_u is the fraction of drug unbound in blood or plasma.

Inspection of the above equation indicates for compounds with low intrinsic clearance compared to blood flow, Q and $(Cl_i + Q)$ effectively cancel and Cl (or Cl_S) approximates to Cl_i . Conversely, when intrinsic clearance is high relative to blood flow,

Fig. 2.2 Inter-relationship between various terms of drug clearance used within pharmacokinetic analysis.



Cl_i and $(Cl_i + Q)$ effectively cancel and Cl (or Cl_s) is equal to blood flow (Q). The implications of this on drugs cleared by metabolism is that the systemic clearance of low clearance drugs are sensitive to changes in metabolism rate whereas that of high clearance drugs are sensitive to changes in blood flow.

It is important to recognize the distinction between the various terms used for drug clearance and the inter-relationship between these. Essentially intrinsic clearance values are independent of flow through the organ of clearance, whilst unbound clearance terms are independent of binding. These relationships are illustrated in Figure 2.2.

2.4

Intravenous Administration: Clearance and Half-life

Clearance is related to the concentrations present in blood after administration of a drug by the equation:

$$Cl = \text{Dose}/\text{AUC} \quad (2.6)$$

where AUC is the area under the plasma concentration time curve. Clearance is a constant with units often given as mL min^{-1} or $\text{mL min}^{-1} \text{kg}^{-1}$ body weight. These values refer to the volume of blood totally cleared of drug per unit time. Hepatic blood flow values are 100, 50 and $25 \text{ mL min}^{-1} \text{kg}^{-1}$ in rat, dog and man respectively. Blood clearance values approaching these indicate that hepatic extraction is very high (rapid metabolism).

Blood arriving at an organ of extraction normally contains only a fraction of the total drug present in the body. The flow through the major extraction organs, the liver and kidneys, is about 3% of the total blood volume per minute, however, for many

drugs, distribution out of the blood into the tissues will have occurred. The duration of the drug in the body is therefore the relationship between the clearance (blood flow through the organs of extraction and their extraction efficiency) and the amount of the dose of drug actually in the circulation (blood). The amount of drug in the circulation is related to the volume of distribution and therefore to the elimination rate constant (k_{el}) which is given by the relationship:

$$k_{el} = Cl/Vd \quad (2.7)$$

The elimination rate constant can be described as a proportional rate constant. An elimination rate constant of 0.1 h^{-1} means that 10 % of the drug is removed per hour.

The elimination rate constant and half-life ($t_{1/2}$), the time taken for the drug concentration present in the circulation to decline to 50 % of the current value, are related by the equation:

$$t_{1/2} = \ln 2/k_{el} \quad (2.8)$$

Half-life reflects how often a drug needs to be administered. To maintain concentrations with minimal peak and trough levels over a dosing interval a rule of thumb is that the dosing interval should equal the drug half-life. Thus for once-a-day administration a 24-h half-life is required. This will provide a peak-to-trough variation in plasma concentration of approximately two-fold. In practice the tolerance in peak-to-trough variation in plasma concentration will depend on the therapeutic index of a given drug and dosing intervals of two to three half-lives are not uncommon.

The importance of these equations is that drugs can have different half-lives due either to changes in clearance or changes in volume (see Section 2.7). This is illustrated in Figure 2.3 for a simple single compartment pharmacokinetic model where the half-life is doubled either by reducing clearance to 50 % or by doubling the volume of distribution.

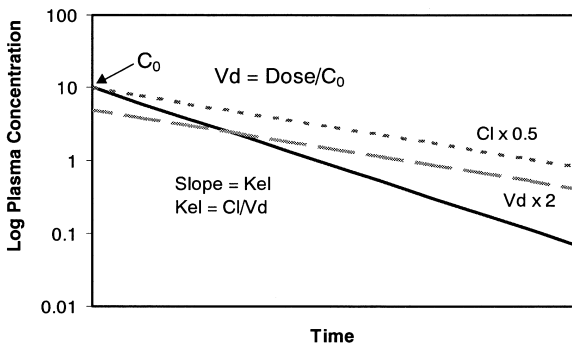


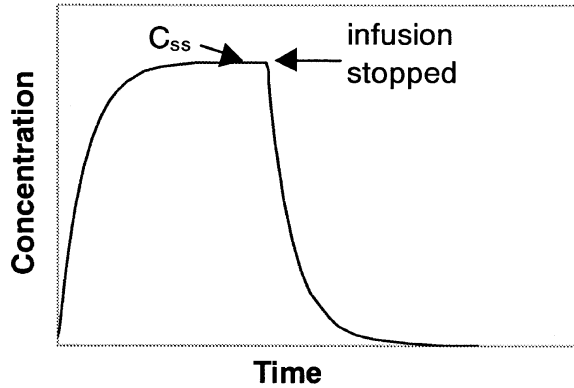
Fig. 2.3 Effect of clearance and volume of distribution on half-life for a simple single compartment pharmacokinetic model.

2.5

Intravenous Administration: Infusion

With linear kinetics, providing an intravenous infusion is maintained long enough, a situation will arise when the rate of drug infused = rate of drug eliminated. The

Fig. 2.4 Plasma concentration profile observed after intravenous infusion.



plasma or blood concentrations will remain constant and be described as “steady state”. The plasma concentration profile following intravenous infusion is illustrated in Figure 2.4.

The steady state concentration (C_{ss}) is defined by the equation:

$$C_{ss} = ko / Cl_p \quad (2.9)$$

where ko is the infusion rate and Cl_p is the plasma (or blood) clearance. The equation which governs the rise in plasma concentration is shown below where the plasma concentration (C_p) may be determined at any time (t).

$$C_p = ko / Cl_p (1 - e^{-k_{el} \cdot t}) \quad (2.10)$$

Thus the time taken to reach steady state is dependent on k_{el} . The larger k_{el} (shorter the half-life) the more rapidly the drug will attain steady state. As a guide 87 % of steady state is attained when a drug is infused for a period equal to three half-lives. Decline from steady state will be as described above, so a short half-life drug will rapidly attain steady state during infusion and rapidly disappear following the cessation of infusion.

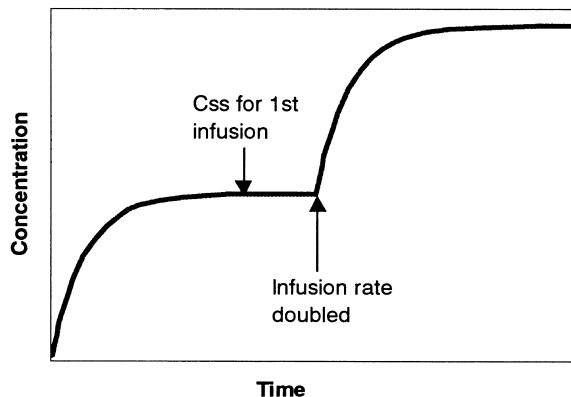


Fig. 2.5 Intravenous infusion with infusion rate doubled.

Increasing the infusion rate will mean the concentrations will climb until a new steady state value is obtained. Thus doubling the infusion rate doubles the steady state plasma concentration as illustrated in Figure 2.5.

2.6

Oral Administration

When a drug is administered orally, it has to be absorbed across the membranes of the gastrointestinal tract. Incomplete absorption lowers the proportion of the dose able to reach the systemic circulation. The blood supply to the gastrointestinal tract (GIT) is drained via the hepatic portal vein which passes through the liver on its passage back to the heart and lungs. Transport of the drug from the gastrointestinal tract to the systemic circulation will mean the entire absorbed dose has to pass through the liver.

On this “first-pass” the entire dose is subjected to liver extraction and the fraction of the dose reaching the systemic circulation (F) can be substantially reduced (even for completely absorbed drugs) as shown in the following equation:

$$F = 1 - E \quad (2.11)$$

Again E is the same concept as that shown in Figure 2.1. This phenomenon is termed the first-pass effect, or pre-systemic metabolism, and is a major factor in reducing the bioavailability of lipophilic drugs. From the concept of extraction shown in Figure 2.1, rapidly metabolized drugs, with high Cl_i values, will have high extraction and high first-pass effects. An example of this type of drug is the lipophilic calcium channel blocker, felodipine. This compound has an hepatic extraction of about 0.80, leading to oral systemic drug exposure (AUC) of only about one-fifth of that observed after intravenous administration [7]. Conversely, slowly metabolized drugs, with low Cl_i values, will have low extraction and show small and insignificant first-pass effects. The class III anti-dysrhythmic drug, dofetilide, provides such an example. Hepatic extraction of this compound is only about 0.07, leading to similar systemic exposure (AUC) after oral and intravenous doses [8].

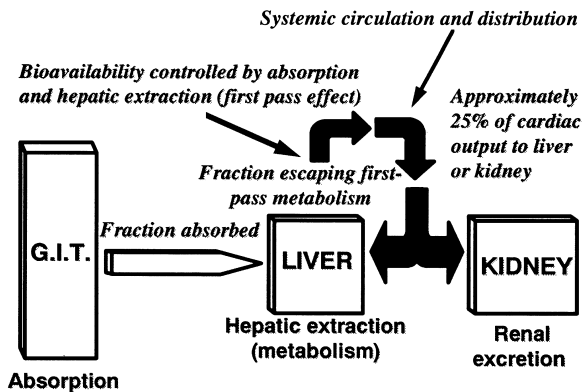


Fig. 2.6 Schematic illustrating the disposition of a drug after oral administration.

A complication of this can be additional first-pass effects caused by metabolism by the gastrointestinal tract itself. In the most extreme cases, such as midazolam, extraction by the gut wall may be as high as 0.38 to 0.54 and comparable to that of the liver itself [9].

The previous equations referring to intravenously administered drugs (e.g. Eq. 2.6) can be modified to apply to the oral situation:

$$Cl_o = F \cdot \text{Dose}/\text{AUC} \quad (2.12)$$

Where Cl_o is the oral clearance and F indicates the fraction absorbed and escaping hepatic first-pass effects. Referring back to the intravenous equation we can calculate F or absolute bioavailability by administering a drug intravenously and orally and measuring drug concentrations to derive the respective AUCs. When the same dose of drug is given then:

$$F = \text{AUC}_{\text{oral}}/\text{AUC}_{\text{i.v.}} \quad (2.13)$$

The estimation of systemic clearance together with this value gives valuable information about the behaviour of a drug. High clearance drugs with values approaching hepatic blood flow will indicate hepatic extraction (metabolism) as a reason for low bioavailability. In contrast poor absorption will probably be the problem in low clearance drugs which show low bioavailabilities.

2.7

Repeated Doses

When oral doses are administered far apart in time they behave independently. This is usually not the desired profile if we assume that a certain concentration is needed to maintain efficacy and if a certain concentration is exceeded side-effects will occur. Giving doses of the drug sufficiently close together so that the following doses are administered prior to the full elimination of the preceding dose means that some accumulation will occur, moreover a smoothing out of the plasma concentration profile will occur. This is illustrated in Figure 2.7.

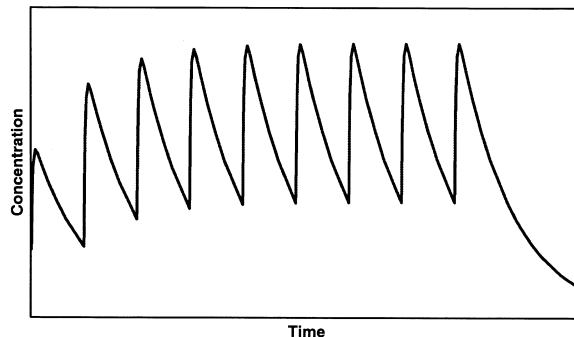


Fig. 2.7 Plasma concentration profile for multiple oral dose administration.

Ultimately if doses are given very close together then the effect is that of intravenous infusion and a steady state occurs. In fact for any drug an average steady state value ($C_{av,ss}$) can be calculated:

$$C_{av,ss} = F \cdot \text{Dose}/Cl \cdot T \quad (2.14)$$

where T represents the interval between doses, Dose is the size of a single administered dose and Cl is clearance. Note that $F \cdot \text{Dose}/T$ in this equation is actually the dosing rate as for intravenous infusion.

The same relationship to k_{el} and half-life also apply, so that as with intravenous infusion 87.5% of the final steady state concentration is achieved following administration of the drug for three half-lives.

This equation can be rewritten to indicate the amount of drug in the body by substitution of k_{el} for Cl . Since $k_{el} = 0.693/t_{1/2}$ the following equation emerges:

$$A_{av} = 1.44 \cdot F \cdot t_{1/2} \cdot (\text{Dose}/T) \quad (2.15)$$

where A_{av} is the average amount of drug in the body over the dosing interval. By relating this to each dose an accumulation ratio (R_{ac}) can be calculated:

$$R_{ac} = A_{av}/F \cdot \text{Dose} = 1.44 \cdot t_{1/2}/T \quad (2.16)$$

The maximum and minimum amounts in the body (A_{max} and A_{min} respectively) are defined by:

$$A_{max} = \text{Dose}/1 - (1/2)^\varepsilon \quad (2.17)$$

$$A_{min} = \text{Dose} \cdot 1[1 - (1/2)^\varepsilon - 1] \quad (2.18)$$

where $\varepsilon = T/t_{1/2}$ or the dosing interval defined in terms of half-life. These equations mean that for a drug given once a day with a 24-h half-life then a steady state will be largely achieved by 3–4 days. In addition, the amount of drug in the body (or the plasma concentration) will be approximately 1.4 times that of a single dose and that this will fluctuate between approximately twice the single dose and equivalent to the dose.

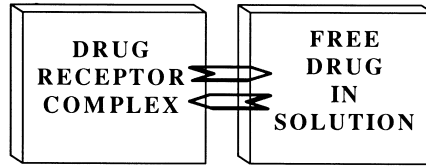
2.8

Development of the Unbound (Free) Drug Model

As outlined earlier, pharmacokinetics based on total drug concentrations proves useful in many situations, but is limited when data from a series of compounds are compared. This is the normal situation in a drug discovery programme and alternative presentations of pharmacokinetic information need to be explored. Since the medicinal chemist is trying to link compound potency in *in vitro* systems (receptor binding, etc.) with behaviour *in vivo*; it is important to find ways to unify the observations.

Measurement of the unbound drug present in the circulation and basing pharmacokinetic estimates on this, allows the *in vitro* and *in vivo* data to be rationalized.

Fig. 2.8 Schematic illustrating equilibrium between drug and receptor.



The first and possibly the simplest biological test for a drug is the *in vitro* assessment of affinity for its target. Such experiments can be shown schematically as illustrated in Figure 2.8 in which the drug is added to the aqueous buffer surrounding the receptor (or cell or tissue) and the total drug added is assumed to be in aqueous solution and in equilibrium with the receptor.

2.9

Unbound Drug and Drug Action

The biological or functional response to receptor activation can be assumed to be directly proportional to the number of receptors (R) occupied by a given ligand (L) at equilibrium. This assumption is termed the occupancy theory of drug response. The equation describing this phenomenon was proposed as:

$$[R] E_F/E_M = [RL]/[R]_T \quad (2.19)$$

where E_F is the fractional response, E_M is the maximal response, $[RL]$ is the concentration of receptor–ligand complex and $[R]_T$ is the total receptor concentration. At equilibrium, $R + L \rightleftharpoons RL$, such that the affinity constant K_A can be defined as $K_A = [RL]/[L][R]$. This is the same equation as that derived from Langmuir's saturation isotherm, which derives from the law of mass action. It is possible to describe the occupancy theory in the following way:

- the receptor/ligand (RL) complex is reversible
- association is a bimolecular process
- dissociation is a monomolecular process
- all receptors of a given type are equivalent and behave independently of one another
- the concentration of ligand is greatly in excess of the receptor and therefore the binding of the ligand to the receptor does not alter the free (F) concentration of the ligand
- the response elicited by receptor occupation is directly proportional to the number of receptors occupied by the ligand

The equilibrium dissociation constant K_d gives a measure of the affinity of the ligand for the receptor.

$$K_d = ([R][L])/[RL] \quad (2.20)$$

K_d can also be defined by the two microconstants for rate on and off k_{+1} and k_{-1} so that $K_d = k_{-1}/k_{+1}$, where K_d is the concentration of the ligand (L) that occupies 50% of the available receptors.

Antagonist ligands occupy the receptor without eliciting a response, thus preventing agonist ligands from producing their effects. Since this interaction is usually competitive in nature, an agonist can overcome the antagonist effects as its concentration is increased. The competitive nature of this interaction allows the determination of a pA_2 value, the affinity of an antagonist for a receptor as shown below.

$$pA_2 = -\log K_B \quad (2.21)$$

where K_B = the dissociation constant for a competitive antagonist and is the ligand concentration that occupies 50 % of the receptors.

We thus have a series of unbound drug affinity measures relating to the action of the drug. The values are those typically obtained by the pharmacologist and form the basis of the structure–activity relationships which the medicinal chemist will work on. It is possible to extend this model to provide a pharmacokinetic phase as shown in Figure 2.9.

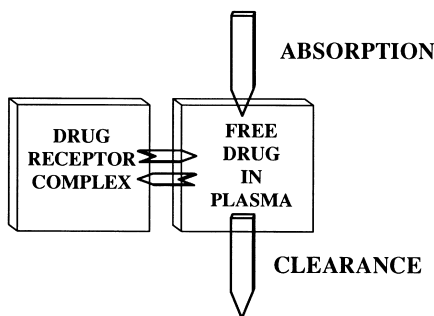


Fig. 2.9 Schematic showing the equilibrium of a drug receptor and unbound (free) drug and the processes that control drug concentration.

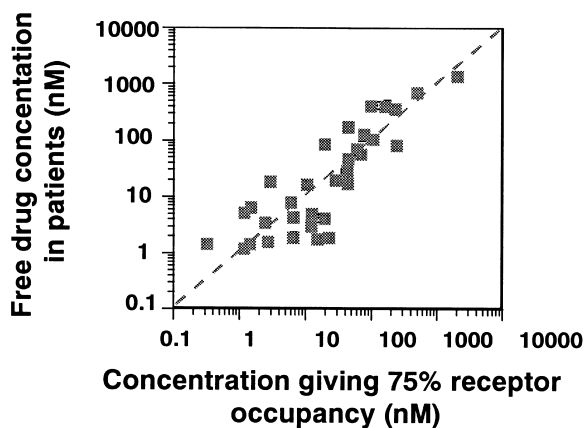
Here we assume that:

- free drug is in equilibrium across the system
- only free drug can exert pharmacological activity (see above)
- drug is reversibly bound to tissues and blood
- only free drug can be cleared

To examine the validity of this model, data from a number of 7 transmembrane (7TM) receptor antagonists (antimuscarinics, antihistaminics, β -adrenoceptor blockers etc.) were examined. The K_B values for these drugs were compared to their free (unbound) plasma concentration. To simplify the analysis the plasma concentration data was taken from patients at steady state on therapeutic doses. Steady state means that the dosing rate (rate in) is balanced by the clearance rate (rate out). This concept is exactly as described earlier for intravenous infusion, however the steady state is an average of the various peaks and troughs that occur in a normal dosage regimen. The relationship between the values was very close and the *in vitro* potency values can be adjusted to 75 % receptor occupancy (RO) rather than 50 % using Eq. (2.21) shown below (where the ligand concentration is represented by L):

$$RO = [L]/[K_B + L] \quad (2.21)$$

Fig. 2.10 Correlation of *in vitro* potency with plasma free drug concentration required for efficacy.



When this relationship is plotted, a 1 : 1 relationship is seen as shown in Figure 2.10. Thus the free concentration present in plasma is that actually seen at the receptor. Moreover, the *in vitro* values (K_B) determined from receptor binding actually represent the concentration required in the patient for optimum efficacy.

We can thus see that the traditional indicators of potency that drive synthetic chemistry, such as pA_2 values, can have direct relevance to the plasma concentration (free) required to elicit the desired response. If we extend this example further it is unlikely that in all cases there is a simple direct equilibrium for all compounds between the free drug in plasma and the aqueous media bathing the receptor. The concentration of the free drug in the plasma is in direct equilibrium with the interstitial fluid bathing most cells of the body, since the capillary walls contain sufficient numbers of pores to allow the rapid passage of relatively small molecules, regardless of physicochemistry. Most receptor targets are accessed extracellularly. We can expect therefore that all drugs, regardless of their physicochemistry, will be in direct equilibrium at these targets, with the free drug in plasma. For instance the G-protein-coupled receptors have a binding site which is accessible to hydrophilic molecules.

This is exemplified by the endogenous agonists of these receptors that are usually hydrophilic by nature. Adrenalin, dopamine and histamine are representative and have $\log D_{7.4}$ values of -2.6 , -2.4 and -2.9 respectively.

The antagonists included in Figure 2.10 range in $\log D_{7.4}$ value. For example, within the β -adrenoceptor antagonists the range is from -1.9 for atenolol to 1.1 for propranolol. This range indicates the ease of passage from the circulation to the receptor site for both hydrophilic and lipophilic drugs.

2.10

Unbound Drug Model and Barriers to Equilibrium

In some cases barriers such as the blood–brain barrier exist, in other cases the target is intracellular. Here the model has to be extended to place the receptor in a biophase

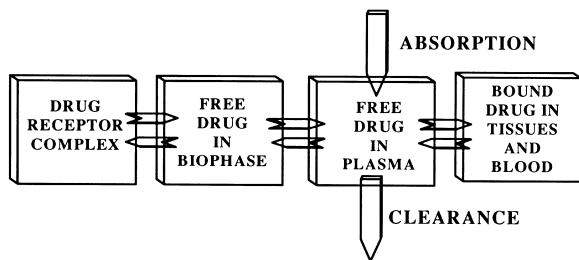


Fig. 2.11 Schematic pharmacodynamic/pharmacokinetic model incorporating a biophase and a drug binding compartment.

(Figure 2.11). The model also includes a “compartment” for the drug that is reversibly bound to tissues and blood. The significance of this will be explored after further examination of the role of the biophase.

Aqueous channels are much fewer in number in the capillaries of the brain (blood–brain barrier) and rapid transfer into the brain fluids requires molecules to traverse the lipid cores of the membranes. Actual passage into cells, like crossing the blood–brain barrier, also requires molecules to traverse the lipid core of the membrane due to the relative paucity of aqueous channels. Distribution of a drug to the target, whether a cell membrane receptor in the CNS or an intracellular enzyme or receptor, therefore critically determines the range of physicochemical properties available for the drug discoverer to exploit. The access of the CNS to drugs is illustrated by reference to a series of dopamine D_2 antagonists. Here receptor occupancy can be measured by the use of PET scanning and this “direct measure” of receptor occupancy can be compared with theoretical occupation calculated from the free drug plasma concentrations in the same experiment. Figure 2.12 shows this comparison for the lipophilic antagonists remoxipride, haloperidol and thioridazine and the hydrophilic compound sulpiride.

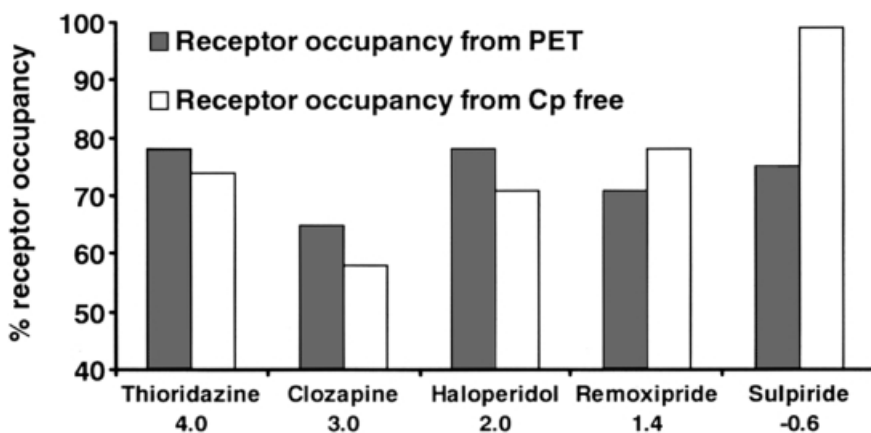


Fig. 2.12 Receptor occupancy based on PET scanning and *in vitro* potency combined with free plasma drug concentration. $\log D_{7,4}$ values shown below compound names.

As for the more comprehensive set of non-CNS site antagonists, referred to above, efficacy is observed at around 75 % receptor occupancy. Noticeably the lipophilic antagonists, thioridazine, clozapine, haloperidol and remoxipride, are in direct equilibrium with the free drug concentration in plasma. In contrast salpiride requires a free plasma concentration over 50-fold greater than that required if there was a simple direct equilibrium between the plasma concentration and the extracellular fluid of the brain. This difference in equilibrium between salpiride and the lipophilic compounds is due to the poor penetration of this hydrophilic molecule across the blood–brain barrier. As explained above, the reasons for this are the low number of aqueous channels or pores in the capillary walls of the blood vessels of the brain, thereby restricting entry of hydrophilic compounds to the extracellular fluid of the CNS. Similar observations can be made for intracellular targets, whether enzymes or receptors. Here the need to penetrate the lipid core is reflected in the physicochemistry of the endogenous agonists. For instance, steroid receptors are intracellular and steroids have $\log D_{7,4}$ values such as 3.3, 1.7 and 2.3 for testosterone, cortisol and corticosterone respectively. These values contrast with the values for the endogenous agonists of G-protein-coupled receptors.

2.11

Slow Offset Compounds

One frequently encounters the case where the equilibrium dissociation constant (K_d , see above) is defined by microconstants with “fast” rates on and off the receptor. However, any change in potency in a chemical series (affinity) must represent an increase in the on (k_{+1}) rate or a decrease in the off rate (k_{-1}). Occasionally, either by accident or design, the off rate is altered dramatically enough to redefine the receptor kinetics of the compound such that the rates influence the actual pharmacodynam-

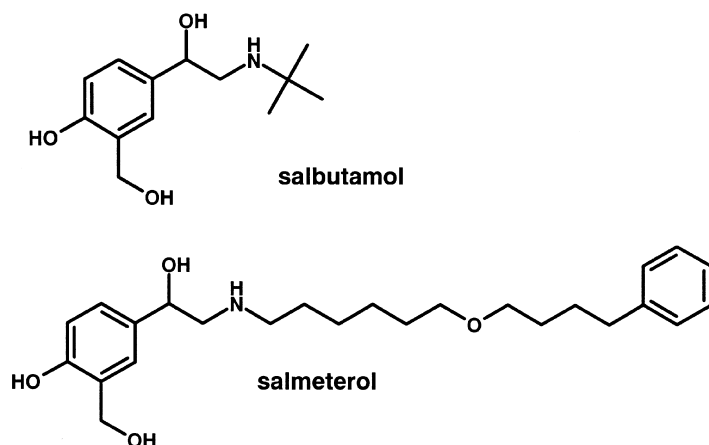


Fig. 2.13 Structures of salbutamol and salmeterol, rapid and slow offset β_2 -adrenoceptor agonists.

ics of the compound. These compounds are termed “slow offset” and their pharmacodynamic action exceeds that which would be predicted from the duration of the plasma concentrations. Often such compounds are detected during *in vitro* studies by increasing affinity or potency with time of incubation or persistence of activity following removal of drug by “wash out”. A number of explanations for this phenomena have been advanced. Extra-receptor binding attempts to explain the slow offset of a compound by invoking a binding site removed from the actual active site domain. This site could be either protein or lipid. Salmeterol (a β_2 adrenoceptor agonist) represents an agent designed in this manner [10]. The lipophilic side chain interacts with an exosite and markedly improves duration against compounds such as salbutamol (Figure 2.13).

The exosite appears to be located at the interface of the cytoplasm and the transmembrane domain of the β_2 -adrenergic receptor [10]. The structures of salbutamol and salmeterol are clearly different, although it is obvious both are based on the “adrenalin” pharmacophore. More subtle changes in structure leading to “slow-offset” can only be rationalized by changes in intra-receptor binding. Possibilities for such increases can include simply increased interaction *per se* and resultant affinity, with an effect largely confined to changes in the off rate. Thus, telenzepine is more potent than pirenzepine as well as showing slow offset from the receptor [11]. This increase in affinity may simply reflect the increased lipophilicity of the telenzepine head group (Figure 2.14).

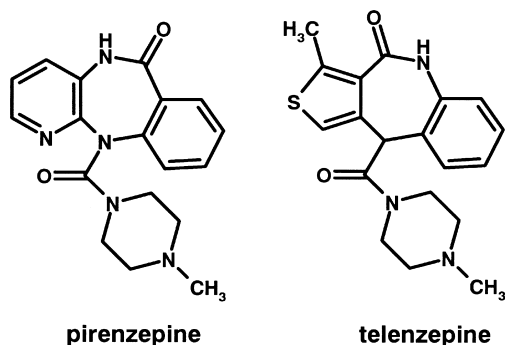


Fig. 2.14 Structures of pirenzepine and its more potent, slow offset M1 antimuscarinic analogue telenzepine.

It is possible to achieve slow offset without a change in potency. Here conformational restriction may be the mechanism. If one assumes a number of binding functions in a molecule, and that for stable binding all have to interact, then probability suggests that in a flexible molecule, association and disassociation will be occurring rapidly (fast on, fast off). With a molecule whose confirmation is restricted to one favourable to the interactions, it is likely that the rate of association and disassociation will be markedly lower (slow on, slow off). Such restrictions may be very simple molecular changes, for instance a single methyl group converts the fast offset compound carfentanil [12] to the slow offset compound lofentanil (Figure 2.15).

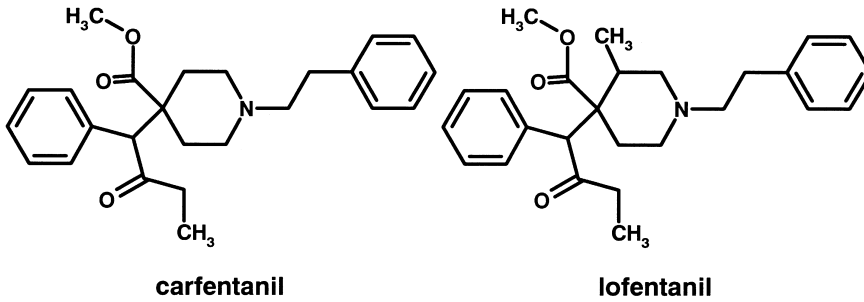


Fig. 2.15 Structures of opioid agonists carfentanil and its slow offset analogue lofentanil.

2.12

Factors Governing Unbound Drug Concentration

We thus have in many cases only two parameters defining drug activity at steady state, receptor affinity and free (unbound) plasma concentration. Occasionally actual persistence at the receptor needs to be taken into account. In some cases, particularly hydrophilic drugs, there is a permeation factor that needs to be defined. The concept of steady state allows simplification of the equations and concepts of pharmacokinetics. Steady state in the context here implies a drug dosed at specific times so that the concentrations between administered doses are effectively an exact image of previous doses and that the difference between the peak and trough levels are small. The factors governing the steady state free plasma concentration $C_{p(f)}$, for an oral drug, are the dosing rate (dose size \times frequency), the fraction of the dose absorbed (F) through the g.i. tract and the free drug clearance (Cl_{iu}) as shown below:

$$\begin{aligned} &\text{at steady state: rate in} = \text{rate out} \\ &(\text{Dose size} \times \text{frequency}) \cdot F = C_{p(f)} \cdot Cl_{iu} \end{aligned} \quad (2.22)$$

True steady state is usually only achieved for a prolonged period with intravenous infusion. If we assume that we wish for a similar steady value after oral administration, then we need to balance our dosing frequency with the rate of decline of drug concentration and the rule of thumb referred to earlier (dosing interval equal to drug half-life) can be applied. Unbound clearance and free drug are particularly applicable to drugs delivered by the oral route. For a well-absorbed compound the free plasma concentrations directly relate to Cl_{iu} (intrinsic unbound clearance).

$$AUC = \text{Dose}/Cl_{iu} \quad (2.23)$$

This simplifies greatly the concepts of first-pass hepatic metabolism and systemic clearance referred to previously. Most importantly Cl_{iu} is directly evolved from the enzyme kinetic parameters, V_{max} and K_m :

$$Cl_{iu} = V_{max}/K_m \quad (2.24)$$

When the drug concentrations are below the K_m , Cl_{iu} is essentially independent of drug concentration. The processes of drug metabolism are similar to other enzymatic processes. For instance most oxidative processes (cytochrome P450) obey Michaelis–Menten kinetics:

$$v = [V_{max} \cdot s]/[K_m + s] \quad (2.25)$$

where v is the rate of the reaction, V_{max} the maximum rate, K_m the affinity constant (concentration at 50% V_{max}) and s the substrate concentration. Substrate concentration (s) is equal to or has a direct relationship to $Cp_{(f)}$. In many cases $Cp_{(f)}$ (or s) are below the K_m value of the enzyme system. However, in some cases (particularly the higher affinity P450s such as CYP2D6, see Chapter 7), $Cp_{(f)}$ (or s) can exceed the K_m and the rate of metabolism therefore approaches the maximum (V_{max}). As such the kinetics move from first order to zero order and the elimination of the drug is capacity limited. The term saturation kinetics is applied. Under these conditions

$$Cl_{iu} = V_{max}/s \quad (2.26)$$

and clearance depends on drug concentration.

These values are obtained from *in vitro* enzyme experiments. From the previous relationship between *in vitro* pharmacology measurements and free drug concentrations and those outlined here, it is reasonable to assume that clinical dose size can be calculated from simple *in vitro* measurements.

It is easiest to understand how clearance relates to the rate of decline of drug concentration (half-life) if we consider the model depicted in Figure 2.9. When a dose (D) is administered intravenously then the initial free concentration achieved in plasma $Cp_{(f_0)}$ is dependant on the volume of extracellular or total body water minus plasma water and the amount of drug bound to tissues and proteins.

Free volume is calculated by equations analogous to those for total drug (see Eq. 2.1).

$$Cp_{(f_0)} = D/Vd_{(f)} \quad (2.27)$$

in which $Vd_{(f)}$ is an apparent volume not only including the actual fluid the drug is dissolved in but also including the drug bound to tissues and protein as if it was an aqueous compartment in direct equilibrium with the free drug. Thus the greater the amount of drug bound, the greater the apparent free volume. The clearance and volume of distribution of unbound drug are related by the equation

$$Cl_u = Vd_{(f)} \cdot k_{el} \quad (2.28)$$

where k_{el} is the elimination rate constant. Note that this equation and others are essentially the same as those for total drug except that free (unbound) drug values are substituted for total drug values. Free volume and free clearance are always equal to or greater than the values calculated from total drug. Moreover increases in plasma protein binding increase free volume but decrease total volume.

These concepts lead to two important observations. Protein binding or tissue binding is not important in daily dose size. The daily dose size is determined by the required free (unbound) concentration of drug required for efficacy. Protein binding

or tissue binding is important in the actual dosage regimen (frequency). The greater the binding the lower and more sustained the free drug concentrations are. Thus a drug with four-fold higher binding and hence free volume than another, with the same unbound (free) clearance, will have a four-fold longer half-life. This could result in a dosage regimen of 20 mg once a day compared to 5 mg four times a day, both giving rise to broadly similar profiles and fluctuations around the average steady state concentration.

References

- 1 Haller M, Akbulut C, Brechtelsbauer H, Fett W, Briegel J, Finsterer U, Peter K, *Life Sci.* **1993**, *53*, 1597–1604.
- 2 Burns E, Triger DR, Tucker GT, Bax NDS, *Clin. Sci.* **1991**, *80*, 155–160.
- 3 Wong WW, Sheng HP, Morkeberg JC, Kosanovich JL, Clarke LL, Klein PD, *Am. J. Clin. Nutr.* **1989**, *50*, 1290–1294.
- 4 Brans YW, Kazzi NJ, Andrew DS, Schwartz CA, Carey KD, *Biol. Neonate* **1990**, *58*, 137–144.
- 5 Gibaldi M, McNamara PJ, *Eur. J. Clin. Pharmacol.* **1978**, *13*, 373–378.
- 6 Stopher DA, Beresford AP, Macrae PV, Humphrey MJ, *J. Cardiovasc. Pharmacol.* **1988**, *12*, S55–S59.
- 7 Edgar B, Regardh CG, Johnsson G, Johansson L, Lundborg P, Loftberg I, Ronn O, *Clin. Pharmacol. Ther.* **1985**, *38*, 205–211.
- 8 Smith DA, Rasmussen HS, Stopher DA, Walker DK, *Xenobiotica* **1992**, *22*, 709–719.
- 9 Thummel KE, Kunze KL, Shen DD, *Adv. Drug Delivery Rev.* **1997**, *27*, 99–127.
- 10 Green SA, Spasoff AP, Coleman RA, Johnson M, Liggett SB, *J. Biol. Chem.* **1996**, *271*, 24029–24035.
- 11 Schudt C, Auriga C, Kinder B, Birdsall NJM, *Eur. J. Pharmacol.* **1988**, *145*, 87–90.
- 12 Leysen JE, Gommeren W, *Drug Dev. Res.* **1986**, *8*, 119–131.

3

Absorption

Abbreviations

AUC	Area under the curve of a concentration time profile
Caco-2	Human colon adenocarcinoma cell line used as absorption model
g. i.	Gastrointestinal
MDCK	Madin–Darby Canine Kidney cell line used as absorption model

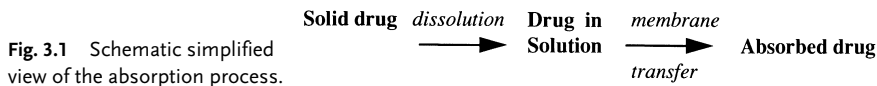
Symbols

A%	Percentage of dose absorbed as measured in portal vein
CLOGP	MedChem/Biobyte log <i>P</i> estimation program
<i>F</i> %	Percentage of dose bioavailable
<i>F</i> _a	Fraction absorbed
<i>F</i> _{non}	Fraction non-ionised at pH 6.5
IFV	Intestinal fluid volume (250 ml)
<i>k</i> _a	Absorption rate constant in rats (min ⁻¹)
log <i>D</i>	Logarithm of distribution coefficient
log <i>P</i>	Logarithm of partition coefficient
log <i>S</i>	Logarithm of solubility in water
RT	Average residence time in the small intestine (270 min)
<i>S</i>	Solubility in phosphate buffer at pH 6.5
<i>S</i> ₀	Intrinsic solubility of the neutral species at 37 °C
<i>V</i> _L	Volume of the luminal contents
<i>X</i> ₀	Dose administered

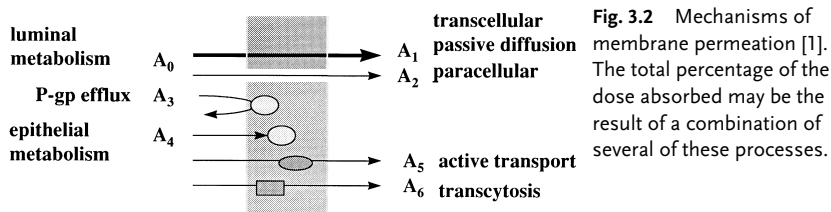
3.1

The Absorption Process

The oral absorption of a drug is dependent on the compound dissolving in the aqueous contents of the gastrointestinal tract (dissolution) and then traversing the actual barrier of the gastrointestinal tract to reach the blood (Figure 3.1).



For a number of reasons membrane transfer may be limited (see Figure 3.2) and therefore absorption incomplete. In this chapter these processes will be discussed.



$$A\% = -a_0A_0 + a_1A_1 + a_2A_2 - a_3A_3 - a_4A_4 + a_5A_5 + a_6A_6$$

3.2

Dissolution

Dissolution depends on the surface area of the dissolving solid and the solubility of the drug at the surface of the dissolving solid. Considering these factors separately surface area is manipulated by the processing and formulation of the compound. Milling and micronization convert the drug into smaller particles with consequently greater surface area. In actual clinical use the compaction of the particles into tablets is offset by formulation with disintegrants. Certain formulations use a co-solvent such as polyethylene glycol (PEG) which is an organic solvent with water miscible properties.

Solubility is manipulated mainly by the structure of the drug. Broadly, solubility is inversely proportional to the number and type of lipophilic functions within the molecule and the tightness of the crystal packing of the molecule. Yalkowski [2] has produced a general solubility ($\log S$) equation, for organic non-electrolytes. The equation incorporates the entropy of melting (ΔS_m) and melting point (m. p. in $^{\circ}\text{C}$) as a measure of crystal packing and $\log P$ as a measure of lipophilicity.

$$\log S = (\Delta S_m (\text{m.p.} - 25)/1364) - \log P + 0.80 \quad (3.1)$$

This equation can be further simplified to

$$\log S = -\log P - 0.01 \text{ m.p.} + 1.2 \quad (3.2)$$

It can be seen from the above that increases in either crystal packing or lipophilicity will decrease solubility.

The rate of dissolution is effected by solubility as is the actual concentration of drug in the bulk of the solution (aqueous contents of gastrointestinal tract). The concentration of drug in solution is the driving force of the membrane transfer of drug

into the body and low aqueous solubility often continues to present itself as a problem even after formulation improvements.

A number of drugs have very low aqueous solubility, mainly due to very high lipophilicity, but also due to lack of ionizable centres, and also the tight crystal packing referred to above. These drugs are erratically and incompletely absorbed due to this inability to dissolve in the gastrointestinal tract following oral administration. Examples of low solubility, dissolution limited drugs include danazole, griseofulvin, halofantrine, ketoconazole, nitrofurantoin, phenytoin and triamterene [3,4]. Poor dissolution is responsible for both intra- and inter-patient variability in drug absorption and therefore represents a major problem in drug design.

If a drug has an ionizable centre then solubility can be improved by salt formation. In the absence of a salt basic drugs will also have increased solubility in the acidic environment of the stomach.

The incorporation of an ionizable centre, such as an amine or similar function, into a template can bring a number of benefits including water solubility. A key step [5] in the discovery of indinavir was the incorporation of a basic amine (and a pyridine) into the backbone of hydroxyethylene transition state mimic compounds (Figure 3.3) to enhance solubility (and potency).

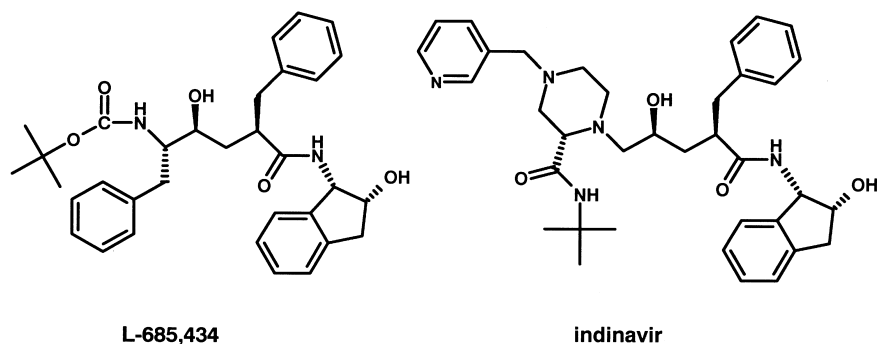


Fig. 3.3 Structures of lead compound L-685,434 and indinavir which incorporates basic functions aiding water solubility.

3.3

Membrane Transfer

The barrier of the gastrointestinal tract is similar to any other that involves the crossing of biological membranes. Biomembranes are composed of a lipid-bilayer [6]. The bilayer results from the orientation of the lipids (phospholipids, glycolipids and cholesterol) in the aqueous medium. Phospholipids are amphipathic with polar head groups and lipid “tails” and align so that the polar head groups orientate towards the aqueous medium and the lipid tails form an inner hydrophobic core. Because of the high flexibility of membrane lipids they are able to perform transversal/lateral movements within the membrane. A variety of proteins such as selective ion channels (Na^+ , K^+ , Ca^{2+} , Cl^-) are embedded within the membrane. Tight junctions are formed

by the interaction of membrane proteins at the contact surfaces between single cells. Tight junctions are in reality small aqueous-filled pores. The dimensions of these pores have been estimated to be in the range of 3–10 Å. The number and dimensions of the tight junctions depend on the membrane type. For the small intestine these tight junctions make up about 0.01 % of the whole surface. Thus the surface area of the actual biological membrane is much greater than that of the aqueous pores (tight junctions).

Compounds can cross biological membranes by two passive processes, transcellular and paracellular mechanisms. For transcellular diffusion two potential mechanisms exist. The compound can distribute into the lipid core of the membrane and diffuse within the membrane to the basolateral side. Alternatively, the solute may diffuse across the apical cell membrane and enter the cytoplasm before exiting across the basolateral membrane. Because both processes involve diffusion through the lipid core of the membrane the physicochemistry of the compound is important. Paracellular absorption involves the passage of the compound through the aqueous-filled pores. Clearly in principle many compounds can be absorbed by this route but the process is invariably slower than the transcellular route (surface area of pores versus surface area of the membrane) and is very dependent on molecular size due to the finite dimensions of the aqueous pores.

The actual amount of a drug absorbed (F_a) is dependent on two rates: the rate of absorption (k_a) and the rate of disappearance of the drug from the absorption site. Disappearance can be due to absorption (k_a) or movement of the drug (k_m) through the gastrointestinal tract and away from the absorption site. The proportion absorbed can be expressed as:

$$F_a = k_a / (k_a + k_m) \quad (3.3)$$

Compounds crossing the gastrointestinal tract via the transcellular route can usually be absorbed throughout the length of the tract. In contrast the paracellular route is only, readily, available in the small intestine and the term “absorption window” is often applied. The calculated human pore sizes (radii) are, jejunum 6–8 Å, ileum 2.9–3.8 Å and colon less than 2.3 Å. In practice the small intestine transit time is around 6 h whilst transit of the whole tract is approximately 24 h. For lipophilic compounds, with adequate dissolution, which have high rates of transcellular passage across membranes, k_a has a high value. Moreover, since the drug is absorbed throughout the g.i. tract k_m is of a low value and therefore the proportion of a dose absorbed is high (complete). For hydrophilic compounds, which are dependent on the slow paracellular pathway, k_a has a low value. Moreover, the “absorption window” referred to above means that the drug rapidly moves away from the absorption site and k_m is high. Consequently paracellularly absorbed compounds show incomplete absorption and the proportion which is absorbed is low. Table 3.1 gives examples of compounds absorbed by the paracellular route.

What is noticeable is that the compounds are of low molecular weight, however, there is no simple relationship between molecular weight and percentage absorbed, probably indicating that shape and possibly flexibility are also of importance. Compounds such as propranolol ($\log D_{7.4}$, 0.9) which are related to those in Table 3.1,

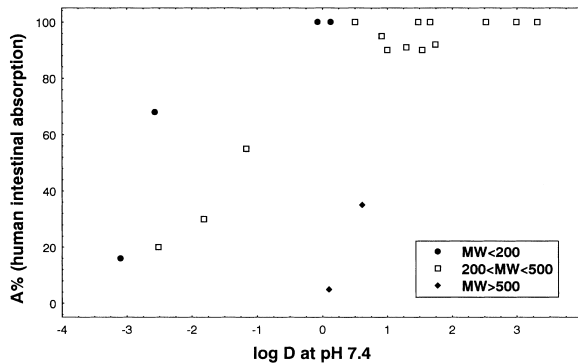
Tab. 3.1 Examples of drugs absorbed by the paracellular route.

Compound	log $D_{7.4}$	Molecular weight	% Absorbed
Nadolol	-2.1	309	13
Sotalol	-1.7	272	100
Atenolol	-1.5	266	51
Practolol	-1.3	266	100
Xamoterol	-1.0	339	9
Amosulalol	-0.8	380	100
Sumatriptan	-0.8	295	60
Pirenzepine	-0.6	351	25
Famotidine	-0.6	338	37
Ranitidine	-0.3	314	50

show high flux rates via the transcellular route and consequently are completely absorbed. Note, however, that lipophilicity correlates with increased metabolic lability and such compounds may have their apparent systemic availabilities decreased by metabolism as they pass through the gut and the liver.

For simple molecules, like β -adrenoceptor antagonists octanol/water log $D_{7.4}$ values are remarkably predictive of absorption potential. Compounds with log $D_{7.4}$ values below 0 are absorbed predominantly by the paracellular route and compounds with log $D_{7.4}$ values above 0 are absorbed by the transcellular route.

Another example of the relationship between log D values and intestinal absorption is taken from reference [1] (see Figure 3.4). Compounds with log $D > 0$ demonstrate a nearly complete absorption. Two exceptions are compounds with a MW above 500. Whether size as such, or the accompanying increase in the number of H-bonds, is responsible for poorer absorption is not fully understood.

**Fig. 3.4** Dependence of oral absorption on log D [1].

However, as the number of H-bonding functions in a molecule rises, octanol/water distribution, in isolation, becomes a progressively less valuable predictor. For such compounds desolvation and breaking of H-bonds becomes the rate-limiting step in transfer across the membrane [7].

Octanol/Cyclohexane Ratio (H-bonding) →

Alkyl Phenyl Halogen (<1)	<i>Tert Amine</i> (2.5) Ester (2.4) Ether (1.8) Ketone (1.8) Nitrile (1.7) Nitro (0.8)	<i>Sec Amine</i> (4.5) <i>Pri Amine</i> (5.1) Amide (8.6) Carboxylate (4.7) Hydroxyl (3.2) Sulphonamide (10.0) Sulphone (4.1) Sulphoxide (3.1)
---	--	---

Fig. 3.5 Raevsky H-bond scores from HYBOT95 (shown in parentheses) and correlation with D_{log} (compare with Figure 1.2 in Chapter 1).

Methods to calculate H-bonding potential range from simple H-bond counts (number of donors and acceptors), through systems that assign a value of 1 for donors and 0.5 for acceptors to sophisticated scoring systems such as the Raevsky H-bond score [8]. The correlation of Raevsky H-bond scores with $\Delta \log D$ shown previously as Figure 1.4 in Chapter 1 (Physicochemistry) is shown as Figure 3.5.

None of these methods gives a perfect prediction, particularly because H-bonding potential needs to be overlaid over intrinsic lipophilicity. For this reason Lipinski's "rule-of-five" becomes valuable in defining the outer limits in which chemists can work [9]. Lipinski defined the boundaries of good absorption potential by demonstrating that poor permeability is produced by:

- more than five H-bond donors (sum of OHs and NHs)
- more than 10 H-bond acceptors (sum of Ns and Os)
- molecular weight over 500
- poor dissolution by $\log P$ over 5

The medicinal chemist can use these rules and understand the boundaries and work towards lowering these values. Figure 3.6 shows a synthetic strategy aimed at removing H-bond donors from a series of endothelin antagonists and a resultant increase in apparent bioavailability as determined by intra-duodenal AUC [10]. Noticeable CLOGP values vary only marginally with the changes in structure, values being 4.8, 5.0, 4.8 and 5.5 for compounds A, B, C and D respectively. In contrast the

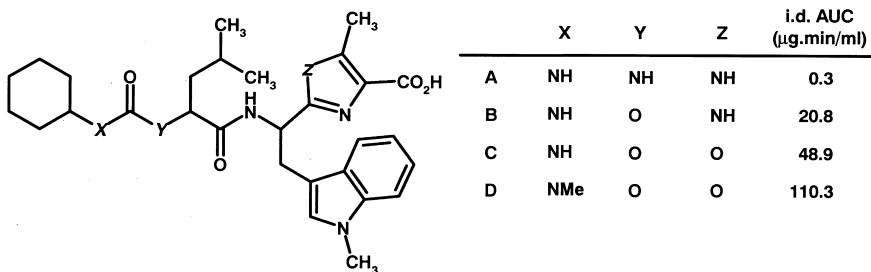
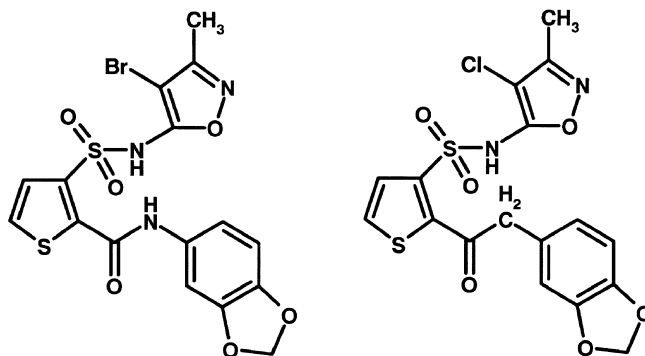


Fig. 3.6 Removal of H-bond donors as a synthetic strategy for a series of azole-containing endothelin antagonists aimed at improving bioavailability by lowering H-bonding potential [10].

Fig. 3.7 Replacement of amide with acetyl in a series of amidothiophenesulfonamide endothelin-A antagonists to improve oral bioavailability [11].



number of H-bond donors is reduced by 3 and the Raevsky score from 28.9 (A) to 21.4 (D).

A similar example, also from endothelin antagonists, is the replacement of the amide group (Figure 3.7) in a series of amidothiophenesulfonamides with acetyl [11]. This move retained *in vitro* potency, but markedly improved oral bioavailability.

3.4

Barriers to Membrane Transfer

The cells of the gastrointestinal tract contain a number of enzymes of drug metabolism and also various transport proteins. Of particular importance in the attenuation of absorption/bioavailability are the glucuronyl and sulphotransferases which metabolize phenol-containing drugs (see below) sufficiently rapidly to attenuate the passage of intact drug across the gastrointestinal tract. Cytochrome P450 enzymes are also present, in particular CYP3A4 (see Chapter 7) and again certain substrates for the drug may be metabolized during passage across the tract. This effect may be greatly enhanced by the action of the efflux pumps, in particular P-glycoprotein. The range of substrates for P-glycoprotein is large but includes a number of relatively large molecular weight drugs which are also CYP3A4 substrates. Cyclosporin A is one example. This drug shows significant attenuation of absorption across the gastrointestinal tract due to metabolism. Metabolism by the gut is greater than many other examples of CYP3A4 substrates. It can be postulated that in effect absorption of the drug is followed by secretion back into the lumen of the gut by P-glycoprotein. This cyclical process effectively exposes cyclosporin A to “multi-pass” metabolism by CYP3A4 and a resultant reduced appearance of intact cyclosporin A in the circulation.

Detailed structure–activity relationships of P-glycoprotein are not yet available. Some understanding is provided by Seelig [12] who has compared structural features in P-glycoprotein substrates. This analysis has indicated that recognition elements are present in structures and are formed by two (type I) or three electron donor groups (type II) with a fixed spatial separation. The type I element consists of two electron donor groups separated by 2.5 Å, whilst the type II elements has a spatial

separation of the outer groups of 4.6 Å. All molecules that are P-glycoprotein substrates contain at least one of these groups and the affinity of the substrate for P-glycoprotein depends on the strength and number of electron donor or hydrogen bond acceptor groups. For the purpose of this analysis all groups with an unshared electron pair on an electronegative atom (O, N, S or F and Cl), or groups with a π -electron orbital of an unsaturated system, were considered as electron donors. However, this analysis did not account for the directionality of the H-bonds.

The dramatic effect of a single unit is shown in Figure 3.8 for a series of beta-adrenoceptor antagonists.

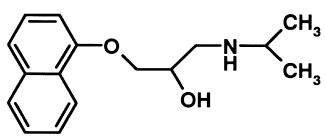
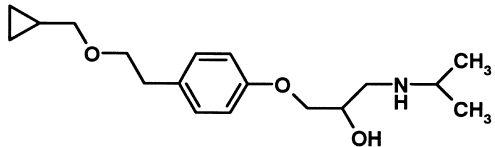
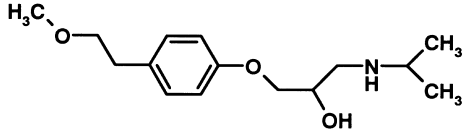
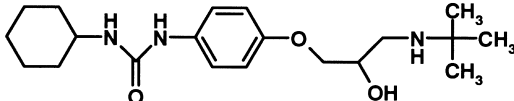
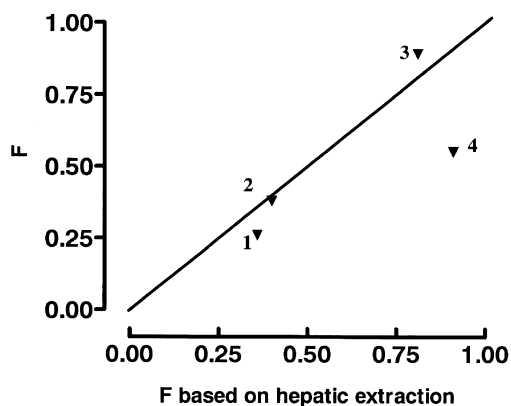
		$E(gi)$	$E(h)$
1		0.10	0.64
2		0.00	0.19
3		0.02	0.60
4		0.36	0.09

Fig. 3.8 Structures of propranolol (**1**), betaxolol (**2**), metoprolol (**3**) and talinolol (**4**) and their respective extraction by the gastrointestinal tract ($E(g. i.)$) and liver $E(h)$

All these compounds are moderately lipophilic and should show excellent ability to cross biological membranes by transcellular absorption. Propranolol, betaxolol and metoprolol all have minimal gut first-pass metabolism, as shown by the low value for $E(g. i.)$. Metabolism and first pass effects for these compounds are largely confirmed to the liver as shown by the values for $E(g. i.)$. In contrast talinolol shows high extraction by the gastrointestinal tract with low liver extraction [13]. These effects are illustrated graphically in Figure 3.9 which shows the bioavailability predicted from hepatic extraction contrasted with that seen *in vivo* in man.

Noticeably propranolol, betaxolol and metoprolol are close or on the borderline for hepatic first-pass effects, whereas talinolol falls markedly below it. Talinolol has been shown to be a substrate for P-glycoprotein [14]. The effect of the urea function is of key importance within this change, as urea lacks a strong type I unit in terms of Seel-

Fig. 3.9 Bioavailability (F) of propranolol (1), betaxolol (2), metoprolol (3) and talinolol (4) found *in vivo* in man compared to that predicted based solely on hepatic extraction.



ig's classification. Other changes in the molecule, such as the tertiary butyl, rather than isopropyl N-substituent are not so important since the related compounds pafenolol and celiprolol (Figure 3.10) also show similar bioavailability.

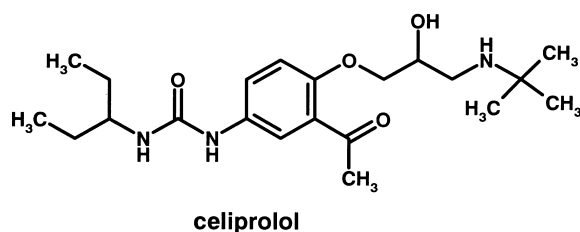
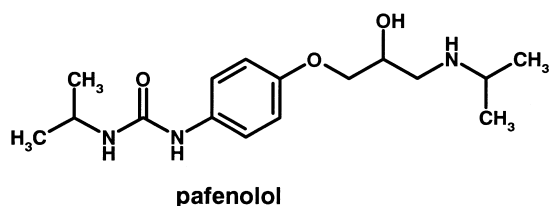


Fig. 3.10 Structures of pafenolol and celiprolol, derivatives of the talinolol (see Figure 3.6) structure which show similar bioavailability characteristics.

These considerations are important in pro-drug design and add to the complexity referred to earlier. Many active principles in pro-drug programmes are non-lipophilic compounds, possessing a number of H-bond donor and acceptor functions (amide or peptide linkages). Addition of a pro-moiety will raise the lipophilicity and molecular weight. In doing so the final molecule may have the required structure to traverse the lipid core of a membrane, but this advantage is lost by it becoming a substrate for efflux. An example (Figure 3.11) of this is the fibrinogen receptor antagonist L-767,679, a low lipophilicity compound ($\log P < -3$) with resultant low membrane flux. The benzyl ester (L-775,318) analogue ($\log P 0.7$) also showed limited absorption, and studies in Caco-2 cells (see Section 3.5) showed the compound to be effluxed by P-glycoprotein [15].

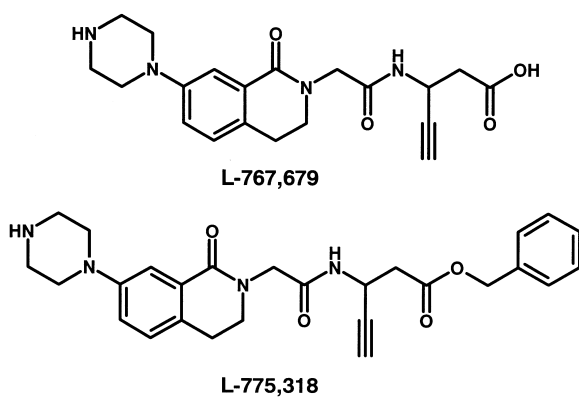


Fig. 3.11 Structures of the fibrinogen receptor antagonist L-767,679 and its benzyl ester (L-775,318) analogue.

3.5

Models for Absorption Estimation

A number of models have been suggested to estimate the absorption potential in humans (see Table 3.2) [16, 17]. These vary from low throughput (*in situ* rat model) to high throughput (*in silico*) models. Most companies will use a combination of these approaches. The human colon adenocarcinoma cell lines Caco-2 and HT-29 are widely used as screening models for absorption [18, 19]. An alternative is offered by the MDCK cell line which is a faster growing cell [20]. These cell lines express typical impediments for absorption such those mentioned above for P-glycoprotein and CYP3A4 isoenzyme. They are thus believed to be a good mimic of the physicochemical and biological barrier of the g. i. tract.

Tab. 3.2 Models for absorption estimation.

-
- *In vivo*
 - *In situ* (rat perfusion)
 - In vitro (Caco-2 and other cell lines; Ussing chamber)
 - Physicochemical properties
 - *In silico* (*in computro*)
-

3.6

Estimation of Absorption Potential

A simple dimensionless number, absorption potential (*AP*), has been proposed to make first approximation predictions of oral absorption (Eq. 3.3) [3].

$$AP = \log P + \log F_{\text{non}} + \log (S_o \cdot V_L/X_o) \quad (3.3)$$

In this equation, $\log P$ is the partition coefficient for the neutral species, $\log F_{\text{non}}$ the fraction of non-ionized compound, S_o the intrinsic solubility, V_L the luminal vol-

ume and X_0 the given dose. By extending this approach the effect of particle size on oral absorption has also been modelled [21].

An approach to estimating the maximum absorbable dose (MAD) in humans is based on Eq. (3.4) [22,23].

$$\text{MAD (mg)} = S \cdot k_a \cdot \text{IFV} \cdot \text{RT} \quad (3.4)$$

S is the solubility in phosphate buffer at the pH 6.5 (in mg mL^{-1}), k_a the absorption rate constant in rats (min^{-1}), IFV is the intestinal fluid volume (250 mL), and RT is the average residence time in the small intestine (270 min).

3.7

Computational Approaches

As mentioned above, hydrogen bonding and molecular size, in combination with lipophilicity have an important influence on oral absorption. A number of methods are available to compute these properties. A further example of the correlation between H-bonding, expressed as polar surface area, is found in Figure 3.12 [24,25]. Such a sigmoidal relationship is found for compounds which are absorbed by passive diffusion only and not hindered by efflux or metabolism, and which are not involved in active uptake. Otherwise deviations will be found [25].

Combination of several descriptors believed to be important for oral absorption have been used in various multivariate analysis studies [26]. The general trend is that a combination of size/shape and a hydrogen bond descriptor, sometimes in combination with $\log D$, has good predictive value. At present such models do not account for the biological function of the membrane, such as P-gp-mediated efflux.

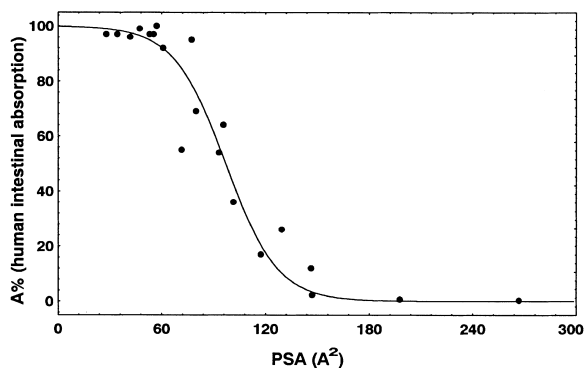


Fig. 3.12 Correlation between polar surface area (PSA) and intestinal absorption [24, 25].

References

- 1 Van de Waterbeemd H, In: *Oral Drug Absorption*. Prediction and Assessment, Dekker, New York, Eds. Dressman J, Lennernäs, H, pp. 31–49.
- 2 Yalkowski SH, Valvani SC, *J. Pharm. Sci.* **1980**, *69*, 912–922.
- 3 Dressman JB, Amidon GL, Fleisher D, *J. Pharm. Sci.* **1985**, *74*, 588–589.
- 4 Amidon GL, Lennernas H, Shah VP, Crison JR, *Pharm. Res.* **1995**, *12*, 413–420.
- 5 Vacca JP, Dorsey BD, Schleif WA, Levin RB, McDaniel SL, Darke PL, Zugay J, Quintero JC, Blahy OM, Roth E, Sardana VV, Schlabach AJ, Graham PI, Condra JH, Gotlib L, Holloway MK, Lin J, Chen I-W, Vastag K, Ostovic D, Anderson PS, Emmini EA, Huff JR, *Proc. Natl Acad. Sci. USA* **1994**, *91*, 4096–4100.
- 6 Macheras P, Reppas C, Dressman JB (Eds) *Biopharmaceutics of Orally Administered Drugs*, Ellis Horwood, London, **1995**.
- 7 Conradi RA, Burton PS, Borchardt RT, In: *Lipophilicity in Drug Action and Toxicology* (Eds Pliska V, Testa B, Van de Waterbeemd H), pp. 233–252. VCH, Weinheim, **1996**.
- 8 Raevsky OA, Grifor'ev VY, Kireev DB, Zefirov, NS, *Quant. Struct. Activity Relat.* **1992**, *14*, 433–436.
- 9 Lipinski CA, Lombardo F, Dominy BW, Feeney PJ, *Adv. Drug Del. Rev.* **1997**, *23*, 3–25.
- 10 Von Geldern TW, Hoffman DJ, Kester JA, Nellans HN, Dayton BD, Calzadilla SV, Marsch KC, Hernandez L, Chiou W, *J. Med. Chem.* **1996**, *39* 982–991.
- 11 Wu C, Chan MF, Stavros F, Raju B, Okun I, Mong S, Keller KM, Brock T, Kogan TP, Dixon RAF, *J. Med. Chem.* **1997**, *40*, 1690–1697.
- 12 Seelig A, *Eur. Biochem.* **1998**, *251*, 252–261.
- 13 Travsch B, Oertel R, Richter K, Gramatt T, *Biopharm. Drug Dispos.* **1995**, *16*, 403–414.
- 14 Spahn-Langguth H, Baktir G, Rad-schuweit A, Okyar A, Terhaag B, Ader P, Hanafy A, Langguth P, *Int. J. Clin. Pharmacol. Ther.* **1998**, *36*, 16–24.
- 15 Prueksaitanont T, Deluna P, Gorham LM, Bennett MA, Cohn D, Pang J, Xu X, Leung K, Lin JH, *Drug Metab. Dispos.* **1998**, *26*, 520–527.
- 16 Borchardt RT, Smith PL, Wilson G, (Eds) *Models for Assessing Drug Absorption and Metabolism*. Plenum Press, New York, **1996**.
- 17 Barthe L, Woodley J, Houin G, *Fund. Clin. Pharmacol.* **1999**, *13*, 154–168.
- 18 Hidalgo IJ, In: *Models for Assessing Drug Absorption and Metabolism* (Eds Borchardt RT, Smith PL, Wilson G), pp. 35–50. Plenum Press, New York, **1996**.
- 19 Artursson P, Palm K, Luthman K, *Adv. Drug Deliv. Rev.* **1996**, *22*, 67–84.
- 20 Irvine JD, Takahashi L, Lockhart K, Cheong J, Tolan JW, Selick HE, Grove JR, *J. Pharm. Sci.* **1999**, *88*, 28–33.
- 21 Oh D-M, Curl RL, Amidon GL, *Pharm. Res.* **1993**, *10*, 264–270.
- 22 Johnson KC, Swindell AC, *Pharm. Res.* **1996**, *13*, 1794–1797.
- 23 Lombardo F, Winter SM, Tremain L, Lowe III JA, In: *Integration of Pharmaceutical Discovery and Development: Case Studies* (Eds Borchardt RT et al.), pp. 465–479. Plenum Press, New York, **1998**.
- 24 Palm K, Luthman K, Ungell A-L, Strandlund G, Beigi F, Lundahl P, Artursson P, *J. Med. Chem.* **1998**, *41*, 5382–5392.
- 25 Clark DE, *J. Pharm. Sci.* **1999**, *88*, 807–814.
- 26 Van de Waterbeemd H, In: *Pharmacokinetic Optimization in Drug Research: Biological, Physicochemical and Computational Strategies* (Eds Testa B, Van de Waterbeemd H, Folkers G, Guy R), Verlag HCA, Basel, **2001**, pp. 499–511.

4

Distribution

Abbreviations

CNS Central nervous system

Symbols

Cl_p Plasma clearance
 Cl_u Unbound clearance of free drug
 $\Delta \log P$ Difference in $\log P$ values in octanol and cyclohexane
 H-bond Hydrogen bond
 k_{el} Elimination rate constant
 $\log D_{7.4}$ Distribution coefficient at pH 7.4 (usually octanol/water)
 $\log P$ Partition coefficient (usually octanol)
 pK_a Ionization constant
 T_{max} Time to maximum observed plasma concentration
 $Vd_{(f)}$ Unbound volume of distribution of the free drug

4.1

Membrane Transfer Access to the Target

Distribution of drugs across the membranes of the body can be regarded as passive diffusion. Similar considerations to those already outlined for oral absorption apply, although for significant penetration to intracellular targets the aqueous pore pathway does not readily apply. Similarly, as previously outlined the tight junctions of the capillaries supplying the CNS render the paracellular pathway very inefficient. These aspects of distribution were also described in Section 2.10, concerning the unbound drug model and barriers to equilibrium. Figure 4.1 depicts a scheme for the distribution of drugs. Penetration from the circulation into the interstitial fluid is rapid for all drugs since the aqueous pores present in capillary membranes have a mean diameter of between 50–100 Å. Thus there is ready access to targets located at the surface of cells such as G-protein coupled receptors. The exception to this is the cerebral capillary network, since here there is a virtual absence of pores due to the continuous tight intercellular junctions. For intracellular targets, if only the free drug is

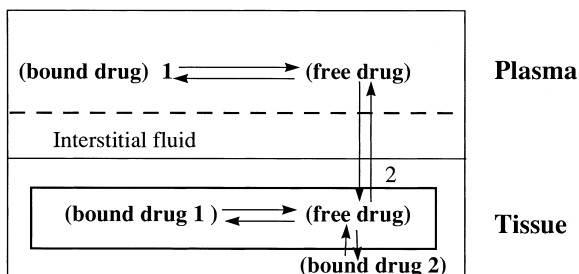


Fig. 4.1 Schematic illustrating drug distribution. Drug is present in the circulation as either free or bound, only the free drug is available for distribution, bound drug 1 in tissues is the drug bound to intracellular proteins and constituents, bound drug 2 is that bound to the cell and intracellular membranes.

considered, then at steady state the concentrations present inside the cell and in the circulation should be similar for a drug that readily crosses the cell membrane.

The overall amount of drug present in a tissue is determined by the amount that is bound either to intracellular proteins or, as discussed below, to the actual cell membranes themselves. Albumin is present in many tissues and organs and is available to bind drugs. Other intracellular proteins that can bind drugs include ligandin, present in liver, kidney and intestine, myosin and actin in muscular tissue and melanin in pigmented tissue, particularly the eye. Normally, as previously discussed, the free drug is that which determines the pharmacological activity. Note also, as previously stated, that the concentration of free drug in the circulation depends at steady state on free drug clearance and not the extent of plasma protein or even blood binding. In certain instances, as will be highlighted later, certain toxicities can derive directly due to membrane interactions (disruption, phospholipidosis, etc.). Key factors which determine the ease of crossing cell membranes are, lipophilicity, as defined by partition coefficient, hydrogen bonding capacity [1] and molecular size [2]. For simple small molecules with a minimum of nitrogen- or oxygen-containing functions, a positive $\log D$ value is a good indicator of ability to cross the membrane. For more complex molecules, size and H-bonding capacity become important.

4.2

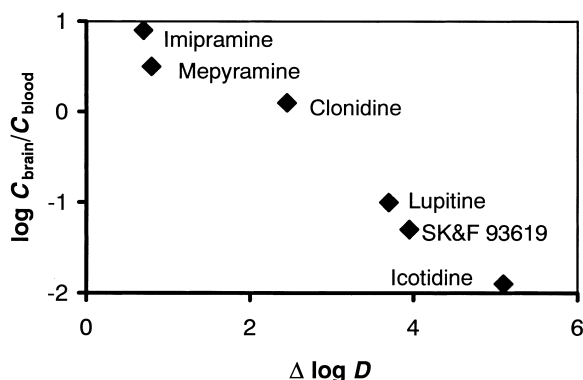
Brain Penetration

The work of Young *et al.* [1] provides a classic example of the role of increased H-bonding potential in preventing access to the CNS (crossing capillary and astrocyte cell membranes; Figure 4.2). In this example $\Delta \log P$ provided a measure of H-bonding potential.

Much of the data produced in studies such as this has measured the partitioning of drugs into whole brain from blood or plasma. The importance of lipophilicity in brain distribution has therefore been highlighted in many reviews [3,4], however the majority of these have concentrated on total drug concentrations which, given the lipid nature of brain tissue, over-emphasizes the accumulation of lipophilic drugs.

Whilst giving some ideas of the penetration into the brain, such data are limited in understanding the CNS activity of drugs. Whole brain partitioning actually repre-

Fig. 4.2 Penetration of anti-histamine compounds into the CNS correlated with $\Delta \log P$ ($\log P_{\text{cyclohexane}} - \log P_{\text{octanol}}$) as a measure of hydrogen bonding potential.



sents partitioning into the lipid of the brain, and not actually access to drug receptors. For instance, desipramine partitions into brain and is distributed unevenly [5]. The distribution corresponds to lipid content of the brain regions and not to specific desipramine binding sites. Thus correlations such as those above describe the partitioning of the drug into lipid against the partitioning of the drug into model lipid. For receptors such as 7TMs ECF concentrations determine activity. The ECF can be considered as the aqueous phase of the CNS. CSF concentrations can be taken as a reasonable guide of ECF concentrations. The apparent dramatic differences in brain distribution described for total brain, as shown above (three to four orders of magnitude), collapse to a small ratio when the free (unbound) concentration of drug in plasma is compared to the CSF concentration. Whole brain/blood partitioning reflects nothing but an inert partitioning process of drug into lipid material.

The lack of information conveyed by total brain concentration is indicated by studies on KA-672 [6], a lipophilic benzopyranone acetylcholinesterase inhibitor. The compound achieved total brain concentrations of $0.39 \mu\text{M}$ at a dose of 1 mg kg^{-1} equivalent to the IC_{50} determined *in vitro* ($0.36 \mu\text{M}$). Doses up to 10 mg kg^{-1} were without pharmacological effect. Analysis of CSF indicated concentrations of the compound were below $0.01 \mu\text{M}$ readily explaining the lack of activity. These low concentrations are presumably due to high (unbound) free drug clearance and resultant low concentrations of free drug in the plasma (and CSF).

Free unbound drug partitioning actually reflects the fact that the drug is reaching the receptor and is having a pharmacological effect. Unless active transport systems are invoked the maximum CSF to plasma partition coefficient is 1. This should be contrasted to the 100- or 1000-fold affinity of total brain compared to blood or plasma. The minimum partitioning based on a limited data set appears to be 0.1. Figure 4.3 compares lipophilicity ($\log D$) in a series of diverse compounds that illustrate the limited range of partitioning. It should be noted that the term $\log D$ is not a perfect descriptor and some of the measures which incorporate size and hydrogen bonding may be better. Clearly though, the CNS is more permeable than imagined, allowing drugs such as sulpiride (Figure 4.3) to be used for CNS applications.

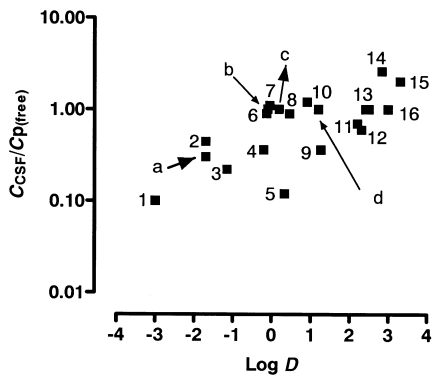


Fig. 4.3 CSF concentration/free (unbound) plasma concentration ratios for neutral and basic drugs: 1, ritropirronium; 2, atenolol; 3, sulpiride; 4, morphine; 5, cimetidine; 6, metoprolol; 7, atropine; 8, tacrine; 9, digoxin; 10, propranolol; 11, carbamazepine; 12, ondansetron; 13, diazepam; 14, imipramine; 15, digitonin; 16, chlorpromazine and acidic drugs, a, salicylic acid; b, ketoprofen; c, oxyphenbutazone and d, indomethacin compared to log *D*.

The use of microdialysis has enabled unbound drug concentrations to be determined in ECF, providing another measurement of penetration across the blood–brain barrier and one more closely related to activity. A review of data obtained by microdialysis [7], showed that free drug exposure in the brain is equal to or less than free drug concentration in plasma or blood, with ratios ranging from 4% for the most polar compound (atenolol) to unity for lipophilic compounds (e.g. carbamazepine). This largely supports the similar conclusions from the CSF data shown above. This relationship is illustrated in Figure 4.4.

Somewhat surprisingly, microdialysis has also revealed that the time to maximum concentration (T_{max}) within the CNS is close to the T_{max} value in blood or plasma, irrespective of lipophilicity. For example, the CNS T_{max} for atenolol ($\log D_{7.4} = -1.8$) occurs at 2 min in the rat after intravenous administration [8]. In addition the rate of elimination (half-life) of atenolol and other polar agents from the CNS is similar to that in plasma or blood. The implication of these data is that poorly permeable drugs do not take longer to reach equilibrium with CNS tissue than more lipophilic agents

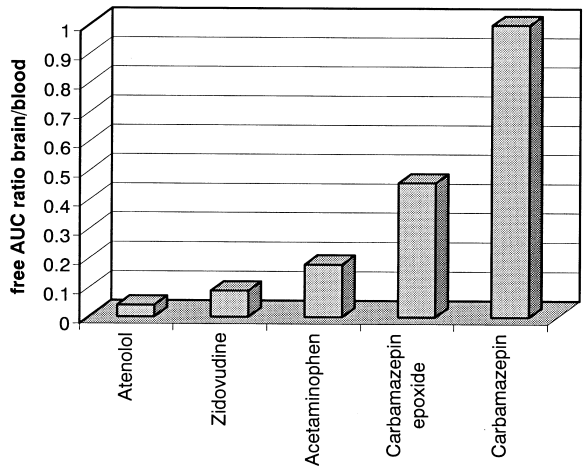
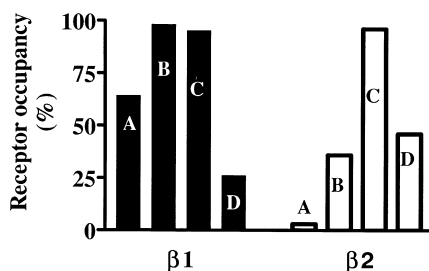


Fig. 4.4 Relationship between lipophilicity and CNS penetration expressed as free drug AUC ratio in brain to blood (data from reference [16]).

as might be assumed. To explain these observations, it has been postulated that non-passive transport (i.e. active) processes play a role in determining CNS exposure [7].

The fact that hydrophilic compounds have ready access to the CNS, albeit up to 10-fold lower than lipophilic compounds, is not generally appreciated. In the design of drugs selectivity over the CNS effects has sometimes relied on making compound hydrophilic. Clearly this will give some selectivity (up to 10-fold), although this may not be sufficient. For instance β -adrenoceptor antagonists are known to cause sleep disorders. In four drugs studied the effects were lowest with atenolol ($\log D = -1.6$), intermediate with metoprolol ($\log D = -0.1$), and highest with pindolol ($\log D = -0.1$) and propranolol ($\log D = 1.2$). This was correlated with the total amount present in brain tissue [9], which related to the $\log D$ values. Further analysis of this data [10] using CSF data and receptor affinity to calculate receptor occupancy, demonstrated that there was high occupation of the β_1 central receptor for all drugs. Propranolol showed a low occupancy, possibly because the active 4-hydroxy metabolite is not included in the calculation. In contrast, occupation of the β_2 central receptor correlated well with sleep disturbances. The incidence of sleep disturbances is therefore not about penetration into the CNS but the β_1/β_2 selectivity of the compounds (atenolol > metoprolol > pindolol = propranolol). The relative receptor occupancies are illustrated in Figure 4.5.

Fig. 4.5 Central receptor occupancy after oral administration of β -adrenoceptor antagonists: A, atenolol; B, metoprolol; C, pindolol; D, propranolol. The high occupancy of β_1 receptors does not correlate with physicochemical properties (lipophilicity). The occupation of β_2 receptors correlates with sleep disturbances and the intrinsic selectivity of the compounds.



For a small drug molecule, penetration into the target may often be easier to achieve than duration of action. Assuming duration of action is linked to drug half-life, then distribution as outlined below can be an important factor.

4.3

Volume of Distribution and Duration

The volume of distribution of a drug molecule is, as described previously, a theoretical number that assumes the drug is at equal concentration in the tissue and in the circulation and represents what volume (or mass) of tissue is required to give that concentration. Volume of distribution, therefore, provides a term that partially reflects tissue affinity. However, it is important to remember that affinity may vary between different tissues and a moderate volume of distribution may reflect moderate concentrations in many tissues or high concentrations in a few. For an illustration of

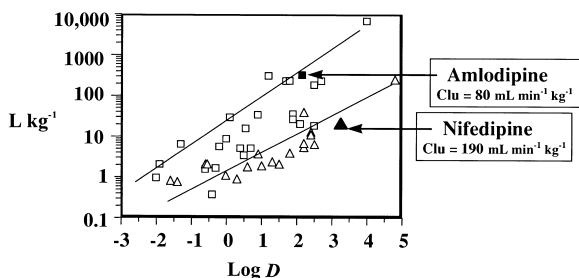


Fig. 4.6 Free (unbound) volumes of distribution of neutral (triangles) and basic (squares) drugs, also indicating amlodipine and nifedipine together with their free (unbound) clearance value (Cl_u).

how the manipulation of distribution affects systemic concentration the following examples will use free volume rather than total, although either could equally apply.

Taking the simplest case of neutral drugs, where increasing $\log D_{7.4}$ reflects increased binding to constituents of blood and cells and increased partitioning of drugs into membranes, there is a trend for increasing volume of distribution with increasing lipophilicity (Figure 4.6). In this case, for uncharged neutral molecules, there are no additional ionic interactions with tissue constituents. In most cases, the volume of distribution is highest for basic drugs ionized at physiological pH, due to ion-pair interactions between the basic centre and the charged acidic head groups of phospholipid membranes as described previously.

This ion pairing for basic drugs results in high affinity and also ensures that the ionized fraction of the drug is the predominant form within the membrane. This is particularly important, since most alkylamines have pK_a values in the range 8-10 and are thus, predominantly in ionized form at physiological pH. The increase in volume for basic drugs is also illustrated in Figure 4.6.

The importance of volume of distribution is in influencing the duration of the drug effect. Since half-life ($0.693/k_{el}$ where k_{el} is the elimination rate constant) is determined by the volume of distribution and the clearance ($Cl_u = Vd_{(f)} \times k_{el}$), manipulation of volume is an important tool for changing duration of action. Here the small amount of drug in the circulation is important, since this is the compound actually passing through and hence available to the organs of clearance (liver and kidney). Incorporation of a basic centre into a neutral molecule is therefore a method of increasing the volume of distribution of a compound. An example of this is the discovery of the series of drugs based on rifamycin SV (Figure 4.7). This compound was one of the first drugs with high activity against *Mycobacterium tuberculosis*. Its clinical performance [11], however, was disappointing due to poor oral absorption (dissolution) and very short duration ascribed at the time to rapid biliary elimination (clearance).

Many different analogues were produced, including introduction of basic functions with a goal of increased potency, solubility, and reduction in clearance. Rifampicin is a methyl-piperazinyl amino methyl derivative [12] with much better duration and has become a successful drug. The basic functionality however does not alter clearance but increases volume substantially (Figure 4.7). Duration is enhanced further [12] by the more basic spiropiperidyl analogue, rifabutin (Figure 4.7). Again

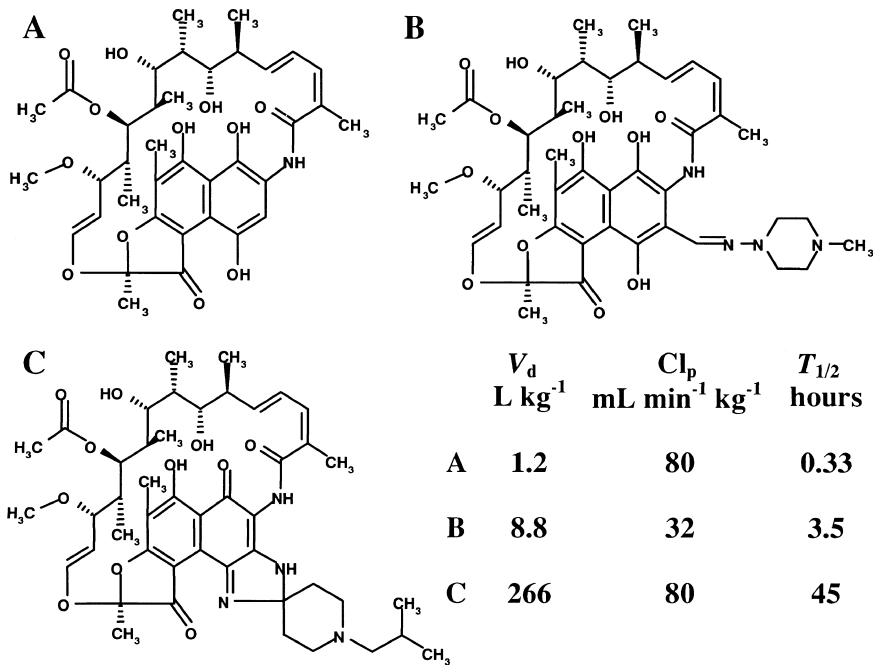


Fig. 4.7 Structures of (A) rifamycin, (B) rifampicin and (C) rifabutin, together with their pharmacokinetic properties. Volume of distribution (V_d) and plasma clearance (Cl_p) are for free unbound drug.

the desirable pharmacokinetic (and pharmacodynamic) properties are due to effects on volume of distribution rather than effects on clearance.

This strategy of modification of a neutral molecule by addition of basic functionality was employed in the discovery of the dihydropyridine calcium channel blocker, amlodipine. The long plasma elimination half-life (35 h) of amlodipine (Figure 4.8) is due, in large part, to its basicity and resultant high volume of distribution [13].

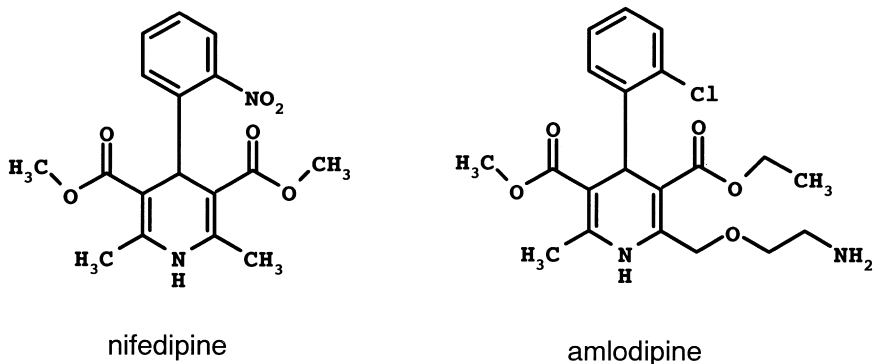


Fig. 4.8 Structures of the dihydropyridine calcium channel blockers, nifedipine (neutral) and amlodipine (basic).

These pharmacokinetic parameters are unique among dihydropyridine calcium channel blockers and allow once-a-day dosing of amlodipine, without the need for sustained release technology. The large volume of distribution is achieved despite the moderate lipophilicity of amlodipine and can be compared to the prototype dihydropyridine drug, nifedipine which is of similar lipophilicity but neutral (Figure 4.8). Notably, these changes in structure do not trigger a large change in clearance. The high tissue distribution of amlodipine is unique amongst dihydropyridine drugs, and has been ascribed to a specific ionic interaction between the protonated amino function and the charged anionic oxygen of the phosphate head groups present in the phospholipid membranes [14] and is as described previously in Chapter 1 (Physicochemistry).

Another basic drug where minor structural modification results in a dramatic increase in volume of distribution is the macrolide antibiotic, azithromycin. The traditional agent in this class is erythromycin, which contains one basic nitrogen, in the sugar side-chain.

Introduction of a second basic centre into the macrolide aglycone ring in azithromycin increases the free (unbound) volume of distribution from 4.8 to 62 L kg⁻¹ (Figure 4.9). Free (unbound) clearance of the two compounds is also changed from 55 mL min⁻¹ kg⁻¹ for erythromycin to 18 mL min⁻¹ kg⁻¹ for azithromycin. The apparent plasma elimination half-life is, therefore, increased from 3 to 48 h. One consequence of the high tissue distribution of azithromycin is that the plasma or blood concentrations do not reflect tissue levels, which may be 10- to 100-fold higher, compared to only 0.5- to 5-fold higher for erythromycin. Azithromycin readily enters macrophages and leukocytes and is, therefore, particularly beneficial against intracellular pathogens. Elimination of azithromycin is also prolonged with reported tissue half-life values of up to 77 h [15]. Overall, the pharmacokinetic properties of azithromycin provide adequate tissue concentrations on a once-daily dosing regimen and provide wide therapeutic applications. The high and prolonged tissue concentrations of azithromycin achieved provide a long duration of

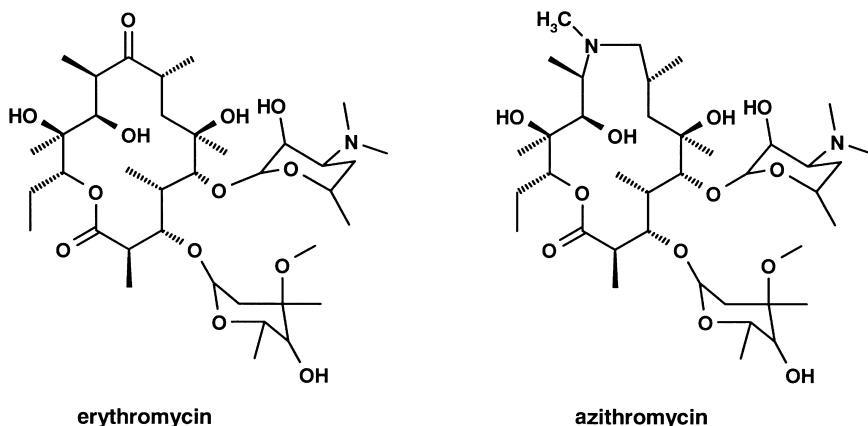


Fig. 4.9 Structures of the macrolide antibiotics, erythromycin (mono-basic) and azithromycin (dibasic).

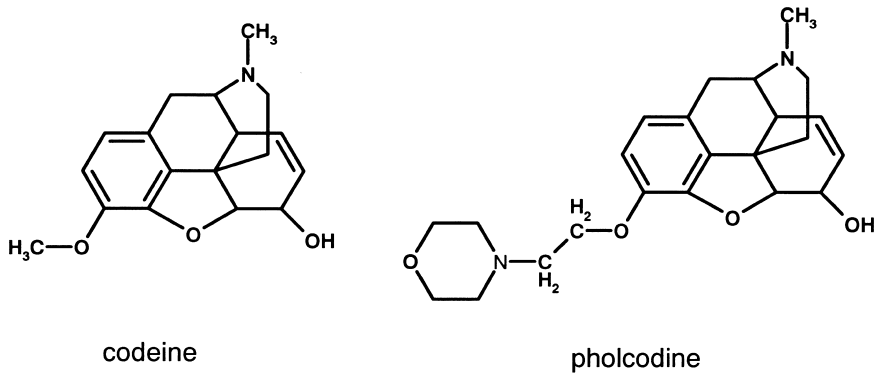


Fig. 4.10 Structures of codeine (monobasic) and pholcodine (dibasic).

action. Only 3–5-day courses of treatment are therefore required, hence improving patient compliance to complete the course and reducing the development of resistance [15].

A similar example to azithromycin, but in a small molecule series is pholcodine (Figure 4.10), where a basic morpholino side chain replaces the methyl group of codeine. Unbound clearance is essentially similar ($10 \text{ mL min}^{-1} \text{ kg}^{-1}$) but the free unbound volume is increased approximately 10-fold (4 to 40 L kg^{-1}) with a corresponding increase in half-life (3 to 37 h) [16].

High accumulation of drug in tissues has also been implicated in the seven-fold longer elimination half-life of the dibasic antiarrhythmic, disobutamide (Figure 4.11) compared to the monobasic agent, disopyramide. The elimination half-life of disobutamide is 54 h compared to approximately 7 h for disopyramide.

Disobutamide has been shown to accumulate extensively in tissues in contrast to disopyramide [17].

It is important to note that in these latter two examples, the high tissue affinity of the well-tolerated, anti-infective, azithromycin, is viewed as a pharmacokinetic advantage, while similar high tissue affinity is viewed as disadvantageous for the antiarrhythmic, disobutamide, which has a low safety margin. Obviously, different therapeutic areas impose different restrictions on the ideal pharmacokinetic profile for management of each condition, hence careful consideration should be paid to this at an early stage in drug discovery programmes.

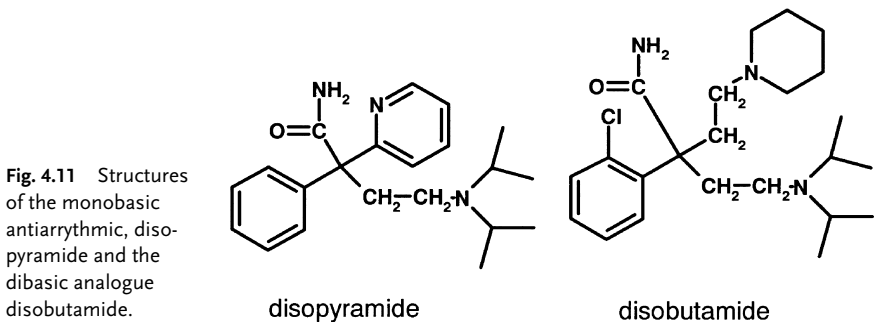


Fig. 4.11 Structures of the monobasic antiarrhythmic, disopyramide and the dibasic analogue disobutamide.

4.4

Distribution and T_{\max}

It has been postulated that high tissue distribution of drugs can lead to a delayed T_{\max} (time to maximum plasma concentration) after oral administration. Amlodipine (Figure 4.5), has a typical T_{\max} value of 6 to 9 h following an oral dose. Given the excellent physicochemical properties (moderately lipophilic and good solubility) of this molecule, slow absorption across the membranes of the gastrointestinal tract is unlikely. In addition the compound appears to be more rapidly absorbed in patients with hepatic impairment with a mean T_{\max} value of 3.8 versus 6.8 h [18]. The apparent slow absorption has been attributed to the considerable partitioning of drugs like amlodipine into the initial tissue beds encountered followed by a slower redistribution. After oral dosing the major tissue bed is the liver. The intrinsic high tissue distribution of amlodipine is reflected in a volume of distribution of 21 L kg^{-1} [19]. Amlodipine, which is a relatively low clearance compound, is thus taken up extensively into the liver and then slowly redistributed back out, thus delaying the time to the maximum observed concentration in the systemic circulation (T_{\max}). In the patients with hepatic impairment, the presence of hepatic shunts (blood vessels bypassing the liver), decreases the exposure of the compound to liver tissue and hence reduces T_{\max} . Studies with isolated rat livers indicated that the apparent volume of distribution in the liver exceeded 100 mL g^{-1} tissue [20] demonstrating very high affinity for this tissue.

This postulated phenomenon can have the beneficial effect of reducing the likelihood of systemic side-effects by effectively buffering the rate at which the drug enters the systemic circulation and hence reducing peak-to-trough variations in concentration. Conversely, high affinity for liver tissue may increase exposure to the enzymes of clearance and may therefore attenuate the first-pass extraction of drugs.

References

- 1 Young, RC, Mitchell RC, Brown TH, Ganellin CR, Griffiths R, Jones M, Rana KK, Saunders D, Smith IR, Sore NE, Wilks TJ, *J. Med. Chem.* **1988**, *31*, 656–671.
- 2 Van de Waterbeemd H, Camenisch G, Folkers G, Chrétien JR, Raevsky OA, *J. Drug Target.* **1998**, *6*, 151–165.
- 3 Brodie BB, Kurz H, Schanker LS, *J. Pharmacol. Exp. Ther.* **1960**, *130*, 20–25.
- 4 Hansch C, Bjorkroth JP, Leo A, *J. Pharm. Sci.* **1987**, *76*, 663–687.
- 5 Wladyslaw D, Leokadia D, Lucyna J, Halina N, Mirosława M, *J. Pharm. Pharmacol.* **1991**, *43*, 31–35.
- 6 Hilgert M, Noldner M, Chatterjee SS, Klein J, *Neurosci. Lett.* **1999**, *263*, 193–196.
- 7 Hammarlund-Udenaes M, Paalzow LK, de Lange ECM, *Pharm. Res.* **1997**, *14*, 128–134.
- 8 De Lange ECM, Danhof M, deBoer AG, Breimer DD, *Brain Res.* **1994**, *666*, 1–8.
- 9 McAinsh J, Cruickshank JM, *Pharm. Ther.* **1990**, *46*, 163–197.
- 10 Yamada YF, Shibuya J, Hamada J, Shawada Y, Iga T, *J. Pharmacokinetic. Biopharm.* **1995**, *23*, 131–145.
- 11 Bergamini N, Fowst G, *Arzneimittel-Forsch.* **1965**, *15*, 951–1002.
- 12 Benet LZ, Oie S, Schwartz JB, In: *Goodman and Gilman's The Pharmacological Basis for Therapeutics*, pp. 1707–1792. McGraw-Hill, New York, **1995**.
- 13 Smith DA, Jones BC, Walker DK, *Med. Res. Rev.* **1996**, *16*, 243–266.
- 14 Mason RP, Rhodes DG, Herbert LG, *J. Med. Chem.* **1991**, *34*, 869–877.
- 15 Foulds G, Shepard RM, Johnson RB, *J. Antimicrob. Chemother.* **1990**, *25* (Suppl. A), 73–82.
- 16 Fowle WA, Butz ASE, Jones EC, Waetherly BC, Welch RM, Posner J, *Br. J. Clin. Pharmacol.* **1986**, *22*, 61–71.
- 17 Cook CS, McDonald SJ, Karim A, *Xenobiotica*, **1993**, *23*, 1299–1309.
- 18 Humphrey MJ, Smith DA, *Br. J. Clin. Pharmacol.* **1992**, *33*, 219P.
- 19 Faulkner JK, McGibney D, Chasseaud LF, Perry JL, Taylor IW, *Br. J. Clin. Pharmacol.* **1986**, *22*, 21–25.
- 20 Walker DK, Humphrey MJ, Smith DA, *Xenobiotica*, **1994**, *24*, 243–250.

5

Clearance

Abbreviations

ATP	Adenosine triphosphate
BTL	Bilitranslocase
CYP450	Cytochrome P450
MOAT	Multiple organic acid transporter
MRP	Multi-drug resistance protein
Natp	Sodium dependent acid transporter protein
OATP	Organic acid transport protein
OCT1	Organic cation transporter 1
OCT2	Organic cation transporter 2
P-gp	P-glycoprotein
TxRA	Thromboxane receptor antagonist
TxSI	Thromboxane synthase inhibitor

Symbols

Cl	Clearance
$\log D_{7.4}$	Distribution coefficient (octanol/buffer) at pH 7.4
$t_{1/2}$	Elimination half-life
V_d	Volume of distribution

5.1

The Clearance Processes

Clearance of drug normally occurs from the liver and kidneys and it is an important assumption that only free (i. e. not protein bound) drug is available for clearance. A diagram of the interaction of the major clearance processes is shown in Figure 5.1.

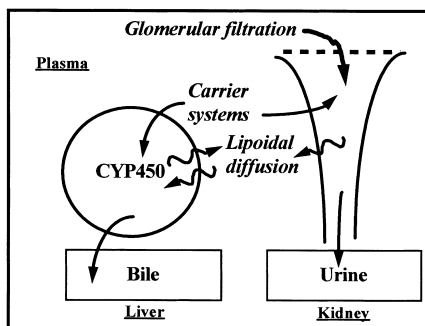


Fig. 5.1 Schematic illustrating the interplay of hepatic and renal clearance processes.

5.2

Role of Transport Proteins in Drug Clearance

For hepatic clearance, passive diffusion through the lipid core of the hepatocyte membranes (available only to lipophilic drugs) is augmented by sinusoidal carrier systems, particularly for ionized molecules (either anionic or cationic) of molecular weights above 400. The presence of these carrier systems provides access to the interior of the hepatocyte to drugs with a wide range of physicochemical properties, ranging from hydrophilic to lipophilic. A schematic illustrating the role of these transport systems both into and out of the liver is shown in Figure 5.2. The transporters exist on the sinusoid face to remove drugs from the blood and transport them into the interior of the hepatocyte [1].

Likewise a different family of transporters exists on the canalicular face to transport drugs or their metabolites into bile. This complex system was originally termed biliary clearance but it is really two separate processes, hepatic uptake and biliary excretion. With small sized lipophilic drugs that readily traverse membranes hepatic uptake is probably not a major factor, since even if compounds are substrates, rapid redistribution across the membrane can occur. With higher molecular weight compounds (molecular weight greater than about 500) and those containing considerable H-bonding functionality (i.e. those that do not readily cross membranes) hepat-

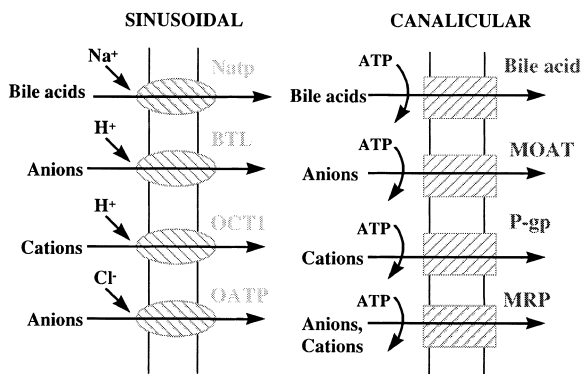


Fig. 5.2 Schematic showing key sinusoidal and canalicular transport proteins and their substrate characteristics.

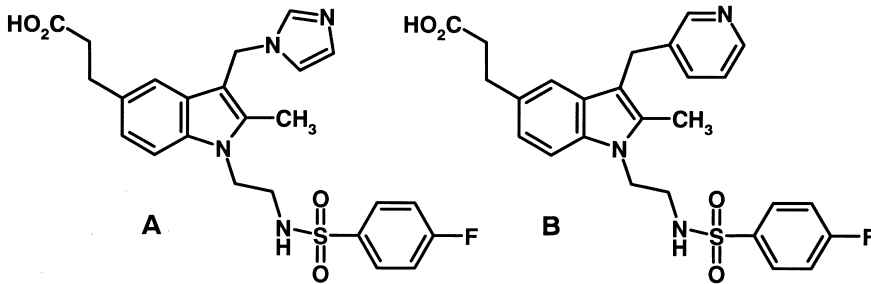


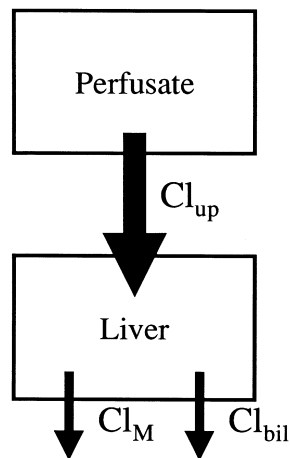
Fig. 5.3 Structures of two combined TxSI/TxRAs subject to high hepatic extraction by sinusoidal transport systems.

ic uptake can become the key clearance process, even if metabolism occurs subsequent to this. Figure 5.3 shows the structure of two combined thromboxane synthase inhibitors/thromboxane A_2 receptor antagonists (TxSI/TxRAs). Both compounds show high hepatic extraction ($E = 0.9$) in the isolated perfused rat liver [2].

Compound A appears mainly as unchanged drug in the bile whereas compound B appears partly as metabolites. Administration of ketoconazole, a potent cytochrome P450 inhibitor, to the preparation dramatically decreases the metabolism of B and the compound appears mainly as unchanged material in the bile. Despite the inhibition of metabolism, hepatic extraction remains high (0.9). This indicates that clearance is dependent on hepatic uptake, via a transporter system, for removal of the compounds from the circulation. Metabolism of compound B is a process that occurs subsequent to this rate-determining step and does not influence overall clearance. This model for the various processes involved in the clearance of these compounds is illustrated in Figure 5.4.

The affinity of compounds for the various transporter proteins vary, but charge, molecular weight and additional H-bonding functionality seem to be particularly important.

Fig. 5.4 Model for the hepatic processes involved in the clearance of the combined TxSI/TxRAs (see Figure 5.3). The clearance by hepatic uptake (Cl_{up}) is the rate-determining step in the removal of the compound from the perfusate. Compounds accumulate within the liver and are subsequently cleared by biliary (Cl_{bil}) or metabolic clearance (Cl_M) (modified from reference [2]).



Lipophilic drugs are metabolized by intracellular membrane-bound enzyme systems (e. g. cytochrome P450s and glucuronyl transferases) to more water soluble derivatives. The active sites of the major forms of the cytochrome P450 superfamily rely heavily on hydrophobic interactions with their substrates, although ion-pair and hydrogen bonding interactions also occur. Exit from the hepatocyte may be by simple passive diffusion back into the plasma or as outlined above via canalicular active transport systems which excrete drugs and their metabolites, again with wide ranging physical properties, into the bile.

5.3

Interplay Between Metabolic and Renal Clearance

Small molecules, with relatively low molecular weight, will appear in the urine due to glomerular filtration. The secretion of drugs into the urine can also occur through tubular carrier systems similar to those present on the sinusoid face of the hepatocyte. For instance, of the carriers illustrated in Figure 5.2, Natp, OATP and OCT1 are also present in the kidney. In addition another organic cation transporter, OCT2, is also present. There is also a vast difference in the volume of fluid formed at the glomerulus each minute and the amount that arrives during the same period at the collecting tubule. The aqueous concentration processes that occur in the kidney mean that for drugs capable of travelling through the lipid core of the tubule membrane, significant reabsorption back into the plasma will occur. The end result of this process is that only hydrophilic molecules are voided in the urine to any substantial degree. This interaction between metabolism and renal clearance can be illustrated by following the fate of the cholinesterase inhibitor SM-10888 [3]. A number of metabolism processes occur on the lipophilic parent molecule involving phase 1 oxidation and phase 2 conjugation reactions. Some of these processes occur sequentially as illustrated in Figure 5.5.

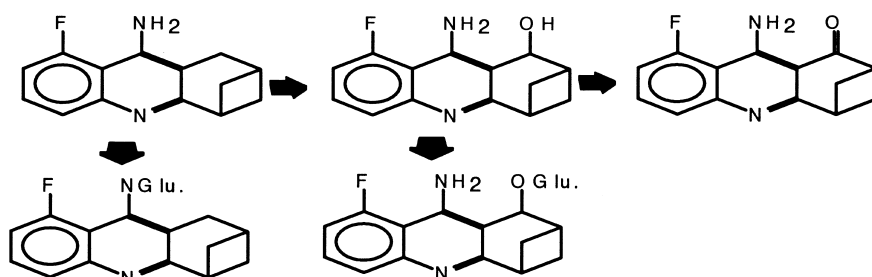


Fig. 5.5 Metabolism of SM-10888, involving phase 1 and phase 2 metabolic processes.

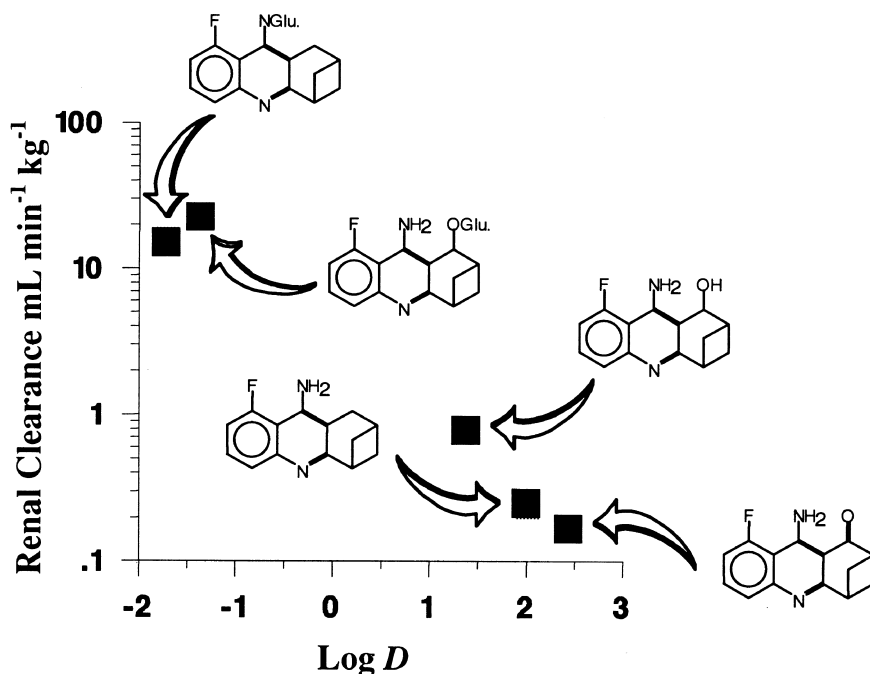


Fig. 5.6 Relationship between lipophilicity and renal clearance for SM-10888 and its metabolites.

5.4

Role of Lipophilicity in Drug Clearance

Most of these steps result in a reduction in lipophilicity compared to the parent molecule. These reductions in lipophilicity lead to increased renal clearance and effectively permit the voiding of the dose from the body as illustrated in Figure 5.6.

This demonstrates the interaction between metabolic and renal clearance. Assuming that SM-10888 is the only pharmacologically active moiety, these processes govern the clearance of active drug and hence determine the required dose. In fact, only the formation of the *N*-glucuronide and the benzylic hydroxyl metabolites are of prime concern to the medicinal chemist. These represent the primary clearance routes of the compound and hence govern the rate of clearance and ultimately the dosage regimen needed to obtain a particular plasma concentration of the active compound, SM-10888 in this example.

Rather than looking at a metabolic pathway, similar models for the control of the mechanism of clearance by lipophilicity are demonstrated by considering drugs in general. Figure 5.7 illustrates free drug renal and metabolic clearance for a series of neutral compounds drawn from the literature [4].

For hydrophilic drugs ($\log D_{7.4}$ below 0) renal clearance is the predominant mechanism. For drugs with $\log D_{7.4}$ values above 0, renal clearance decreases with lipophilicity. In contrast to renal clearance, metabolic clearance increases with in-

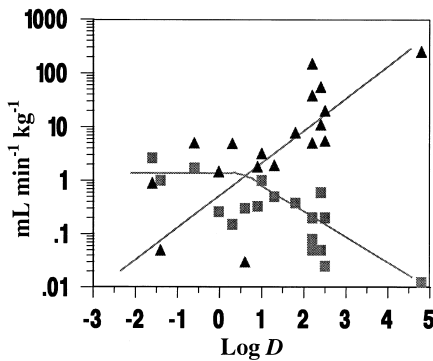


Fig. 5.7 Relationship between lipophilicity and unbound renal (squares) and metabolic clearance (triangles) for a range of neutral drugs in man.

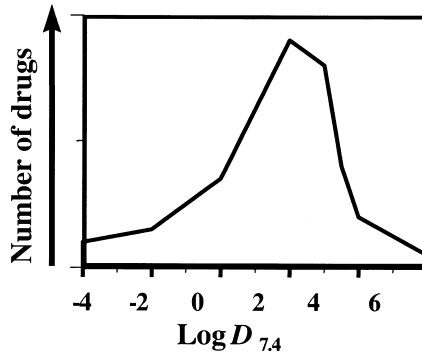
creasing log D and this becomes the major clearance route of lipophilic compounds. Noticeably, considering the logarithmic scale in Figure 5.7, overall clearance declines with decreasing lipophilicity. The lowest clearances, achieved by the combined renal and metabolic processes, are observed below log $D_{7.4}$ values of 0 where metabolic clearance is negligible. This apparent advantage needs to be offset against the disadvantages of reliance on gastrointestinal absorption via the aqueous pore pathway that will tend to predominate for hydrophilic compounds. Moreover the actual potency of the compound is also normally affected by lipophilicity with potency tending to increase with increasing lipophilicity [5]. Furthermore as shown previously, volume of distribution also increases with increasing lipophilicity and hence tends to increase the elimination half-life ($t_{1/2} = 0.693 \times V_d/Cl$). Therefore the duration of the drug in the system is a fine balance between the relationship of lipophilicity and its effects on volume of distribution and clearance.

This balance is illustrated by reference to two β -adrenoceptor antagonists, atenolol and propranolol [6]. These have differing physicochemical properties. Atenolol is a hydrophilic compound which shows reduced absorption, low clearance predominantly by the renal route and a moderate volume of distribution. Note that absorption by the paracellular route is still high, due to the small size of this class of agent. In contrast, propranolol, a moderately lipophilic compound, shows high absorption, high clearance via metabolism and a large volume of distribution. Because of this balance of properties both compounds exhibit very similar elimination half-lives. These half-lives are sufficiently long for both drugs to be administered on twice daily

Tab. 5.1 Physicochemical, pharmacological and pharmacokinetic properties for atenolol and propranolol illustrating their interdependence.

	Log $D_{7.4}$	Affinity (nM)	Absorption (%)	Oral clearance (unbound) $\text{mL min}^{-1} \text{kg}^{-1}$	Volume of distribution (unbound) L kg^{-1}	Half-life (h)
Atenolol	-1.9	100	50	4	0.8	3-5
Propranolol	1.1	4	100	700	51	3-5

Fig. 5.8 Analysis of marketed oral drugs and their lipophilic properties.



(b. d.) dosage regimens due to the relatively flat dose–response curves of this class of agent (Table 5.1).

Propranolol is considerably more potent (albeit less selective) than atenolol. Thus despite a much higher clearance than atenolol, both agents have a daily clinical dose size of around 25–100 mg.

Optimal properties may reside over a span of lipophilicities as illustrated by the β -adrenoreceptor antagonists. However analysis of over 200 marketed oral drugs illustrates the distribution shown in Figure 5.8, where most drugs reside in the “middle ground” of physiochemical properties with log $D_{7.4}$ values in the range 0 to 3. This is probably a result of good fortune rather than design, but intuitively it fits with the idea of maximizing oral potency, absorption and duration by balancing intrinsic potency, dissolution, membrane transfer, distribution and metabolism.

References

- 1 Muller M, Jansen, PLM, *Am. J. Physiol.* **1997**, *272*, G1285–G1303.
- 2 Gardner IB, Walker DK, Lennard MS, Smith DA, Tucker GT, *Xenobiotica*. **1995**, *25*, 185–197.
- 3 Yabuki M, Mine T, Iba K, Nakatsuka I, Yoshitake A, *Drug Metab. Dispos.* **1994**, *22*, 294–297.
- 4 Smith DA, In: *Computer-Assisted Lead Finding and Optimisation* (Eds Van de Waterbeemd H, Testa B, Folkers G), pp. 265–276. Wiley-VCH, Weinheim, **1997**.
- 5 Lipinski CA, Lombardo F, Dominy BW, Feeney PJ, *Adv. Drug Del. Rev.* **1997**, *23*, 3–25.
- 6 Yamada Y, Ito K, Nakamura K, Sawada Y, Tatsuji I, *Biol. Pharm. Bull.* **1993**, *16*, 1251–1259.

6

Renal Clearance

Abbreviations

GFR Glomerular filtration rate

Symbols

$C_{p(f)}$ Free (unbound) plasma concentration

$\log D_{7.4}$ Logarithm of distribution coefficient (octanol/buffer) at pH 7.4

6.1

Kidney Anatomy and Function

The kidney can be subdivided in terms of anatomy and function into a series of units termed nephrons. The nephron consists of the glomerulus, proximal tubule, loop of Henle, distal tubule and the collecting tubule. Filtration by the glomerulus of plasma water is the first step in urine formation. A large volume of blood, approximately 1 L min^{-1} (or 25 % of the entire cardiac output at rest) flows through the kidneys. Thus in 4–5 min a volume of blood equal to the total blood volume passes through the renal circulation, of this volume approximately 10 % is filtered at the glomerulus. Small molecules are also filtered at this stage. The concentration of drug is identical to that present unbound in plasma ($C_{p(f)}$). The rate at which plasma water is filtered (125 mL min^{-1}) is termed the glomerular filtration rate (GFR). In addition to the passive filtration, active secretion may also occur. Various transport proteins are present in the proximal tubule which are selective for acidic and basic compounds (ionized at physiological pH) [1]. For acidic compounds (organic anions), the transporter is located at the contraluminal cell membrane and uptake is a tertiary, active transport process. Physicochemical properties that determine affinity for this transporter are lipophilicity, ionic charge strength (decreasing the pK_a increases the affinity for the transporter) and electron attracting functions in the compound structure. The lipophilic region must have a minimal length of 4 Å and can be up to 10 Å. In addition hydrogen bond formation increases the affinity for the transporter, and there is a direct relationship between the number of H-bond acceptors and affinity. A trans-

port system for basic compounds (organic cations) is situated at the contraluminal membrane. Lipophilicity and ionic charge strength (increasing the pK_a increases affinity for the transporter) govern affinity. The transporter can also transport unionized compounds that have hydrogen-bonding functionality. At the luminal membrane an electroneutral H^+ organic cation transporter is also present. Compounds such as verapamil have similar affinity for this transporter compared to the contraluminal system, whilst cimetidine has higher affinity for it. Unlike glomerular filtration, all the blood passing through the kidney has access to the transporter so clearance rates can be much higher than GFR.

6.2

Lipophilicity and Reabsorption by the Kidney

Reabsorption, as highlighted previously, is the most important factor controlling renal handling of drugs. The degree of reabsorption depends on the physicochemical properties of the drug, principally its degree of ionization and intrinsic lipophilicity ($\log D$). The membranes of the cells that form the tubule are lipoidal (as expected) and do not represent a barrier to lipophilic molecules. Reabsorption occurs all along the nephron. Reabsorption re-establishes the equilibrium between the unbound drug in the urine (largely the case) and the unbound drug in plasma. As the kidney reabsorbs water so the drug is concentrated and hence if lipophilic, reabsorbed by passive diffusion. The majority (80–90%) of filtered water is reabsorbed in the proximal tubule. Most of the remainder is reabsorbed in the distal tubule and collecting ducts. From initial filtration the urine is concentrated approximately 100-fold. We can thus expect that for neutral compounds renal clearance (unbound values) will range between GFR, for compounds that are not reabsorbed, and a value some 100-fold below this for compounds that are completely reabsorbed to an equilibrium with free drug in plasma. Figure 6.1 illustrates this relationship between lipophilicity and renal clearance for a series of neutral compounds.

Clearly, the ability to cross membranes, as represented by octanol partitioning, correlates with the extent of reabsorption, with reabsorption only occurring at $\log D_{7,4}$ values above 0.

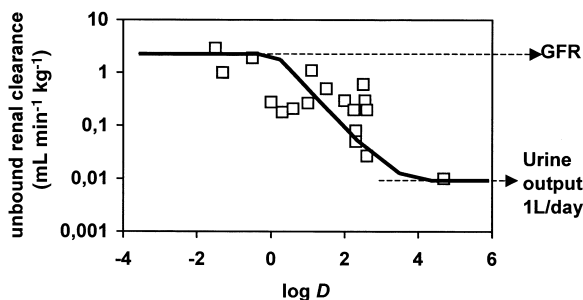


Fig. 6.1 Relationship between lipophilicity and unbound renal clearance (highlighting GFR and urine output) for a series of neutral drugs in man.

6.3

Effect of Charge on Renal Clearance

Similar patterns occur for acidic and basic drugs, however, tubular pH is often more acidic (pH 6.5) than plasma. Because of this, acidic drugs are reabsorbed more extensively and basic drugs less extensively than their $\log D_{7.4}$ would suggest. Moreover, much greater rates of excretion/clearance can occur for these charged moieties due to the tubular active transport proteins. The effects of tubular secretion are particularly apparent as lipophilicity increases (as indicated by the structural features required by the transport systems described above) but before substantial tubular reabsorption occurs. With the shift in tubular pH the value of 0 as a threshold for reabsorption for neutral drugs (see Figure 6.1) correlates to a value of -1 for acid drugs and $+1$ for basic drugs. These effects are illustrated in Figure 6.2.

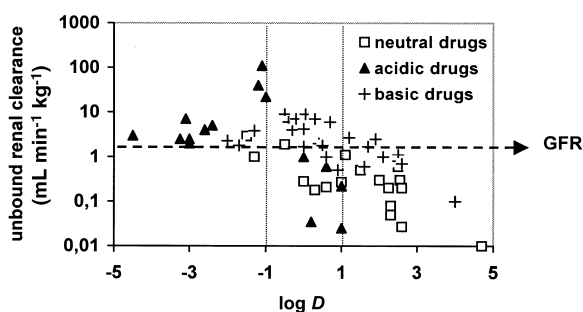


Fig. 6.2 Relationship between lipophilicity, GFR and unbound renal clearance for neutral, acidic and basic drugs in man.

Figure 6.2 highlights the role of lipophilicity in the active transport of drugs. Peak values for renal clearance for these compounds occur at $\log D_{7.4}$ values between -2 and 0 . These values span the region where the compounds have sufficient lipophilicity to interact with the transport proteins but are not substantially reabsorbed.

6.4

Plasma Protein Binding and Renal Clearance

As only unbound drug is available for renal clearance by filtration at the glomerulus, drugs with high plasma protein binding will only appear slowly in the filtrate. Hence considerations of the renal clearance process based on total drug concentrations either in plasma or urine may be misleading.

For example, a series of class III antidysrhythmic agents (Figure 6.3) exhibited decreasing renal clearance in the dog with increasing lipophilicity over a $\log D_{7.4}$ range of 0.7 to 2.1 [2].

However, the major contributing factor to the decreased renal clearance of total drug was increasing plasma protein binding with increasing lipophilicity. When the extent of plasma protein binding was taken into account, the unbound renal clear-

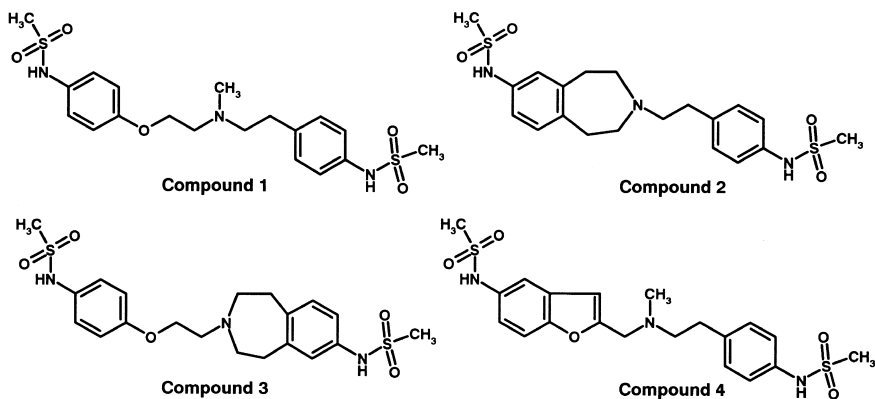


Fig. 6.3 Structures of a series of class III antidysrhythmic agents.

ance for the three least lipophilic compounds was virtually identical at around $6 \text{ mL min}^{-1} \text{ kg}^{-1}$ as shown in Figure 6.4.

The value for unbound renal clearance of $6 \text{ mL min}^{-1} \text{ kg}^{-1}$ is in excess of GFR in the dog ($\sim 4 \text{ mL min}^{-1} \text{ kg}^{-1}$) indicating a degree of tubular secretion in the renal clearance of these basic molecules (pK_a values of 7.8–8.2). The unbound renal clearance of compound 4 is about $1.5 \text{ mL min}^{-1} \text{ kg}^{-1}$ and indicates substantial tubular reabsorption of this, the most lipophilic member of the series. This compound is also substantially less basic than the others (pK_a of 7.3) and as such may be subject to reduced tubular secretion.

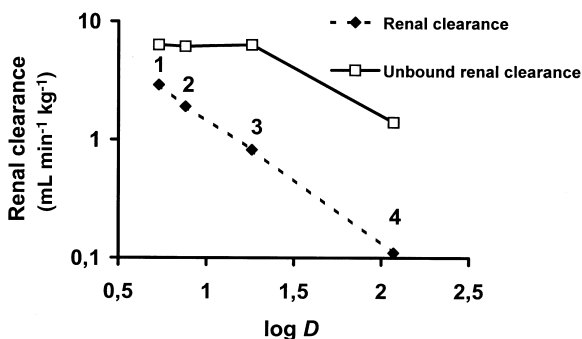


Fig. 6.4 Relationship between lipophilicity and total and unbound renal clearance in the dog for a series of class III antidysrhythmic agents (compounds 1 to 4 in Figure 6.3).

6.5

Balancing Renal Clearance and Absorption

As a clearance route the renal route has attractive features for the design of drugs. For instance clearance rates, certainly for neutral compounds, are low. Moreover, the clearance process by filtration is not saturable and tubular secretion is only saturated at high doses with acidic and basic compounds. In a similar vein drug interactions

Tab. 6.1 Correlation between paracellular absorption and renal clearance.

Compound	log $D_{7,4}$	% cleared renally
Atenolol	- 1.5	85
Practolol	- 1.3	95
Sotalol	- 1.7	80
Xamoterol	- 1.0	60
Nadolol	- 2.1	65
Sumatriptan	- 0.8	25
Pirenzipine	- 0.6	40
Famotidine	- 0.6	88
Ranitidine	- 0.3	70
Amosulalol	- 0.8	34

also only occur at high doses for acidic and basic compounds and will not occur for neutral compounds. Renal function is also easily measured in patients (creatinine clearance) so variation in the process due to age or disease can be readily adjusted for by modification of the dosage regime. On the negative side, low lipophilicity is usually necessary for the renal route to predominate over the metabolic route (see Chapter 5, Figure 5.7). This requirement means that oral absorption of such compounds is likely to be via the paracellular pathway (see Chapter 3). This trend is highlighted in Table 6.1. In this table, the extent of renal clearance of compounds, previously exemplified in Chapter 3 (Absorption) as those absorbed by the paracellular route, is listed. Hence the positive aspects of clearance predominantly by the renal route have to be carefully balanced against the negative aspects of absorption by the paracellular pathway.

6.6

Renal Clearance and Drug Design

Small molecules with relatively simple structures (molecular weights below 350) can successfully combine paracellular absorption and renal clearance. Table 6.1 lists examples of this. Noticeably the compounds are all peripherally acting G-protein-coupled receptor antagonists. When a compound has to cross membrane barriers to access an intracellular target (see Chapter 2, Section 2.10) or cross the blood–brain barrier, then these physicochemical properties are generally unsuitable. It is possible to design molecules of high metabolic stability that “defy” the general trends shown in Figure 5.7 of Chapter 5.

Fluconazole (Figure 6.5) is an example where knowledge of the relationship between physicochemical properties and drug disposition has allowed optimization of the drug’s performance [3]. The project’s goal was a superior compound to ketoconazole, the first orally active azole antifungal drug. Ketoconazole (Figure 6.5) is cleared primarily by hepatic metabolism and shows irregular bioavailability, due partly to

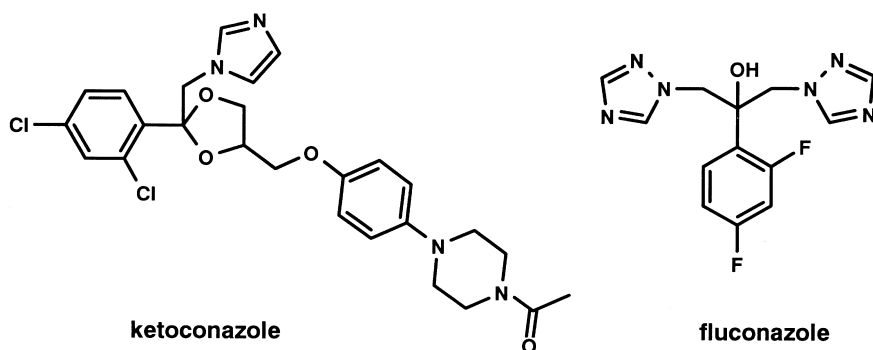


Fig. 6.5 Structures of the antifungal agents, ketoconazole and fluconazole.

this, and also its poor aqueous solubility and consequent erratic dissolution. Ketoconazole is a neutral molecule with a $\log D_{7.4}$ value greater than 4.0. Its high lipophilicity leads to its dependence on metabolic clearance and its low solubility.

Synthesis was directed towards metabolic stability and this was found in the bis-triazole series of compounds. Metabolic stability is achieved by the relative resistance of the triazole moiety to oxidative attack, the presence of halogen functions on the phenyl grouping, another site of possible oxidative attack, and steric hindrance of the hydroxy function, a site for possible conjugation.

Due to the metabolic stability, low molecular weight and absence of ionization at physiological pH, fluconazole has to rely on renal clearance as its major clearance mechanism. The compound has a $\log P$ or $D_{7.4}$ value of 0.5, which means following filtration at the glomerulus a substantial proportion (80%) of the compound in the filtrate will undergo tubular reabsorption. The resultant low rate of renal clearance gives fluconazole a 30-h half-life in man and is consequently suitable for once-a-day administration.

References

- 1 Ullrich KJ, *Biochim. Biophys. Acta* **1994**, 1197, 45–62.
- 2 Walker DK, Beaumont KC, Stopher DA, Smith, DA, *Xenobiotica* **1996**, 26, 1101–1111.
- 3 Smith DA, Jones BC, Walker DK, *Med. Res. Rev.* **1996**, 16, 243–266.

7

Metabolic (Hepatic) Clearance

Abbreviations

COMT	Catechol- <i>O</i> -methyl transferase
CYP	Cytochrome P450
CYP3A4	3A4 isoenzyme of the cytochrome P450 enzyme family
GST	Glutathione- <i>S</i> -transferase
NEP	Neutral endopeptidase
P450	Cytochrome P450
PAPS	3'-Phosphoadenosino-5-phosphosulfate
UGT	UDP-glucuronosyltransferases

7.1

Function of Metabolism (Biotransformation)

Drug metabolism is traditionally divided into phase I and phase II processes. This classical division into primarily oxidative and conjugative processes whilst useful is not definitive. The division is based on the observation that a compound will first undergo oxidative attack (e. g. benzene to phenol) and then the newly introduced hydroxyl function will undergo glucuronidation (phenol to phenyl glucuronic acid). A listing of typical enzymes assigned to phase I and phase II is listed in Table 7.1.

As was shown previously for SM-10888, compounds do not necessarily have to undergo phase I metabolism prior to phase II processes. Either or both (as with SM-10888) can be involved in the primary clearance of a drug. However, in general phase I enzymes are normally of greater import with the cytochrome P450 system occupying a pivotal role in drug clearance. Cytochrome P450 is a haem-containing superfamily of enzymes. The superfamily consists of isoenzymes that are highly selective for endogenous substrates and isoenzymes that are less selective and metabolize exogenous substrates including drugs.

Tab. 7.1 Division of enzymes into phase I and phase II. Phase I enzymes are normally oxidative and phase II conjugative.

Cytochrome P450 monooxygenase	
Azo and nitro group reductase	
Aldehyde dehydrogenase	
Alcohol dehydrogenase	Phase I
Epoxide hydrolase	
Monoamine oxidase	
Flavin monoamine oxidase	
Non-specific esterases	
<hr/>	
Non-specific N- and O-methyltransferases	
D-glucuronic acid transferase	
Catechol O-methyltransferase	Phase II
Glutathione transferase	
Sulphate transferase	

7.2

Cytochrome P450

The cytochrome P450 system can carry out a variety of oxidation reactions as listed in Table 7.2.

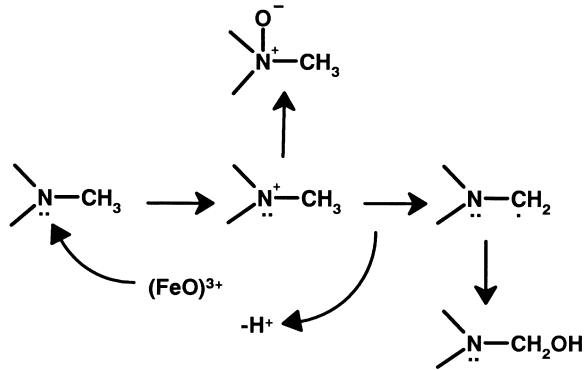
The overall scheme for these reactions is the insertion of a single oxygen atom into the drug molecule. Current views indicate that the chemistry of cytochrome P450 is radical by nature.

The mechanism of cytochrome P450 catalysis is probably constant across the system. It is determined by the ability of a high valent formal $(\text{FeO})^{3+}$ species to carry out one-electron oxidations through the abstraction of hydrogen atoms or electrons. The resultant substrate radical can then recombine with the newly created hydroxyl radical (oxygen rebound) to form the oxidized metabolite. Where a heteroatom is the (rich) source of the electron more than one product is possible. There can be direct recombination to yield the heteroatom oxide or radical relocalization within the

Tab. 7.2 Reactions performed by the cytochrome P450 system.

Reaction	Product	Typical example
Aromatic hydroxylation	Phenyl to phenol	Phenytoin
Aliphatic hydroxylation	Methyl to carbinol	Ibuprofen
N-dealkylation	Tertiary to secondary amine	Lidocaine
O-dealkylation	Ether to alcohol	Naproxen
S-dealkylation	Thioether to thiol	6-methylthiopurine
N-oxidation	Pyridine to pyridine N-oxide	Voriconazole
S-oxidation	Sulphoxide to sulphone	Omeprazole
Alcohol oxidation	Alcohol to carboxylic acid	Losartan

Fig. 7.1 Heteroatom oxidation of drugs by cytochrome P450 leading to heteroatom oxides or dealkylation products.



substrate to a carbon and oxidation of this function to form the unstable carbinol and ultimately heteroatom dealkylation. A possible reaction sequence is illustrated as Figure 7.1.

Many of the investigations into the enzymology of cytochrome P450 over the previous 20 years have focused on the pathway that generates this reactive species as illustrated in Figure 7.2 particularly the donation of electrons and protons to yield the (FeO)³⁺ substrate complex which is the oxidizing species. As part of the cycle substrate binds to the enzyme as an initial step before the addition of electrons and molecular oxygen. The final stage of the cycle is the actual attack of the (FeO)³⁺ species on the substrate.

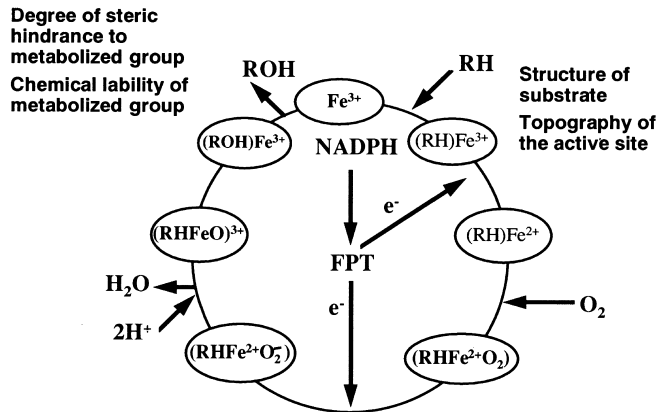


Fig. 7.2 Cytochrome P450 cycle showing the key stages of substrate interaction.

The critical points of the cycle involving substrate–enzyme interactions are illustrated in Figure 7.2 and explored below:

- The initial binding of the substrate to the CYP which causes a change in the spin state of the haem iron eventually resulting in the formation of the (FeO)³⁺-substrate complex. This is obviously a key substrate–protein interaction and depends on the actual 3D-structure of the substrate and the topography of the active site.

However, it cannot be assumed that this initial binding is the same as the final conformation that the protein and substrate adopt during actual substrate attack.

b) The final stages of the cycle, when the geometry and chemical reactivity of this complex determine the structure of the metabolite produced.

Analysis of the literature indicates that three major forms of CYPs are involved in the metabolism of pharmaceuticals in man: CYP2D6, CYP2C9 and CYP3A4, CYP1A2, CYP2C19 and CYP2E1 are also involved, but this involvement is much less extensive. The catalytic selectivity of the major CYPs has been reviewed [1].

7.2.1

Catalytic Selectivity of CYP2D6

Substrates for CYP2D6 include tricyclic antidepressants, β -blockers, class 1 antiarrhythmics. In brief, the structural similarities of many of the substrates and inhibitors in terms of position of hydroxylation, overall structure (aryl-alkylamine) and physicochemistry (ionized nitrogen at physiological pH), have allowed template models such as that illustrated as Figure 7.3 to be constructed.

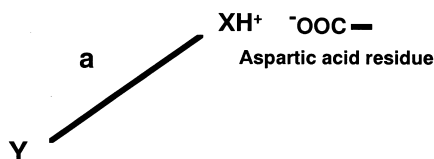


Fig. 7.3 Template model for CYP2D6 with Y the site of oxidation, a is the distance from Y to a heteroatom which is positively charged (normally 5–7 Å).

All the template models produced have the same common features of a basic nitrogen atom at a distance of 5–7 Å from the site of metabolism which is in general on or near a planar aromatic system. It is currently believed that aspartic acid residue 301 provides the carboxylate residues which binds the basic nitrogen of the substrates.

With CYP2D6 therefore the catalytic selectivity relies heavily on a substrate–protein interaction. The relative strength of the proposed ion pair association between the basic nitrogen and the active site of aspartic acid means that the affinity for substrates will be high. This is borne out by the enzyme having lower K_m and K_i values than other CYPs. Thus CYP2D6 is often a major enzyme in drug oxidation despite its low abundance in human liver. This statement is particularly true for low concentrations or doses of drugs, the low K_m values rendering the enzyme easily saturable

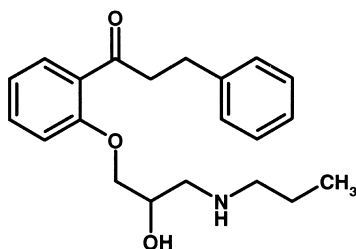
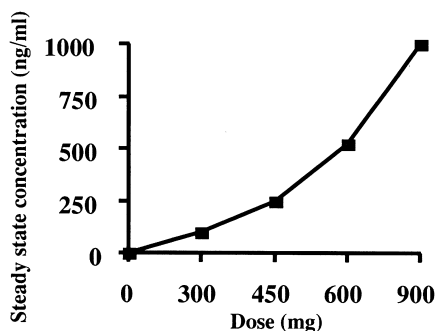


Fig. 7.4 Structure of propafenone.

(see Section 2.12). An example of this is the antiarrhythmic compound propafenone (Figure 7.4) [2] which is converted to 5-hydroxy propafenone by CYP2D6.

The dependence on CYP2D6 metabolism and the relatively high clinical dose (see Figure 7.5) mean that the metabolism is readily saturable over a narrow clinical dose range, so that small increases in dose can lead to disproportionate increases in plasma concentration, and a resultant steep dose–response curve.

Fig. 7.5 Relationship between plasma concentration and dose of propafenone, a CYP2D6 substrate.



CYP2D6 is also problematic in drug therapy since the enzyme is absent in about 7% of Caucasians due to genetic polymorphism. In these 7% (poor metabolizers) clearance of CYP2D6 substrates such as propafenone (Figure 7.4) [3] are markedly lower and can lead to side-effects in these subsets of the population. This correlation of enhanced side-effects in poor metabolizers (lacking CYP2D6) compared to extensive metabolizers (active CYP2D6) has been made for propafenone. The example of betaxolol [4] shows how knowledge of the properties that bestow pharmacological activity can be combined with metabolism concepts to produce a molecule with improved performance. Cardioselectivity for β -adrenoceptor agents can be conferred by substitution in the para position of the phenoxy-propanolamine skeleton. The para position or methoxyethyl substituents (e.g. metoprolol) in this position are the major sites of metabolism for these compounds. This reaction is catalysed by CYP2D6, and the efficiency of the enzyme means that metoprolol shows high clearance and resultant low bioavailability and short half-life. Manoury *et al.* [4] designed the series of compounds leading to betaxolol on the hypothesis that bulky stable substituents in the para position (Figure 7.6) would be resistant to metabolism and also cardioselective.

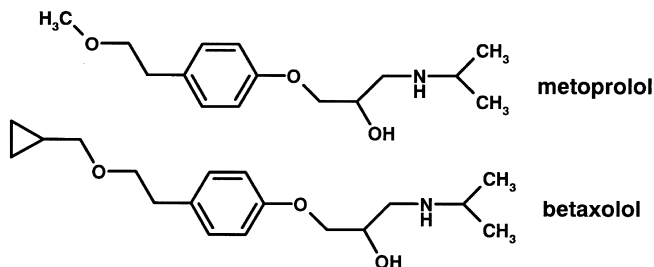


Fig. 7.6 Structures of metoprolol and betaxolol an analogue designed to be more metabolically stable.

Beside the actual steric bulk of the substituent, cyclopropyl is much more stable to hydrogen abstraction than other alkyl functions and represents an ideal terminal group. These changes make betaxolol a compound with much improved pharmacokinetics compared to its lipophilic analogues.

7.2.2

Catalytic Selectivity of CYP2C9

Substrates for CYP2C9 include many non-steroidal anti-inflammatory drugs plus a reasonably diverse set of compounds including phenytoin, (S)-warfarin and tolbutamide. All the substrates with routes of metabolism attributable to CYP2C9 have hydrogen bond donating groups a discrete distance from a lipophilic region which is the site of hydroxylation. The hydrogen bond donating groups and sites of metabolism on each of the substrates have been overlaid with those of phenytoin to produce a putative template of the active site of CYP2C9 (Figure 7.7).

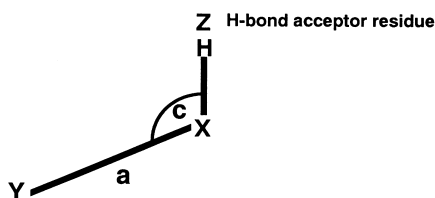


Fig. 7.7 Template model of CYP2C9; Y is the site of oxidation, a is the distance from Y to a heteroatom which can act as a H-bond donor and c defines the angle of the H-bond.

The mean dimensions (\pm SD) for the eight compounds ($a = 6.7 \pm 0.8 \text{ \AA}$, $C = 133 \pm 20^\circ$) illustrates the degree of overlap achieved. Like CYP2D6 the catalytic selectivity of CYP2C9 is dominated by substrate–protein interactions.

Tolbutamide (Figure 7.8) is metabolized via the benzylic methyl group by CYP2C9 as the major clearance mechanism. Chlorpropamide is a related compound incorporating a chlorine function in this position. The resultant metabolic stability gives chlorpropamide a lower clearance and a longer half-life (approximately 35 h compared to 5 h) than tolbutamide, resulting in a substantial increase in duration of action [5].

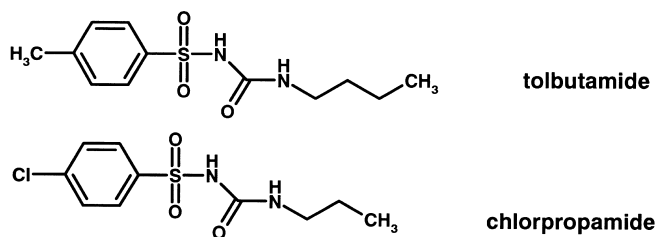
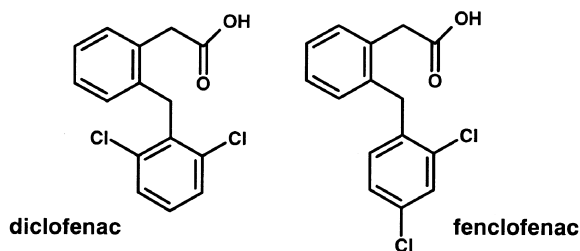


Fig. 7.8 Structures of tolbutamide and the metabolically more stable analogue chlorpropamide.

The mechanism of action of CYPs is radical rather than electrophilic and the actual substitution pattern is important: the role of chlorine is one of blocking rather than deactivation. Many non-steroidal anti-inflammatory drugs are substrates for the

Fig. 7.9 Structures of diclofenac and fenclofenac. Fenclofenac is much more resistant to aromatic hydroxylation.



CYP2C9 enzyme and analogous structures show how metabolic stability to *p*-hydroxylation is achieved with only small changes in substitution.

Diclofenac, with ortho substitution in the aromatic ring (Figure 7.9) is metabolized principally to 4-hydroxydiclofenac by CYP2C9. In man, the drug has a short half-life of approximately 1 h due to the relatively high metabolic (oxidative) clearance. In contrast, the analogous compound, fenclofenac, is considerably more metabolically stable, due to the *p*-halogen substitution pattern, and exhibits a half-life of over 20 h [6].

7.2.3

Catalytic Selectivity of CYP3A4

CYP3A4 attacks lipophilic drugs in positions largely determined by their chemical lability: that is, the ease of hydrogen or electron abstraction. CYP3A4 SAR is dominated therefore by substrate–reactant interaction. Binding of substrates seems to be essentially due to lipophilic forces and results in the expulsion of water from the active site. Such an expulsion of water provides the driving force for the spin state change and hence the formation of the $(\text{FeO})^{3+}$ unit. However, the lipophilic forces holding the substrate in the active site are relatively weak ($\sim 1 \text{ kcal mole}^{-1}$) and would allow motion of the substrate in the active site. Hence, since the substrate is able to adopt more than one orientation in the active site, the eventual product of the reaction is a product of the interaction between one of these orientations and the $(\text{FeO})^{3+}$ unit – a substrate–reactant interaction. This lack of apparent substrate structure similarity (apart from chemical reactivity) indicates a large active site that allows substrate molecules considerable mobility. The selectivity of CYP3A4 to its substrates may also be directed by the conformation they adopt within a lipophilic environment such as we are suggesting for the access channel and active site of CYP3A4. We have previously illustrated this point with cyclosporin A. In an aprotic (lipophilic) solvent cyclosporin A adopts a conformation which allows the major allylic site of CYP3A4 metabolism to extend out away from the bulk of the molecule. This is a different conformation from the one adopted in aqueous solution where the lipophilic sites are internalized and thus shielded from the solvent. As a general rule this “spreading out” of apparently sterically hindered molecules as judged by X-ray or aqueous solution structure, may help to further understand the selectivity of CYP3A4. The principle of extension of lipophilic functions normally hidden from solvent is further supported by the

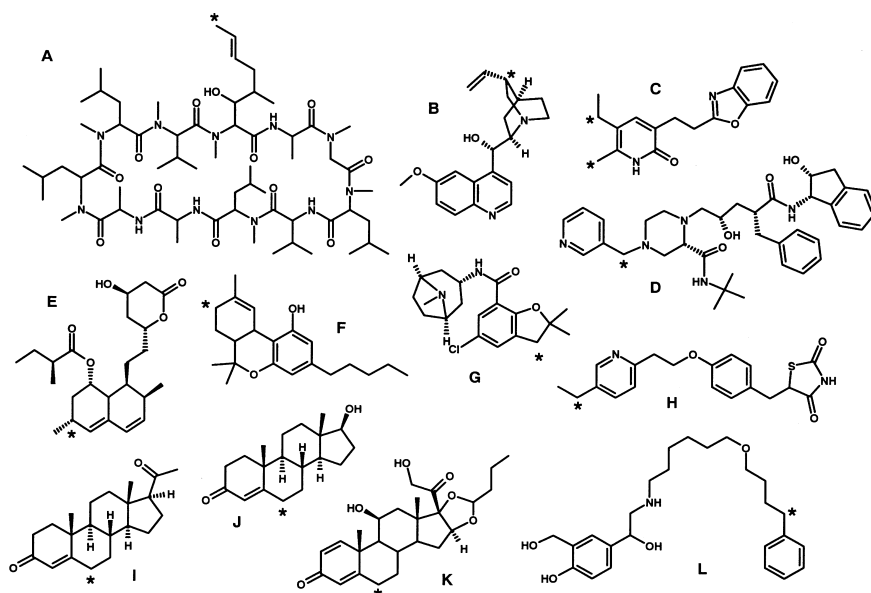


Fig. 7.10 Substrates for CYP3A4 illustrating the diversity of structure and the “selectivity” for attack at allylic and benzylic positions (major sites of metabolism indicated by asterisks). Substrates are A, cyclosporin A; B,

quinidine; C, L-696229; D, indinavir; E, lovastatin; F, D-THC; G, zatosetron; H, pioglitazone; I, progesterone; J, testosterone; K, budesonide and L, salmeterol.

study of the soluble bacterial P450BM₃. In this case the substrates are fatty acids, which in aqueous solution adopt a “globular” conformation. However, upon entering the lipophilic access channel, the fatty acid opens out in an extended conformation with the lipophilic head group directed at the haem and the polar acid function directed at the solvent.

The enzyme is the principal participant in *N*-demethylation reactions where the substrate is a tertiary amine. The list of substrates includes erythromycin, ethylmorphine, lidocaine, diltiazem, tamoxifen, toremifene, verapamil, cocaine, amiodarone, alfentanil and terfenadine. Carbon atoms in the allylic and benzylic positions, such as those present in quinidine, steroids and cyclosporin A, are also particularly prone to oxidation by CYP3A4, a range of substrates is illustrated in Figure 7.10.

Both these routes of metabolism reflect the ease of hydrogen or electron abstraction from these functions. As with conventional radical chemistry, reactivity needs to be combined with probability. Thus, in molecules such as terfenadine the tertiary butyl group will be liable to oxidation due to its “maximum number” of equivalent primary carbons. Thus, although not a specially labile function, the site of metabolism becomes dominated by statistical probability. Terfenadine, as expected, also undergoes *N*-dealkylation by CYP3A4, illustrating the ability of the enzyme to produce multiple products (as for cyclosporin A, midazolam, etc.) and underlining the “flexibility” of CYP3A4 substrate binding.

Overcoming metabolism by CYP3A4 is difficult due to the extreme range of substrates and the tolerance of the enzyme to variations in structure. Two strategies are available: removal of functionality and reduction of lipophilicity.

Allylic and benzylic positions are points of metabolic vulnerability. SCH48461 is a potent cholesterol absorption inhibitor [7]. Metabolic attack occurred at a number of positions including benzylic hydroxylation. Dugar and co-workers substituted oxygen for the C-3' carbon to remove this site of metabolism. This step however, produces an electron-rich phenoxy moiety in comparison to the original phenyl group and possibly makes this function more amenable to aromatic hydroxylation. Blocking of the aromatic oxidation with fluorine introduced in the para-position was required to produce the eventual more stable substitution. These steps are shown in Figure 7.11.

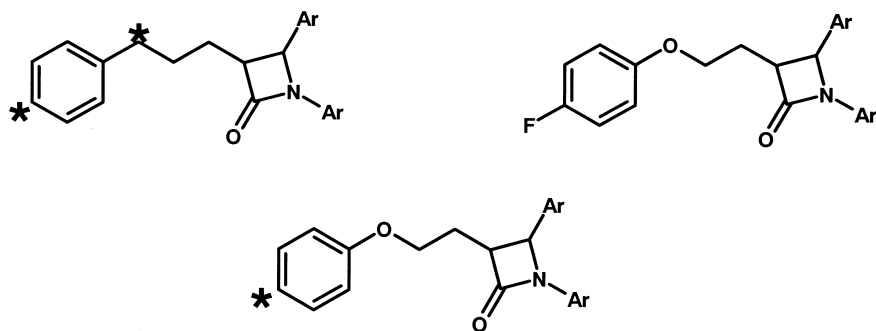


Fig. 7.11 Synthetic strategies to overcome benzylic hydroxylation in a series of cholesterol absorption inhibitors. Positions of metabolism are marked with an asterisk.

The lability of benzylic positions to cytochrome P450 metabolism has been exploited to decrease the unacceptably low clearance and resultant long half-life of various compounds. For example celecoxib, a selective cyclooxygenase inhibitor, has a half-life of 3.5 h in the rat. Early structural leads, represented by compounds in

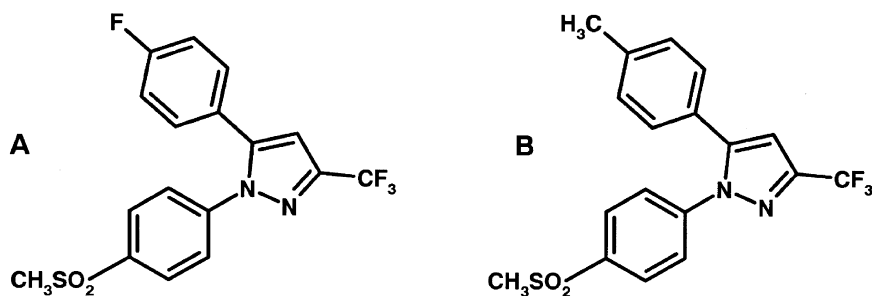


Fig. 7.12 Structures of early long half-life COX2 inhibitor (A) and the candidate compound celecoxib (B) with a moderate half-life.

which the benzylic methyl in celecoxib was substituted with a halogen (Figure 7.12), resulted in compounds with half-life values (in the male rat) of up to 220 h [8].

Diltiazem (Figure 7.13), a calcium channel blocker, is a drug that is extensively metabolized by at least five distinct pathways including *N*-demethylation, deacetylation, *O*-demethylation, ring hydroxylation and acid formation. The enzyme responsible for at least the major route (*N*-demethylation), has been shown to be CYP3A4 [8]. Although widely used in therapy, the compound has a relatively short duration of action. In the search for superior compounds, Floyd *et al.* [9] substituted the benzazepinone ring structure for the benzothiazepinone of diltiazem. Metabolic studies on this class of compound showed that the principal routes of metabolism were similar to that for diltiazem with *N*-demethylation, conversion to an aldehyde (precursor of an acid), deacetylation and *O*-demethylation all occurring. It was also noted that the *N*-desmethyl derivative was equipotent to the parent but much more stable metabolically. This can be rationalized as the decreased substitution on the nitrogen (secondary versus tertiary) stabilizing the nitrogen to electron abstraction (decreased radical stability). This stabilization is particularly important, since electron abstraction is the first step to both the *N*-desmethyl and aldehyde products (a total of 84 % of the total metabolism). The evidence of stability of secondary amines was capitalized on by synthesis of *N*-1 pyrrolidinyl derivatives, which were designed to achieve metabolic stability both by the decreased radical stability of secondary compounds to tertiary amines and steric hindrance afforded by β -substitution (Figure 7.11). The success of this strategy indicates how even the vulnerable alkyl substituted nitrogen grouping can be stabilized against attack.

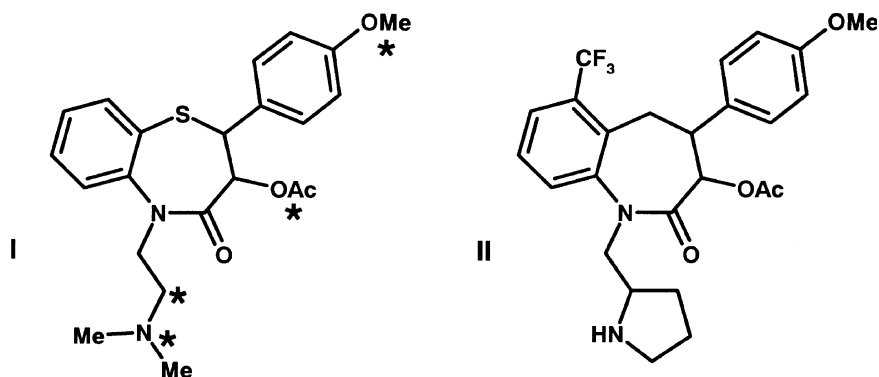
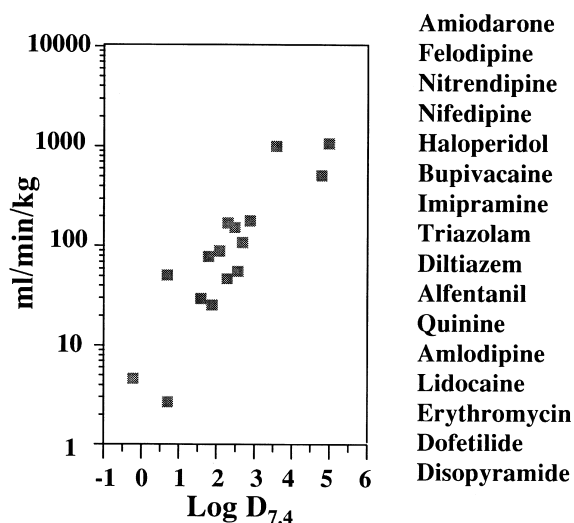


Fig. 7.13 Structures of diltiazem and a benzazepinone analogue resistant to metabolism.

The predominant interaction of CYP3A4 is via hydrophobic forces and the overall lowering of lipophilicity can reduce metabolic lability to the enzyme. Figure 7.14 shows the relationship between unbound intrinsic clearance in man and lipophilicity for a variety of CYP3A4 substrates. The substrates are cleared by a variety of metabolic routes including *N*-dealkylation, aromatization and aromatic and aliphatic hydroxylation. The trend for lower metabolic lability with lower lipophilicity is maintained regardless of structure or metabolic route.

Fig. 7.14 Unbound intrinsic clearance of CYP3A4 substrates and relationship with lipophilicity. The data has been calculated from various clinical studies with the drugs listed in order of decreasing lipophilicity.



7.3

Oxidative Metabolism and Drug Design

In addition to the examples indicated above the design of orally-active cholesterol absorption inhibitors combines both the concept of preventing metabolism and the serendipity of metabolites being more active than the parent drug [10]. On the basis of metabolite structure–activity relationships for SCH 48461 (Figure 7.15), SCH 58335 was designed to combine activity-enhancing oxidation and to remove or block sites of detrimental metabolic oxidation. The improvement in the pharmacodynamics of the compound is illustrated by the ED_{50} being reduced in the cholesterol hamster model from 2.2 to 0.04 $mg\ kg^{-1}\ day^{-1}$.

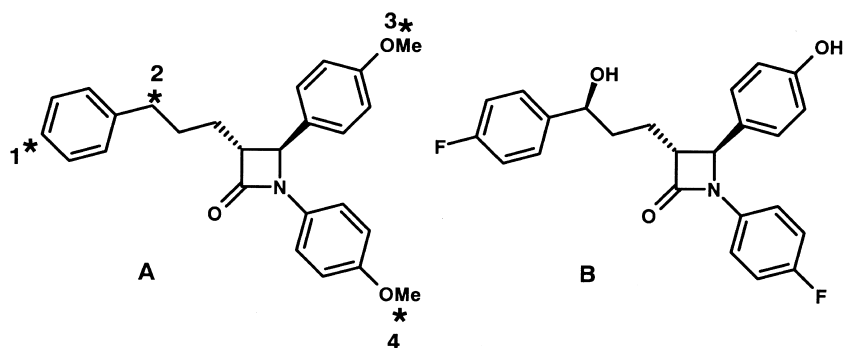


Fig. 7.15 Structures of cholesterol absorption inhibitors SCH 48461 (A) and SCH 58335 (B). Metabolism of SCH 48461 occurs by aromatic hydroxylation (1) benzylic hydroxylation (2) and *O*-demethylation (3, 4). Metabolism is blocked in SCH 58235 at 1 and 4 or results in increases in potency at 2 and 3.

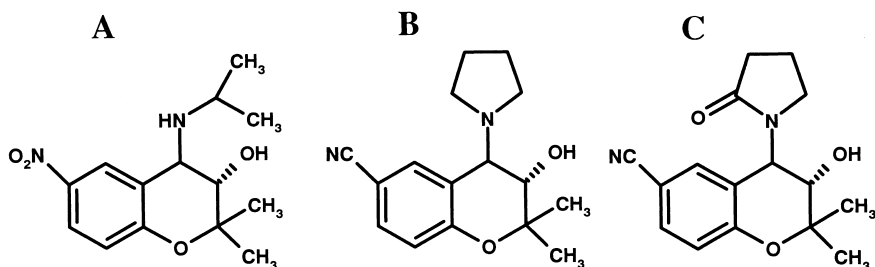


Fig. 7.16 Steps in the discovery of cromakalim: initial structure (A), more potent pyrrolidine analogue (B) and active metabolite (cromakalim C).

The discovery of the potassium channel opener cromakalim is another example of metabolism providing novel active molecules [11]. The programme was designed to find agents that were antihypertensive without having β -adrenoceptor blocking activity. This was due to the belief that β -adrenoceptor blockade was not solely responsible for the antihypertensive effects of β -adrenoceptor blockers. Early compounds were synthesized as cyclized derivatives of β -adrenoceptor blockers. The initial lead is illustrated in Figure 7.16. The gem-dimethyl group and an electron-withdrawing group on the aromatic ring were essential. Cyclic amino groups were preferred to the original isopropylamine, leading to the pyrrolidine derivative. The eventual candidate cromakalim was produced by investigating the metabolites of the pyrrolidine derivative, an oxidation to amines to produce amides being a common metabolic step in cyclic amide systems.

7.4

Non-Specific Esterases

7.4.1

Function of Esterases

Non-specific esterases are distributed widely throughout the body. The activity of these enzymes varies markedly within different tissues. In mammals the highest levels are found in liver and kidney. Numerous isoenzymes exist which have broad substrate overlap. A loose categorization divides the two enzyme types likely to be involved in drug hydrolysis into arylesterases and aliesterases. Aliesterases have a wide substrate range, arylesterases require a phenolic ester. Since most of the major tissues contain a mixture this division is not of great importance. Where esters are of great benefit to drug design is in the design of rapidly cleared molecules, either to an inactive or active form. The most rapid clearance is by blood metabolism. An important point in the screening of compounds designed for rapid metabolism is that the erythrocyte surface has a high esterase content and whole blood is therefore the medium of choice. Moreover rodent blood has very high esterase levels, and may

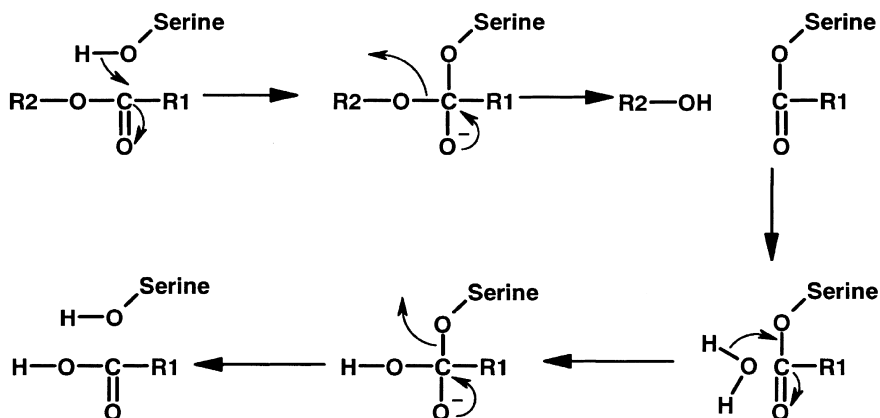


Fig. 7.17 Proposed mechanism for non-specific esterase catalysis involving a serine residue.

give a misleading view of stability if this species is used in isolation. It is highly likely that many of these enzymes are serine esterases and a suggested mechanism is proposed in Figure 7.17.

Ester functions present in molecules tend to be considered labile although steric effects etc. may be utilized to produce drugs without inherent chemical or metabolic problems due to ester lability. For instance a series of antimuscarinic compounds which had selectivity for the M3 receptor (Figure 7.18) were stabilized by the incorporation of a hydroxyethyl side chain or a cyclic ring system at positions surrounding the ester function. Presumably the proximity of these groups to the ester function (carbonyl) prevents close approach of the “attacking” nucleophile, in this case probably a serine hydroxyl.

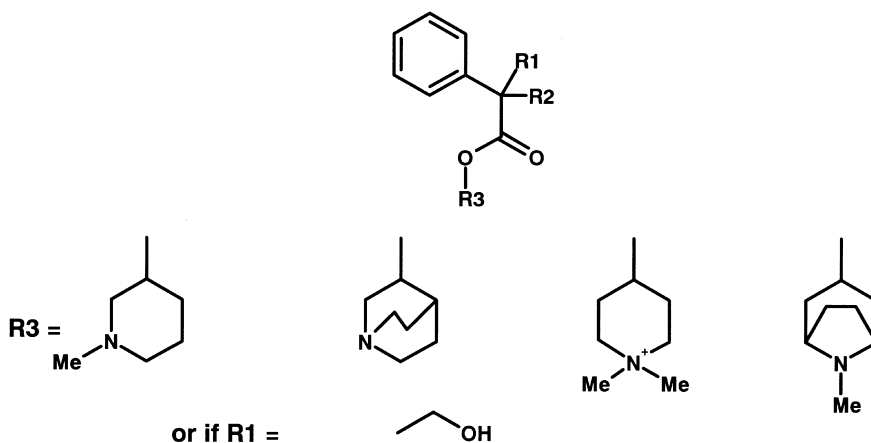


Fig. 7.18 Stabilization of antimuscarinic compounds to esterase activity by steric effects. Stability was achieved when groupings corresponding to those illustrated were incorporated.

7.4.2

Ester Drugs as Intravenous and Topical Agents

Lability can be used to advantage to create drugs that are designed for topical or intravenous infusion administration. For topical administration compounds may benefit from rapid systemic clearance to overcome possible side-effects. Thus the compound is stable at its topical site of action (skin, eye etc.) but rapidly degraded by the esterases present in blood, liver and kidneys to its inactive metabolites. This approach renders the compound selective.

The aim of intravenous infusion is often to achieve a steady state plasma concentration as rapidly as possible and to ensure that the concentration of the drug declines as rapidly as possible once the infusion is stopped. This gives the clinician complete control and the opportunity to react quickly to the patient's needs. Figure 7.19 shows how existing drugs such as the anaesthetic/analgesic sulfentanil, the β -blocker propranolol and the ACE inhibitor captopril, have been used as the starting point for the design of short-acting infusion agents. Essential to this design is the

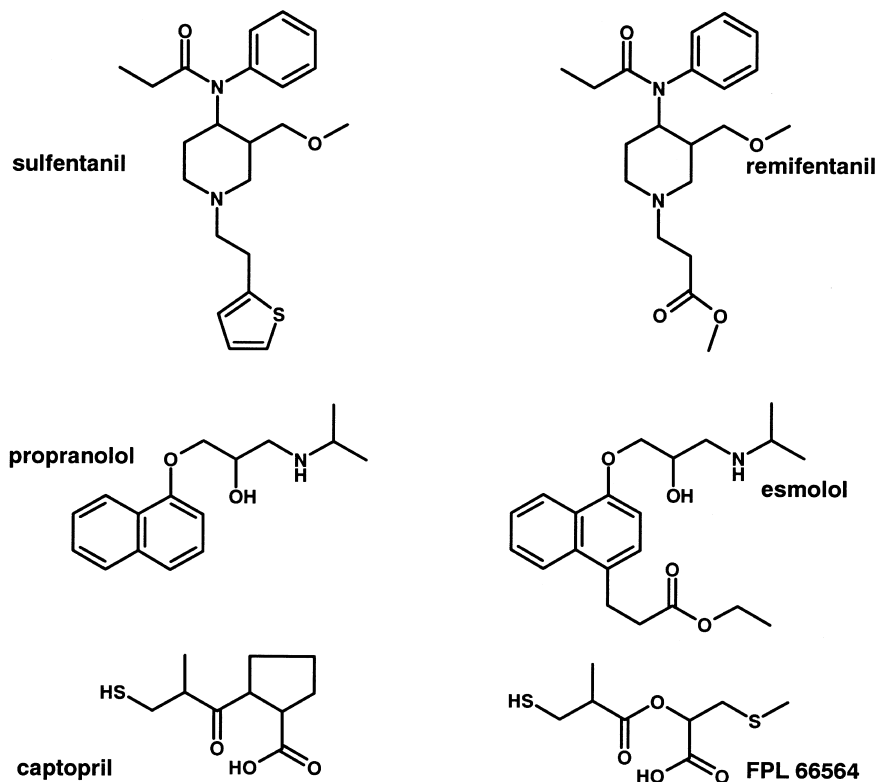


Fig. 7.19 Design of rapidly cleared ester analogues of sulfentanil, propranolol and captopril. The compounds remifentanil, esmolol and FPL 66564 are all cleared to inactive metabolites.

need for the acid metabolites produced from ester hydrolysis to be devoid of activity. In the case of remifentanyl two sites of hydrolysis were incorporated into the molecule to provide sufficient metabolic lability [12, 13].

Topical agents can also be produced by the “soft-drug” approach. Bodor [14] has produced “soft” analogues of methatropine and methscopolamine. These are potent anticholinergics with a short duration of mydriatic action. Moreover the compounds show no systemic side-effects. They thus have a highly selective local action with a much decreased potential for systemic side-effects. Again the design of these drugs depends on knowing that the acidic metabolites produced are inactive.

7.5

Pro-drugs to Aid Membrane Transfer

Esterification of a carboxylic acid function in a molecule has the immediate effect of a reduction in H-bonding potential and an increase in lipophilicity. Such parameters are important in the oral absorption of compounds as described earlier. Candoxatriilat (Figure 7.20), an inhibitor of neutral endopeptidase (NEP), has poor oral bioavailability [15]. The compound has a $\log D$ of -2 . The indanyl ester analogue candoxatril (Figure 7.20) has a $\log D$ of 1.5 , and a reduced Raevsky score [15]. As such the compound is well within the requirements expected for an oral agent. The pro-drug is well absorbed, rapidly hydrolyzed but complete conversion is not achieved. The proportion of candoxatriilat liberated depends on competing clearance processes for candoxatril clearance e. g. hepatic uptake/ biliary clearance. For candoxatriilat the values of systemic availability after oral administration to the mouse, rat, dog and man are 88, 53, 17 and 32 % respectively and depend on the esterase activity (which in rodents is the highest) and the competing processes (which in man are probably the lowest).

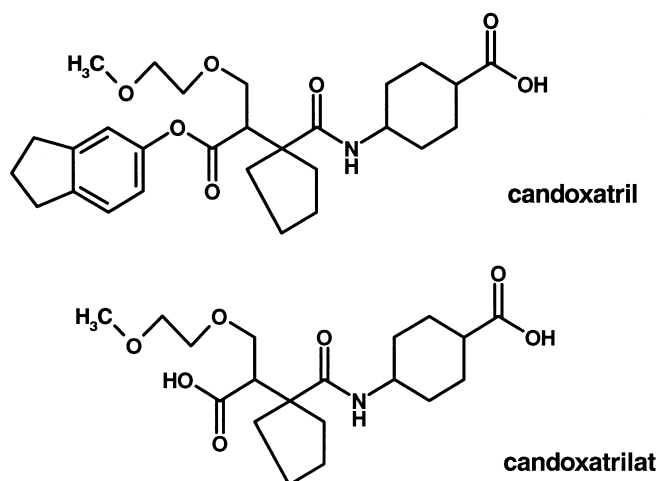


Fig. 7.20 Structures of candoxatril, the orally absorbed indanyl ester pro-drug of candoxatriilat.

7.6

Enzymes Catalysing Drug Conjugation

7.6.1

Glucuronyl- and Sulpho-Transferases

One of the most important phase II conjugation reactions is that catalyzed by the glucuronyl transferases. A number of functional groups have the potential to be glucuronidated as shown in Table 7.3, but phenol and carboxylic acid functions are of prime importance to the medicinal chemist.

Tab. 7.3 Reactions performed by the glucuronyl transferases.

Function	Typical example
Aliphatic hydroxyl	Tiaramide
Phenol	Morphine
Aromatic carboxyl	Furosemide
Aromatic tetrazole	Losartan
Aliphatic carboxyl	Benoxaprofen
Immidazole	Tioconazole
Aromatic amine	Dapsone
Tertiary amine	Chlorpromazine
Triazine	Lamotrigine

Glucuronidation involves the transfer of D-glucuronic acid from UDP- α -glucuronic acid to an acceptor compound. The family of enzymes which catalyze this reaction are the UDP-glucuronyl transferases [16]. The reaction proceeds by nucleophilic S_N2 substitution of the C-1 carbon of glucuronic acid, the product undergoing inversion of configuration. The mechanism is illustrated schematically in Figure 7.21.

Deprotonation

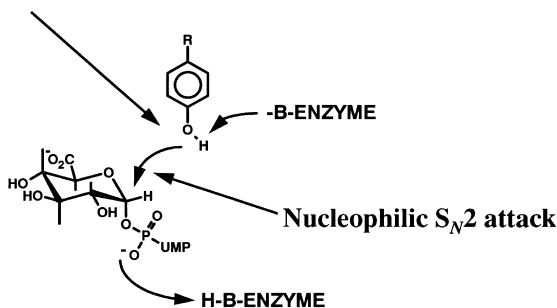


Fig. 7.21 Schematic showing mechanism of glucuronidation reactions.

Similar mechanisms apply to sulphate transferases in which the donor is 3'-phosphoadenosine-5-phosphosulphate (PAPS). The accepting groups in the molecule are phenols, alcohols and hydroxylamines. The sulphotransferases are relatively non-specific, however, phenol-sulphotransferase is probably the most relevant to the medicinal chemist. The similarity in mechanism [17, 18] is shown by comparing the V_{\max} values for glucuronyl transferase and sulphotransferase for a series of power substituted phenols. Figure 7.22 shows the $\log V_{\max}$ for these series plotted against the Hammett sigma value.

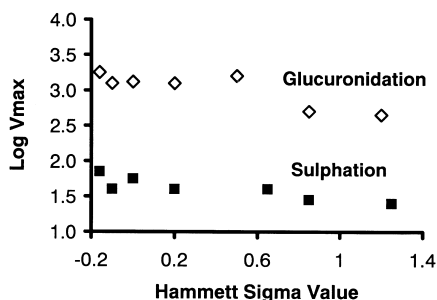


Fig. 7.22 Relationship between sigma value and enzyme rate for glucuronyl and sulphotransferases indicating the role of nucleophilicity.

The negative slope of both curves indicates the greater the nucleophilicity (electron-donating ability) of the phenolate anion the faster the rate of the reaction. The initial deprotonation of the phenol is apparently not rate limiting but must occur rapidly so that those compounds with high pK_a values can be deprotonated. Recently X-ray crystallography data [19, 20] has been obtained for various sulphotransferases. The active site comprises a hydrophobic pocket formed by phenylalanine residues (see Figure 7.23). In the case of the catecholtransferase SULT1A3, a glutamic acid residue provides an ion pair interaction with the basic nitrogen of many of its natural substrates such as dopamine. A critical residue in the catalytic process is a lysine which stabilizes the transition state and via a hydrogen bond interaction with the bridge oxygen, between the 5'-phosphate group and the sulphate group of PAPS, acts as a catalytic acid to enhance the dissociative nature of the sulphuryl transfer mechanism. The other critical residue is an histidine, which acts as the base which deprotonates the phenol (or other group) to a phenoxide. The resultant nucleophile can then attack the sulphur atom of the transferring sulphuryl group.

The glucuronide and sulphotransferases are present in the gut as well as the liver and catalyze the metabolism of many phenol- or catechol-containing drugs (morphine, isoprenaline etc.) during their passage through the gut. The ready conjugation of phenolic functions by both glucuronyl and sulphotransferase systems means that drugs such as morphine are cleared as both glucuronide and sulphate metabolites.

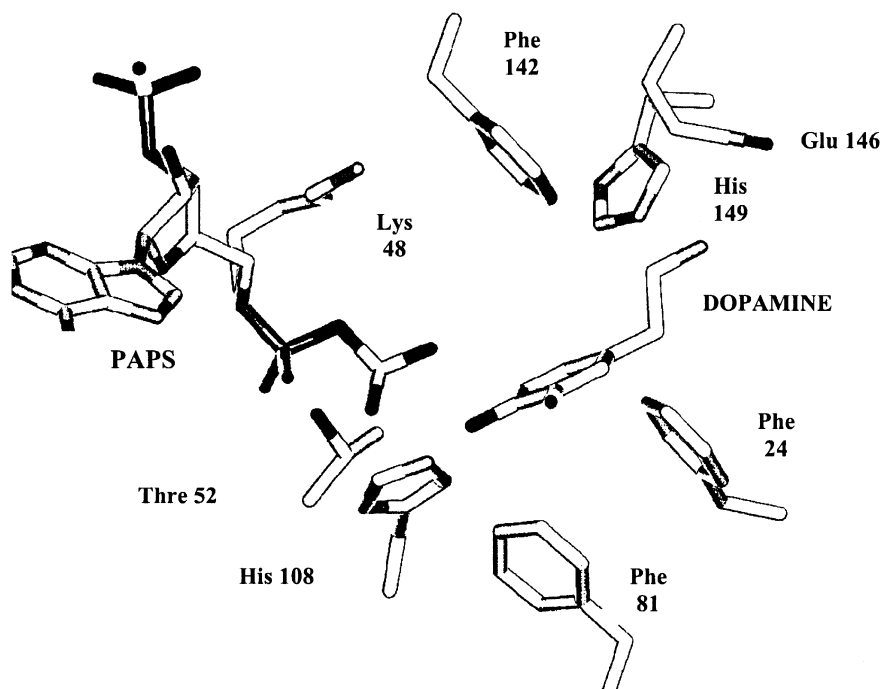


Fig. 7.23 Schematic of the active site of catechol sulphotransferase (SULT1A3), with dopamine in the active site. Phe 142, 81 and 24 form a hydrophobic pocket whilst Glu 146 provides an ion pair interaction with the sub-

strate. Leu 48 stabilizes the transition state and His 108 deprotonates one of the catechol hydroxyls to form the phenoxide nucleophile to allow the reaction to proceed.

7.6.2

Methyl Transferases

Structural data is available on a third member of the transferases, catechol methyl transferase. This crystal structure data gives further clues on how the transferases metabolize their substrates, particularly with regard to the deprotonation step [21]. This enzyme catalyzes the transfer of the methyl group from *S*-adenosyl-L-methionine (SAM) to one of the hydroxyl group of catechols. Catechols are occasionally present in drug candidates (e. g. felodopam) but are frequently encountered as metabolites of drugs (e. g. methylene dioxy-containing compounds such as zamifenacin and paroxetine). The active site of COMT includes the co-enzyme-binding motif and the catalytic site situated in the vicinity of the Mg^{2+} ion. The methyl transfer from SAM to the catechol substrate catalyzed by COMT is a direct bimolecular transfer of the methyl group from the sulphur of α -Me-DOPA to the oxygen of the catechol hydroxyl in an S_N2 -like transition state. The exact juxtaposition of the substrate to the methyl group is possible because of the binding of the two hydroxyl groups to a Mg^{2+}

ion. One hydroxyl of the substrate is surrounded by three positively charged groups inducing it to release its proton to become a negatively charged phenolate ion. These moieties are the Mg^{2+} , the methyl group of SAM and Lys 144. The Mg^{2+} ion in particular probably lowers the pK_a of the hydroxyl group significantly. In contrast, the proton of the other hydroxyl is stabilized by the negatively charged carboxyl group of Glu 199. The ionized hydroxyl makes a direct nucleophilic attack on the electron-deficient methyl of α -Me-DOPA.

7.6.3

Glutathione-S-Transferases

Glutathione-S-transferases (GSTs) are the most important family of enzymes involved in the metabolism of alkylating compounds and their metabolites. They are a major defence system in deactivating toxic materials within the body. The cytosolic GSTs function as dimeric proteins that are assembled from identical or non-identical subunits. Catalytic diversity for the cytosolic isoenzymes originates from the multiplicity of different homo- and hetero-dimeric forms that collectively metabolize a very broad range of structurally diverse electrophilic substrates, although all are highly specific for the thiol-containing substrate glutathione. Understanding the mechanism is considerably helped by the availability of X-ray crystallography data [22].

Each subunit has an active site that appears as a cleft along the domain interface. Each site can be separated into two distinct functional regions: a hydrophilic G-site for binding the physiological substrate glutathione, and an adjacent hydrophobic H-site for binding structurally diverse electrophilic substrates. Although the active sites of glutathione S-transferases are catalytically independent, the full active site is formed by structural elements from both subunits of the dimer. Residues contributing to binding glutathione at the G-site form a network of specific polar interactions. Of key importance is a hydrogen bond between a conserved G-site tyrosine residue and the glutathione thiol group. This hydrogen bond stabilizes the thiolate anion of the active site-bound glutathione. Estimated pK_a values for the bound glutathione are at least two pK_a units below the pK_a value for glutathione free in aqueous solution. The H-site is formed of clusters of non-polar amino acid side chains which provide a highly hydrophobic surface, which, in the absence of a drug substrate is open to bulk solvent. Binding of substrates to this site has been shown to relate to increased lipophilicity for substrates (4-hydroxyalkenes). The actual conjugation reaction, with the thiolate anion acting as a nucleophile proceeds via an S_N2 -type mechanism yielding the “deactivated” product.

7.7

Stability to Conjugation Processes

Conjugation with glucuronic acid or sulphate requires a nucleophilic substituent to be present in the molecule, normally an hydroxyl function. In the case of the glu-

curonyl transferases this can be phenol, primary, secondary or even tertiary alcohol or carboxylate or in the case of sulphotransferases, normally phenol. In some cases primary alcohols can also form sulphate conjugates. The most “reactive” grouping is the phenol and a simple rule is to eliminate such groupings unless essential for activity. In some cases bioisosteres can be introduced to retain pharmacological activity and overcome conjugation. To act as agonists of the dopamine receptor an H-bond donor group is essential in the correct position on a phenyl ring whose centre is situated 5.1 Å from a protonated nitrogen atom [23]. Figure 7.24 illustrates 7-hydroxy-(amino) tetralin analogues which are potent agonists.

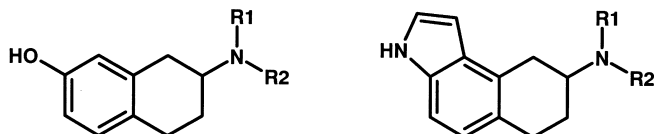


Fig. 7.24 Substitution of a pyrrolo for a phenolic function to act as a H-bond donor for receptor interactions but is resistant to glucuronidation.

These compounds have very low bioavailability and short duration due to extremely rapid glucuronidation [24]. Substitution of the phenolic hydroxy group with a pyrrolo ring (Figure 7.20) gives a series of compounds with a suitable H-bond donor in the correct position (also the geometry matches that of the phenolic hydroxyl), but resistant to glucuronidation [23]. It is not sufficient to replace functionality with

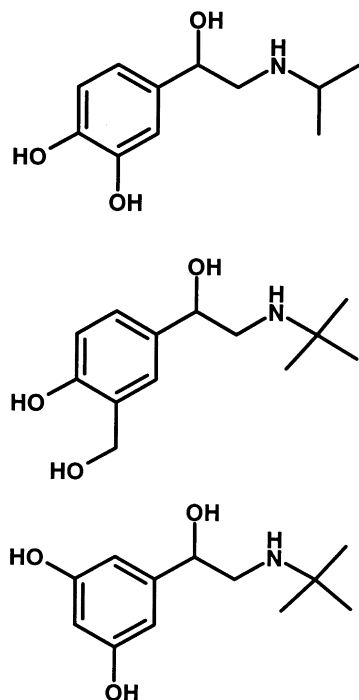


Fig. 7.25 Design of beta-2 selective adrenoceptor agonists resistant to catechol *O*-methyl transferase (COMT).

groupings with similar chemical properties. For instance tetrazolyl is almost an exact mimic of the carboxyl group and readily undergoes glucuronidation.

Catechol methyl transferases require the catechol function to be present to bind to the Mg^{2+} ion. In the search for β_2 -adrenoceptor selectivity to produce potent bronchodilators with low cardiovascular effects, changing the 3,4-hydroxy grouping of the catechol to 3,5- or 3-hydroxyl, 4-methyl-hydroxy, proved to be important (Figure 7.25). These compounds now have much improved bioavailability and pharmacokinetics due to their resistance to catechol methyl transferases.

7.8 Pharmacodynamics and Conjugation

In a number of cases the transferase enzymes metabolize compounds to active species. Morphine is a highly potent opioid analgesic (Figure 7.26) and is metabolized by glucuronidation of both its hydroxyl functions in both the gastrointestinal tract and the liver. Glucuronidation of the 6-position to form morphine-6-glucuronide gives a compound that is also active [25]. Given systemically, the metabolite is twice as potent as morphine itself. When administered intrathecally the compound is approximately 100-fold more potent than the parent morphine.

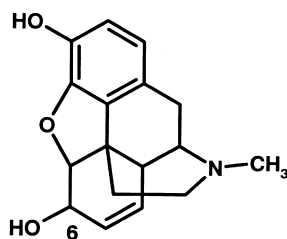


Fig. 7.26 Structure of morphine, which is metabolized to a more active opioid analgesic by glucuronidation at the 6 position.

Unlike morphine, minoxidil [26] is not active itself but is metabolized by hepatic sulphotransferases to minoxidil *N*-*O* sulphate (Figure 7.27).

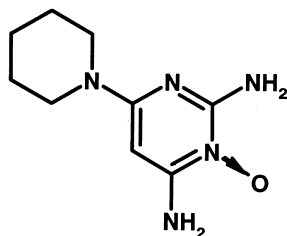


Fig. 7.27 Structure of minoxidil a compound metabolized by sulphotransferases to a potassium channel activator.

Minoxidil sulphate is a potent activator of the ATP-modulated potassium channel and thereby relaxes vascular smooth muscle to give a resultant antihypertensive effect. The actual sulphate metabolite is a relatively minor metabolite, the principal

metabolite being the *N-O* glucuronide. The discovery of minoxidil illustrates the caution which should be applied to screening compounds solely *in vitro*. Occasionally *in vivo* experiments will provide significant advances as a result of the metabolism of novel active agents.

References

- 1 Smith DA, Jones BC, *Biochem. Pharmacol.* **1992**, *44*, 2089–2104.
- 2 Gillis AM, Kates RE, *Clin. Pharmacokinet.* **1984**, *9*, 375–403.
- 3 Lee JT, Kroemer HK, Silberstein DJ, Funck-Brentano C, Lineberry MD, Wood AJ, Roden DM, Woosley RL, *New Engl. J. Med.* **1990**, *322*, 1764–1768.
- 4 Manoury PM, Binet JL, Rousseau J, Leferre-Borg FM, Cavero IG, *J. Med. Chem.* **1987**, *30*, 1003–1011.
- 5 Marchetti P, Natalesi R, *Clin. Pharmacokinet.* **1989**, *16*, 100–1286.
- 6 Verbeck RK, Blackburn JL, Loewen GR, *Clin. Pharmacokinet.* **1983**, *8*, 297–331.
- 7 Dugar S, Yumibe N, Clader JW, Vizziano M, Huie K, Heek MV, Compton DS, Davis HR, *Biorg. Med. Chem. Lett.* **1996**, *6*, 1271–1274.
- 8 Penning TD, Talley JJ, Bertenshaw SR, Carter JS, Collins PW, Docter S, Graneto MJ, Lee LF, Malecha JW, Miyashiro JM, Rogers RS, Rogier DJ, Yu SS, Anderson GD, Burton EG, Cogburn EG, Gregory SA, Koboldt CM, Perkins WE, Seibert K, Veenhuizen AW, Zhang AW, Isaakson PC, *J. Med. Chem.* **1997**, *40*, 1347–1365.
- 9 Floyd DM, Dimball SD, Drapcho J, Das J, Turk CF, Moquin RV, Lago MW, Duff KJ, Lee VG, White RE, Ridgewell RE, Moreland S, Brittain RJ, Normandin DE, Hedberg SA, Cucinotta GC, *J. Med. Chem.* **1992**, *35*, 756–772.
- 10 Rosenblum SB, Huynh T, Afonso A, Davis HR, Yumibe N, Clader JW, Burnett DA, *J. Med. Chem.* **1998**, *41*, 973–980.
- 11 Evams ME, Stemp G, *Chem. Brit.* **1991**, *27*, 439–442.
- 12 Hoke F, Cunningham F, James MK, Muir KT, Hoffman WE, *J. Pharmacol. Exp. Ther.* **1997**, *281*, 226–232.
- 13 Baxter AJ, Carr RD, Eyley SC, Fraser-Rae L, Hallam C, Harper ST, Hurved PA, King SJ, Menchani P, *J. Med. Chem.* **1992**, *35*, 3718–3720.
- 14 Kumar GN, Bodor N, *Curr. Med. Chem.* **1996**, *3*, 23–36.
- 15 Kaye B, Brearley CJ, Cussans NJ, Herron M, Humphrey MJ, Mollatt AR, *Xenobiotica* **1997**, *27*, 1091–1102.
- 16 Burchell B, In: *Handbook of Drug Metabolism.* (Ed. Woolf TF), pp. 153–173. Marcel Dekker, New York, **1999**.
- 17 Yin H, Bennett G, Jones JP, *Chemico-Biol. Int.* **1994**, *90*, 47–58.
- 18 Duffel MW, Jacoby WB, *J. Biol. Chem.* **1981**, *256*, 11123–11127.
- 19 Dajani R, Cleasby A, Neu M, Wonacott AJ, Jhoti H, Hood AM, Modi S, Hersey A, Taskinen J, Cooke RM, Manchee GR, Coughtrie MWH, *J. Biol. Chem.* **1999**, *274*, 37862–37868.
- 20 Kakuta Y, Petrotchenko EV, Pedersen LC, Negishi M, *J. Biol. Chem.* **1998**, *273*, 27324–27330.
- 21 Vidgren J, Svensson LA, Liijas A, *Nature* **1994**, *368*, 354–358.
- 22 Dirr H, Reinemer P, Huber R, *Eur. J. Biochem.* **1994**, *220*, 645–661.
- 23 Asselin AA, Humber LG, Roith K, Metcalf G, *J. Med. Chem.* **1986**, *29*, 648–654.
- 24 Stjernlof P, Gullme M, Elebring T, Anderson B, Wikstrom H, Lagerquist S, Svensson K, Ekman A, Carlsson A, Sundell S, *J. Med. Chem.* **1993**, *36*, 2059–2065.
- 25 Paul D, Standifer KM, Inturrisi CE, Pasternack GW, *J. Pharmacol. Exp. Ther.* **1989**, *251*, 477–483.
- 26 McCall JM, Aiken JW, Chidester CG, DuCharme DW, Wendling MG, *J. Med. Chem.* **1983**, *26*, 1791–1793.

8

Toxicity

Abbreviations

ANF	Atrial natriuretic factor (also ANP: atrial natriuretic peptide)
COX	Cyclooxygenase
ENCC	Electroneutral Na–Cl co-transporter
hFGF	Human fibroblast growth factor
GSH	Glutathione
HMG-CoA	3-Hydroxy-3-methylglutaryl coenzyme A
LH	Luteinizing hormone
5-LPO	5-Lipoxygenase
NK	Neurokinin
NKCC	Old name for ENCC
PBPK/PD	Physiologically-based pharmacokinetic/pharmacodynamic (modelling)
PCNA	Proliferating cell nuclear antigen
PPAR- γ	Peroxisome proliferator-activated receptor γ
TA2	Thromboxane
VEGF	Vascular endothelial growth factor

8.1

Toxicity Findings

A complex series of *in vitro* tests, animal test and then human exposure can at any stage reveal adverse findings that can be termed toxicity. Broadly, toxicity findings can be broken down into the following three sub-divisions.

8.1.1

Pharmacophore-induced Toxicity

This involves findings relating to the pharmacology of the compound. Within this category the adverse effects are either a direct or an indirect extension of the pharmacology. With the indirect extension the original selectivity of the compound for a target is lost at elevated doses and the effects seen are triggered by effects on proteins

etc., which are closely related structurally to the original target. Pharmacophore-induced toxicity is usually seen at doses in excess of the therapeutic dose.

Pharmacophore-induced toxicity does not necessarily occur within the organ or site of intended therapy. An example of this is the toxicity of loop diuretics [1]. The target for this class of drugs are the Na-(K)-Cl co-transporters of the kidney. These co-transporters play a major role in the ion transport and fluid secretion of the utricle and semicircular canal of the ear. Perhaps not surprisingly loop diuretics are associated with ototoxicity. The selectivity and potency of various diuretics can explain their different toxicity profiles. Kidney-specific co-transporters ENCC1 and ENCC2 are expressed in the thick ascending limb and distal convoluted tubule, respectively. ENCC3 is expressed in many tissues including the cochlea. Thiazide diuretics only have activity against ENCC1 and show no toxicity. Loop diuretics inhibit NKCC2 with potencies for bumetanide $< 0.2 \mu\text{M}$ and NKCC3 $> 0.5 \mu\text{M}$. The selectivity of the compound for NKCC2 is lost under the conditions which cause ototoxicity: intravenous administration of high doses.

Unexpected or polypharmacology in a structure can occasionally lead to additional benefits in drugs. In the same way polypharmacology can have dramatic consequences in toxicity. Thalidomide was used as an anti-nausea drug to control morning sickness. Its use in pregnant women had terrible consequences due to the teratogenic nature of the drug.

Recently thalidomide and some of its metabolites (Figure 8.1) and related analogues have been shown to be inhibitors [2] of hFGF- and VEGF-induced neovascularization (angiogenesis). Such a finding readily provides an hypothesis for the causes of teratogenicity associated with thalidomide, since limb development (the site of teratogenesis) is dependent on the formation of new blood vessels.

A problem with toxicity produced by an extension of the pharmacology of a compound, is that the conventional use of no-effect doses based on pre-clinical animal studies may not apply. Moreover pre-clinical studies may be complicated by the often understated ranges of response seen across species due to species differences in the receptors, enzymes and ion channels that comprise drug targets. Table 8.1 lists some of these known variations and the consequences range from an exaggerated response, to an absence of a response.

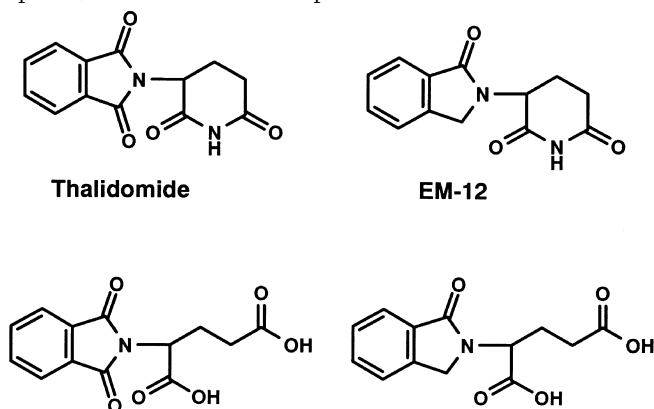


Fig. 8.1 Structures of thalidomide, EM-12 and their metabolites which are all angiogenesis inhibitors and teratogens or potential teratogens.

Tab. 8.1 Receptors, ion channels and enzymes which are drug targets and show species differences.

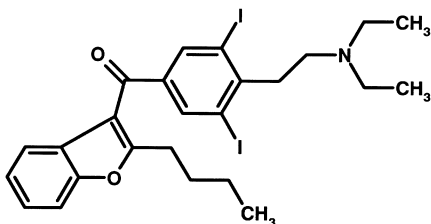
Receptors			
Adenosine	A ₁ , A ₂	Luteinizing hormone	LH
Adrenoceptors	α _{1B} , α _{1C} , α _{2A}	Muscarinic	M ₂
Atrial natriuretic factor	ANF-R1	Neurokinin	NK ₁ , NK ₃
Bradykinin	B ₂	Purinoreceptors	P ₂
Cholecystokinin	CCK	Thromboxane	TA ₂
Dopamine	D ₁	Vanilloid	
Endothelin	ET _B	Vasopressin	V ₁
Serotonin	5-HT _{1A, B, D} 5-HT ₂ , 5-HT ₃ , 5-HT ₄		
Ion Channels			
Rapidly activating delayed rectifier K ⁺ channel			
Enzymes			
Carboxypeptidase B	Renin		
Na ⁺ /K ⁺ ATPase	HMG-CoA reductase		

8.1.2

Structure-related Toxicity

Findings related to the structure of the compound but not related to the pharmacology can provide another possible source of toxicity. This category is distinguished by the adverse events or effects being triggered by structural features or physicochemical properties etc. which allow the compound or metabolites to interact at sites distinct from the intended target or related proteins, etc. This type of toxicity can occur at any dose level including the therapeutic dose.

Amiodarone (Figure 8.2) is an efficacious drug that causes a number of side-effects. The presence of iodine in the molecule is unusual and hypo- and hyperthyroidism have been reported in patients. Although the loss of iodine is relatively slow the relatively large daily dose size and long half-life of the drug and its de-ethylated metabolite suggest that the presence of iodine in the molecule is responsible for its toxicity [3].

**Fig. 8.2** Structure of the highly lipophilic anti-arrhythmic, amiodarone.

The drug is also a highly lipophilic base and accumulates in a number of tissues including the lung. This combination of extreme physicochemical properties can result in more specific interactions such as the condition of phospholipidosis (increase in total lung phospholipids) caused by inhibition of phospholipid breakdown [4]. The medicinal chemist has to decide if extreme lipophilicity and the presence of iodine are essential for activity and, in the case of amiodarone, proven clinical efficacy or whether alternative structures are possible.

Proxicromil and FPL 52757 [5] were oral anti-allergy agents that utilized the strongly acidic “chromone” skeleton as a starting point (Figure 8.3). This skeleton contained the pharmacophore. To achieve oral absorption substantial lipophilicity was added and these changes resulted in surface active (detergent) molecules. The hepatobiliary route of excretion and resultant high concentrations of the compounds at the biliary cannaliculus resulted in hepatotoxicity [5].

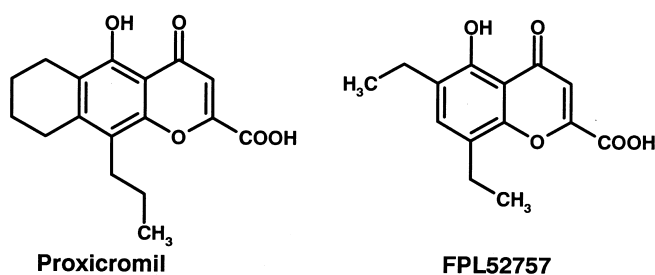


Fig. 8.3 Structures of proxicromil and FPL 52757, two compounds which exhibited toxicity due to their physicochemical properties.

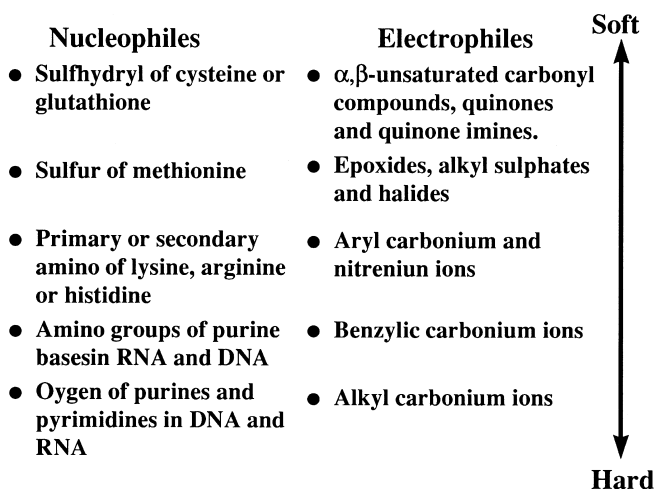
8.1.3

Metabolism-induced Toxicity

Metabolism-induced toxicity results when a key function or grouping is altered by oxidation, reduction or conjugation to become reactive, normally an electrophile [6]. The electrophilic group is then capable of reacting with nucleophiles in the body. Nucleophilic functions are present in proteins, nucleic acids and small peptides such as glutathione (see Section 8.1.2). Reactions with these targets can lead to organ toxicity including carcinogenesis or simply excretion from the body (glutathione conjugates). Some indication of the possible targets [7] is indicated by the nature of the electrophile produced (soft–hard), as indicated in Figure 8.4.

Compounds that react with amino acids or proteins can trigger toxicity by two mechanisms. The direct mechanism involves reaction with specific proteins thus altering their function such that cell death and necrosis occurs. Such toxicities are often seen in a large number of subjects and are dose related. They are also often predicted from animal studies. Alternative mechanisms of toxicity involve an immune component, whereby the protein–metabolite conjugate triggers an immune response. Such toxicity is termed idiosyncratic, occurring in only a subset of the patients receiving the drug. This type of toxicity is not predicted normally by animal studies. These two types of toxicity are illustrated in the schematic shown in Figure 8.5. Glutathione and the glutathione transferase enzymes protect the body from

Fig. 8.4 Schematic showing relative softness and hardness of nucleophiles and electrophiles as an indicator of sites of reaction of electrophilic metabolites.



the reactive metabolites. This system is saturable, so that a threshold dose, or other factors leading to glutathione depletion, is needed to trigger toxicity.

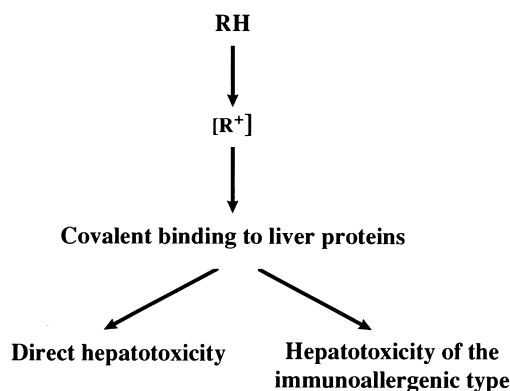


Fig. 8.5 Schematic showing the generation of a reactive metabolite, its reaction with a protein target, and toxicity resulting from a direct mechanism (protein essential to cell function) or one involving the immune system.

8.2 Epoxides

Epoxide metabolites can be generated from a variety of aromatic systems. Anticonvulsants are a class of drug whose side-effects, such as hepatic necrosis and aplastic anaemia, are thought to be mediated by chemically reactive epoxide metabolites formed by cytochrome P450 oxidation. For instance phenytoin (Figure 8.6) toxicity is correlated with oxidation and the inhibition of epoxide hydrolase [8].

Carbamazepine exerts its anticonvulsant activity through its own action on voltage sensitive sodium channels and those of its relatively stable 10-11-epoxide. The compound shows a number of potential toxicities including skin rash, hepatic necrosis and teratogenicity. It is possible the 10-11-epoxide is the causative agent, but struc-

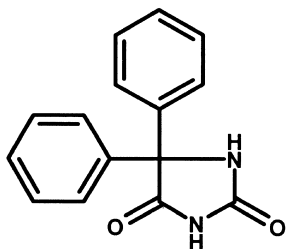


Fig. 8.6 Structure of phenytoin, a drug believed to assert its toxicity through reactive epoxide metabolites.

tural studies [9] suggest other epoxide metabolites of the aromatic ring may be responsible in part. Oxcarbazepine (Figure 8.7) is a related drug that cannot form the 10-11-epoxide and owes part of its activity to its hydroxyl metabolite. Oxcarbazepine is much less teratogenic in animal models and shows a lower preponderance of skin rash [8,10].

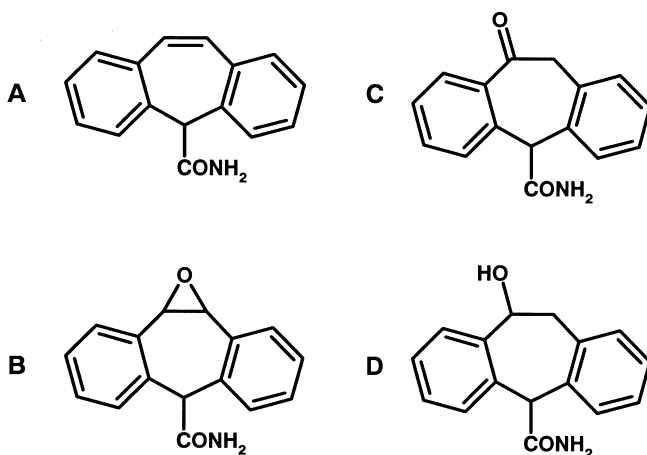


Fig. 8.7 Structures of carbamazepine (A), its 10-11-epoxide metabolite (B), and oxcarbazepine (C) and its hydroxyl metabolite (D).

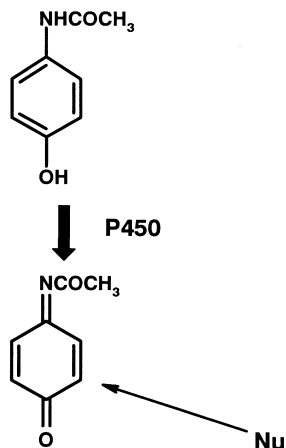
8.3

Quinone Imines

Phenacetin is a classical example of a quinone imine, with oxidation of the compound by cytochrome P450 leading to a benzoquinone intermediate (Figure 8.8). The benzoquinone reacts with various cytosolic proteins to trigger direct hepatotoxicity [6].

Toxicity by metabolism is not confined to the liver since oxidative systems occur in many organs and cells. Amodiaquine is a 4-aminoquinoline antimalarial that has been associated with hepatitis and agranulocytosis. Both side-effects are probably triggered by reactive metabolites produced in the liver or in other sites of the body. For instance polymorphonuclear leucocytes can oxidize amodiaquine. It appears that amodiaquine is metabolized to a quinone imine by the same pathway as that seen in

Fig. 8.8 Oxidation of phenacetin to a benzoquinone intermediate.



the case of acetaminophen [11] (Figure 8.9), suggesting that such structural features in a molecule should be avoided.

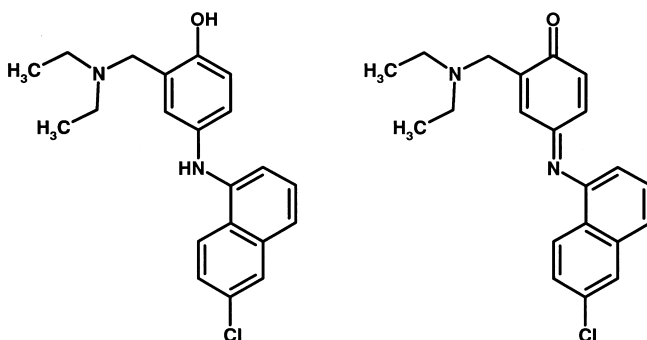


Fig. 8.9 Structures of amodiaquine and its quinone imine metabolite.

Such reactions can occur in other molecules containing aromatic amine functions without a para oxygen substituent. For instance diclofenac can be oxidized to a minor metabolite (5-OH) diclofenac which can be further oxidized [12] to the benzoquinone imine metabolite (Figure 8.10). Again, the reactivity of this intermediate has been implicated in the hepatotoxicity of the compound.

Another drug with a high incidence of hepatotoxicity is the acetylcholinesterase inhibitor tacrine. Binding of reactive metabolites to liver tissue correlated with the formation of a 7-hydroxy metabolite [13], highly suggestive of a quinone imine metabolite as the reactive species. Such a metabolite would be formed by further oxidation of 7-hydroxy tacrine (Figure 8.11).

Indomethacin is associated, in the clinic, with a relatively high incidence of agranulocytosis. Although indomethacin itself is not oxidized to reactive metabolites, one of its metabolites, dsemethyldeschlorobenzoylindomethacin (DMBI) forms an iminoquinone [14]. Formation of the iminoquinone from DMBI is catalysed by

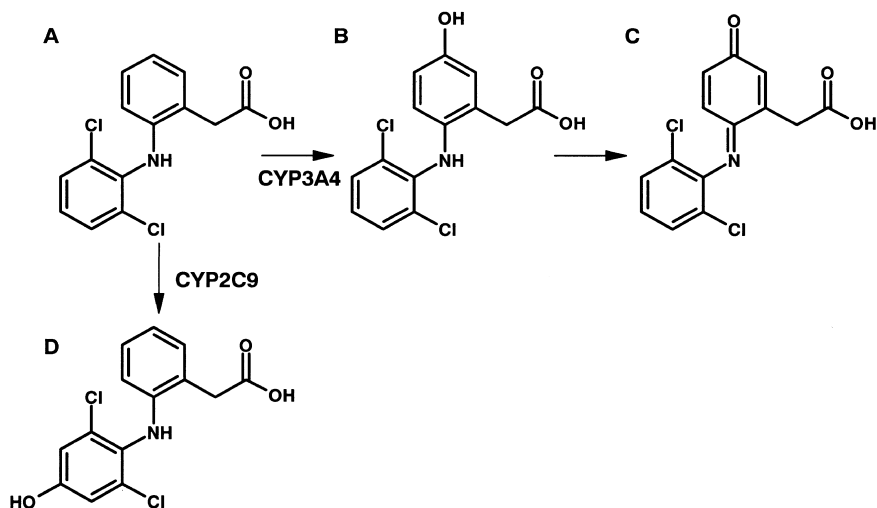


Fig. 8.10 Scheme showing metabolism of diclofenac by oxidation (A) to benzoquinone imine (C) metabolites.

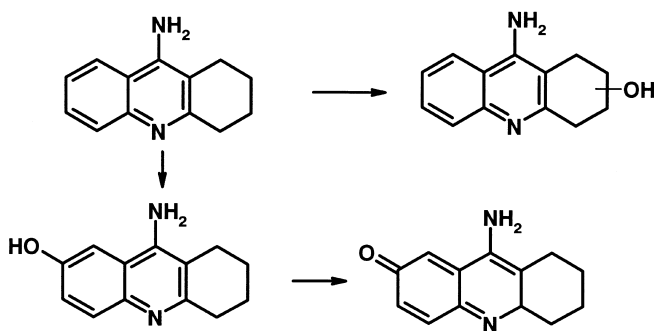


Fig. 8.11 Metabolism of tacrine to hydroxyl metabolites, the 5-hydroxy derivative of which can be further oxidized to the reactive quinone imine.

myeloperoxidase (the major oxidizing enzyme in neutrophils) and HOCl (the major oxidant produced by activated neutrophils). The pathway for formation of the iminoquinone is illustrated in Figure 8.12.

Practolol (Figure 8.13) was the prototype cardioselective β -adrenoceptor blocking agent. Selectivity was achieved by substitution in the para position with an acetyl anilino function. The similarity of this drug with those outlined above is obvious. Practolol caused severe skin and eye lesions in some patients which led to its withdrawal from the market [6]. These lesions manifested as a rash, hyperkeratosis, scarring, even perforation of the cornea and development of a fibrovascular mass in the conjunctiva, and sclerosing peritonitis. Some evidence is available that the drug is oxidatively metabolized to a reactive product that binds irreversibly to tissue pro-

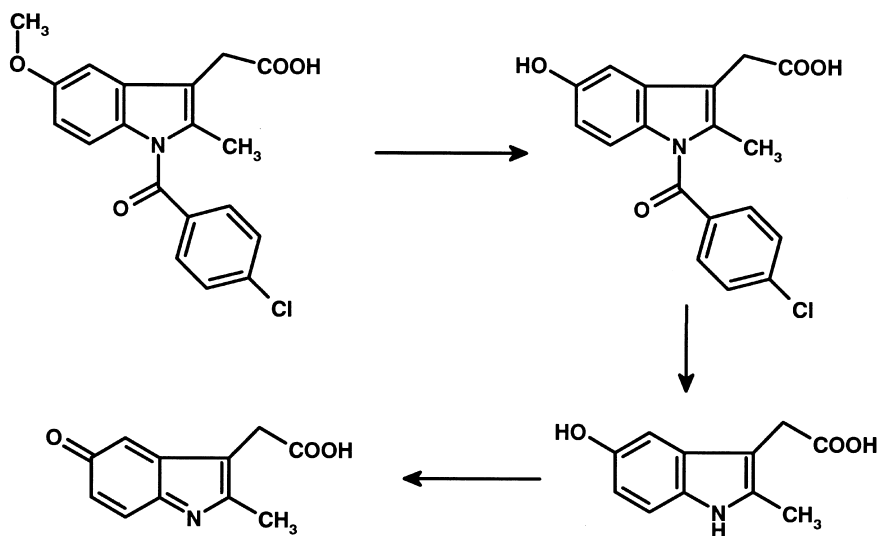


Fig. 8.12 Metabolism of indomethacin to a reactive iminoquinone metabolite.

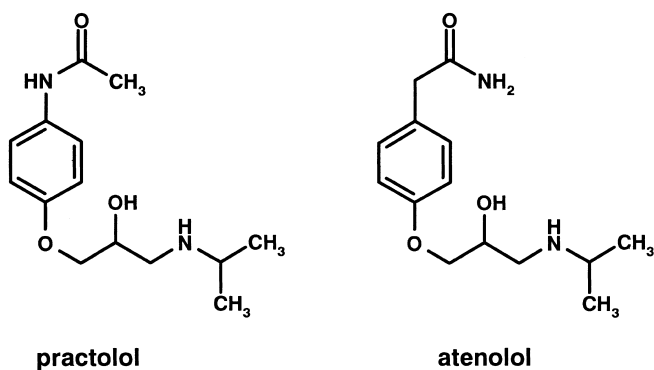


Fig. 8.13 Structures of practolol and atenolol.

teins. That the toxic functionality is the acetanilide is confirmed by the safety of a follow-on drug atenolol. Atenolol (Figure 8.13) has identical physicochemical properties and a very similar structure except that the acetyl-amino function has been replaced with an amide grouping. This structure cannot give rise to similar aromatic amine reactive metabolites. The withdrawal of practolol from the market is obviously a severe blow to the manufacturer and to those patients who benefited from it. Although not shown to be the cause of toxicity the presence of an aromatic amine in the structure of nomifensine (Figure 8.14) has to be treated with suspicion, the compound was also withdrawn from the market 9 years after its launch due to a rising incidence of acute immune haemolytic anaemia [15].

Carbutamide was the first oral anti-diabetic, and the prototype for the sulphonamide type of agent. Carbutamide caused marked bone marrow toxicity in man, but derivatives of this, not containing the anilino function, such as tolbutamide

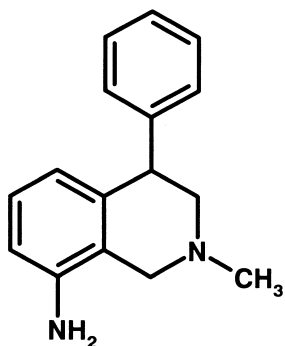


Fig. 8.14 Structure of normifensine, an antidepressant associated with acute immune haemolytic anaemia.

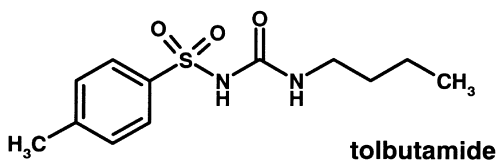
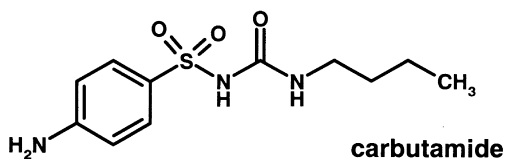


Fig. 8.15 Structures of carbutamide an oral anti-diabetic, associated with bone marrow toxicity, and tolbutamide a compound without similar effects.

(Figure 8.15), were devoid of such toxicity. As for many of the agents featured in this section the structural similarity between carbutamide and tolbutamide clearly implicates the anilino function as the toxicophore.

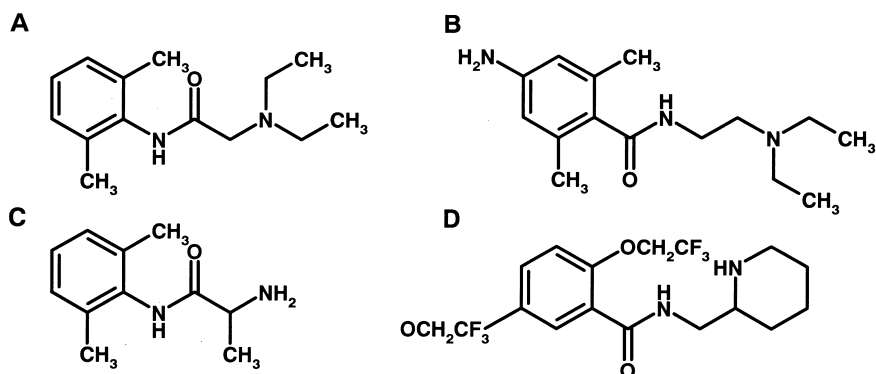


Fig. 8.16 Structures of Na⁺ channel blocker antiarrhythmics: lidocaine (A), procaineamide (B), tocainide (C) and flecainide (D).

A further example of the design of drugs to remove aromatic amine functionalities even when present as an amide, is illustrated by the Na^+ channel class of antiarrhythmic drugs [16]. Lidocaine is very rapidly metabolized (Figure 8.16) and so is only useful as a short-term intravenous agent. Oral forms include procainamide, tocainide and flecainide (Figure 8.16). Procainamide causes fatal bone marrow aplasia in 0.2% of patients and lupus syndrome in 25–50%. Tocainide also causes bone marrow aplasia and pulmonary fibrosis. In contrast, flecainide, whose structure contains no aromatic amine, masked or otherwise, has adverse effects related directly to its pharmacology. Interestingly, the lupus syndrome seen with procainamide is largely absent when *N*-acetyl procainamide is substituted.

8.4

Nitrenium Ions

Clozapine, an antipsychotic agent, has the potential to cause agranulocytosis with an incidence of 1%. The major oxidant in human neutrophils, HOCl, oxidizes clozapine to a nitrenium ion (Figure 8.17) in which the positive charge is highly delocalized. This metabolite is capable of binding irreversibly to the neutrophil [17]. A variety of cells including liver, neutrophils and bone marrow can form reactive clozapine metabolites which react to form glutathione thioether adducts [18].

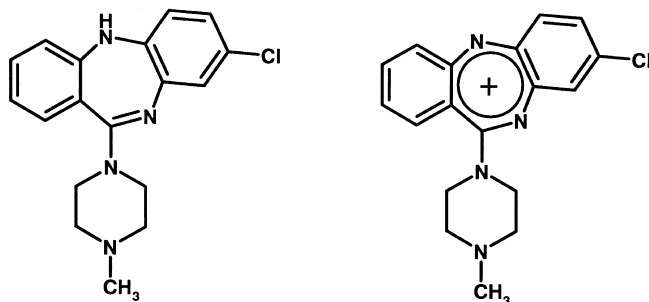


Fig. 8.17 Structures of clozapine and its nitrenium ion, the postulated reactive metabolite generated by oxidation.

Various analogues have been investigated indicating that the nitrogen-bridge between the two aromatic rings is the target, at least for HOCl oxidation. When alter-

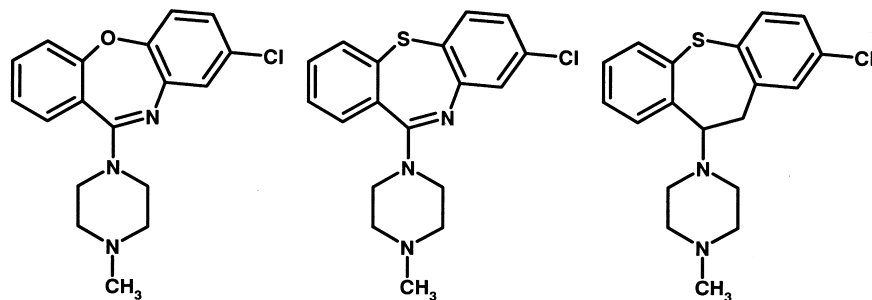


Fig. 8.18 Alternative structures which will not generate the nitrenium ion observed with clozapine.

native bridging heteroatoms are used (Figure 8.18) similar reactive metabolites are not observed [19].

8.5

Iminium Ions

Mianserin is a tetracyclic antidepressant that causes agranulocytosis in isolated cases in patients. Detailed structural analysis [20] has indicated that oxidation by cytochrome P450 to one or more iminium ions is the likely causative first step in this toxicity, the most likely being the C4–N5 version (Figure 8.19). Evidence for this is provided by the C14 β methyl and the O10 analogues which cannot form the corresponding nitrenium and carbonium ions, but are cytotoxic. Removal of the N5 nitrogen atom in analogous structures abolishes production of the reactive metabolites (Figure 8.20).

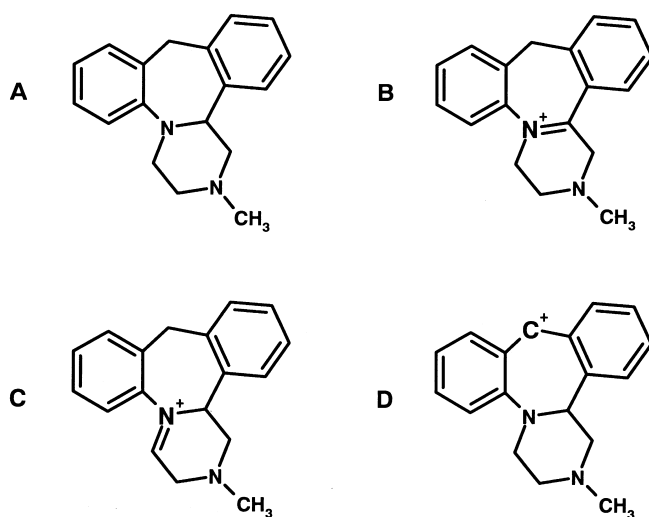


Fig. 8.19 Structures of mianserin (A) with N5 shown and its putative reactive metabolites: N5–C14 β iminium ion (B), C4–N5 iminium ion (C) and carbonium ion at C10 (D). Evidence indicates that metabolite B is the causative agent.

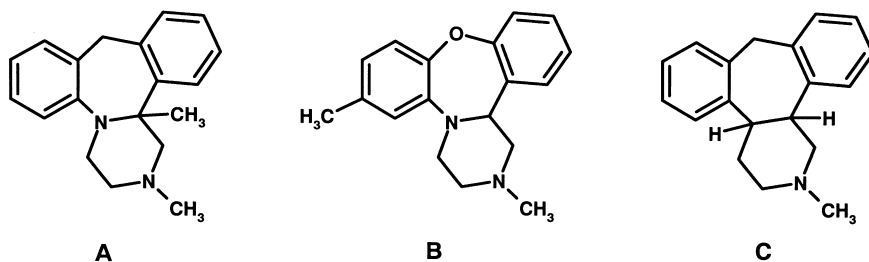


Fig. 8.20 Structures of mianserin analogues. A and B cannot form the N5–C14 β iminium and C10 carbonium ion but are still toxic. C without the N5 nitrogen is not toxic implicating the C4–N5 iminium ion.

Vesnarinone is a drug used to treat congestive heart failure and is associated with a 1% incidence of agranulocytosis. When metabolized by activated neutrophils the major metabolite is veratrylpiperazinamide (Figure 8.21). This unusual *N*-dealkylation (of an aromatic ring) can be rationalized by chlorination of the nitrogen to which the aromatic ring is attached by HOCl, followed by the loss of HCl to form the reactive iminium ion, which itself can react with nucleophiles. Hydrolysis of the iminium ion yields veratrylpiperazinamide and another reactive species, the quinone imine (see Section 8.3).

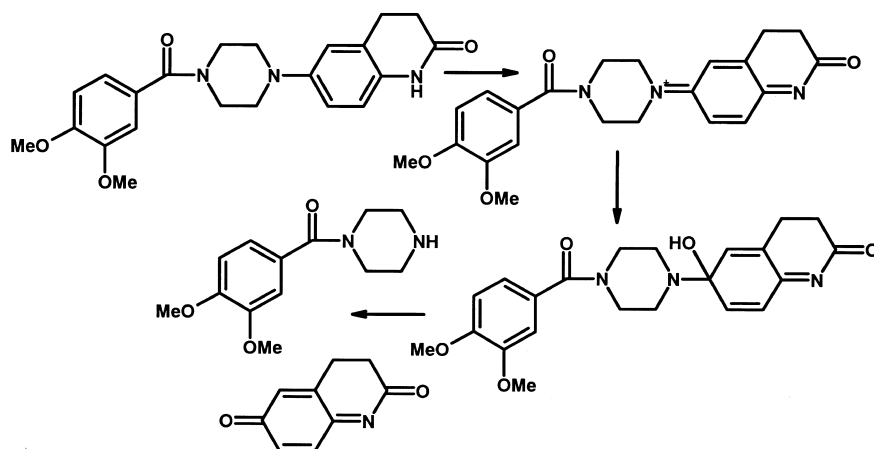


Fig. 8.21 Structures of vesnarinone, and its major metabolite veratrylpiperazinamide. The pathway metabolized by activated neutrophils gives rise to two highly reactive species, an iminium ion and a quinone imine.

8.6

Hydroxylamines

Sulphonamide antimicrobial agents (Figure 8.22) such as sulphamethoxazole [21] are oxidized to protein-reactive cytotoxic metabolites in the liver and also other tissues. These include hydroxylamines and further products such as nitroso-derivatives. Sulphonamide drugs are linked with agranulocytosis, aplastic anaemia and

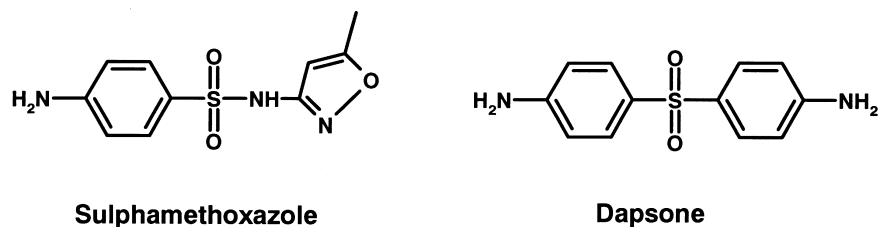


Fig. 8.22 Structures of sulfamethoxazole and dapsone, drugs which form toxic hydroxylamine metabolites.

skin and mucous membrane hypersensitivity reactions including Stevens-Johnson syndrome, and others. Dapsone [22] is a potent anti-inflammatory and anti-parasitic compound, which is metabolized by cytochrome P450 to hydroxylamines, which in turn cause methaemoglobinemia and haemolysis.

8.7

Thiophene Rings

Thiophene rings comprise another functionality that is easily activated to electrophilic species. Thiophene itself is metabolized to the *S*-oxide, which is viewed as the key primary reactive intermediate. Nucleophilic groups such as thiols react at position 2 of the thiophene *S*-oxide via a Michael-type addition [23]. Tienilic acid (Figure 8.23) is oxidized to an *S*-oxide metabolite [24], creating two electron-withdrawing substituents on C2 and a resultant strongly electrophilic carbon at C5 of the thiophene ring [24]. This highly reactive metabolite covalently binds to the enzyme metabolizing it (CYP2C9), triggering an autoimmune reaction resulting in hepatitis. Rotation of the thiophene ring leads to a compound in which the sulphoxide is less reactive and [24] can create a less reactive sulphoxide metabolite which reacts primarily at C2 with nucleophiles. This metabolite is stable enough to escape the enzyme and alkylate other proteins leading to direct toxicity.

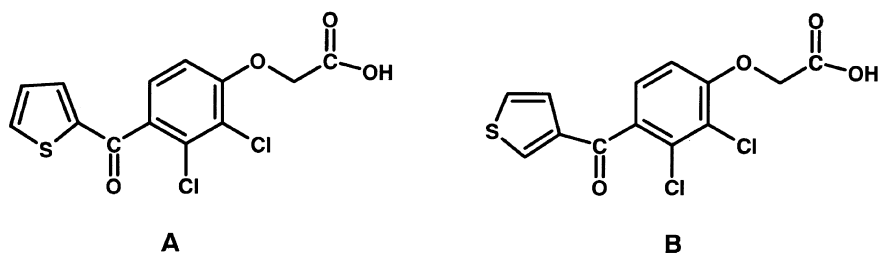


Fig. 8.23 Structure of tienilic acid (A) and an isomeric variant (B) which cause hepatotoxicity by autoimmune and direct mechanisms respectively, following conversion to sulphoxide metabolites and resultant electrophilic carbon atoms.

The thiophene ring has also been incorporated into a number of drugs which have diverse toxicities associated with them (Figure 8.24). Ticlopidine, a platelet function inhibitor, is associated with agranulocytosis in patients [25]. Suprofen, a non-

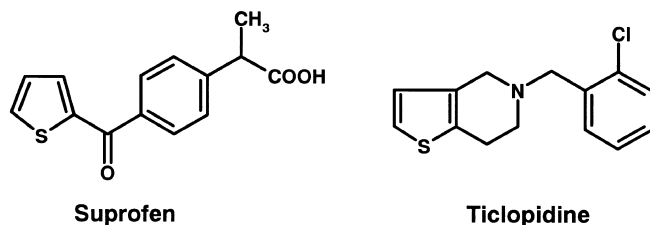


Fig. 8.24 Structures of suprofen and ticlopidine, compounds containing a thiophene ring and associated with diverse toxicities in patients.

steroidal anti-inflammatory agent has been withdrawn from the market due to acute renal injury [26].

The association of ticlopidine with agranulocytosis has been further investigated [27]. A general hypothesis for white blood cell toxicity is the activation of the drug to a reactive metabolite by HOCl, the principal oxidant being generated by activated neutrophils and monocytes (as in Section 8.4). Under these types of oxidation conditions ticlopidine is activated to a thiophene-S-chloride (Figure 8.25) which reacts further to form other products including a glutathione conjugate.

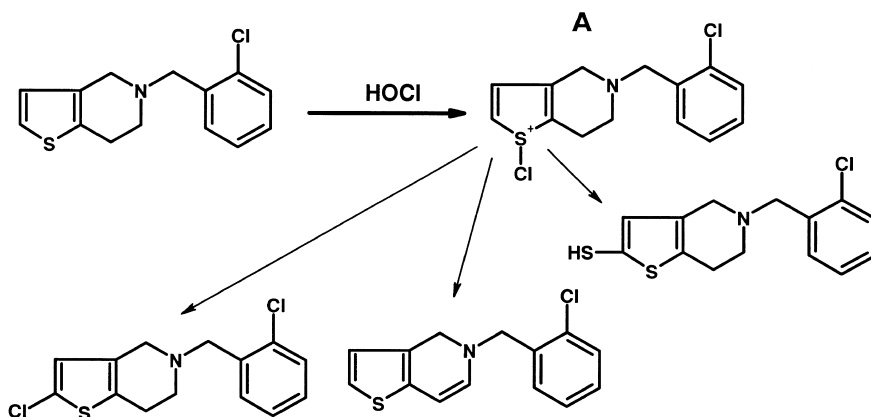


Fig. 8.25 Metabolism of ticlopidine by white blood cells to the reactive thiophene-S-chloride (A) and further breakdown products of this reactive metabolite.

Tenidap (Figure 8.26) is a dual cyclooxygenase (COX) and 5-lipoxygenase (5-LPO) inhibitor developed as an anti-inflammatory agent. Severe abnormalities in hepatic function were reported in Japanese clinical trials [28]. Although the thiophene is not directly implicated in these findings, the ready activation of this system to potential reactive metabolites may be suggestive of the involvement of this function.

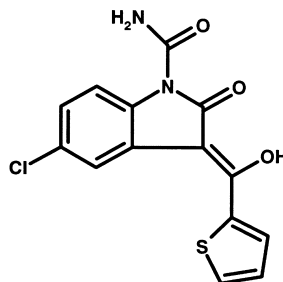


Fig. 8.26 Structure of tenidap, a compound containing a thiophene ring and associated with changes in hepatic function.

8.8

Thioureas

The thiourea group has been incorporated into a number of drugs. The adverse reactions of such compounds are associated with the thioncarbonyl moiety. The thioncarbonyl moiety can be metabolized by flavin-containing monooxygenases and cytochrome P450 enzymes to reactive sulphenic, sulphinic and sulphonic acids which can alkylate proteins. The prototype H₂ antagonist metiamide [29] incorporated a thiourea group. This compound caused blood dyscrasias in man. Replacement of the thiourea [29] with a cyanimino grouping produced the very successful compound cimetidine (Figure 8.27).

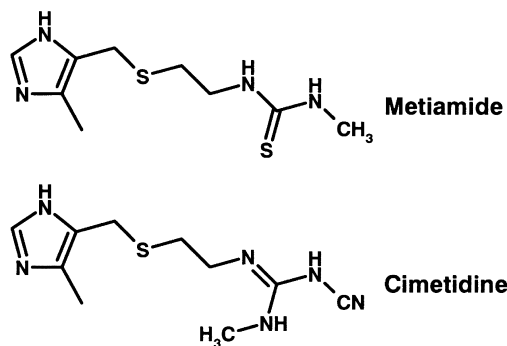


Fig. 8.27 Structures of the thiourea-containing H₂ antagonist metiamide, which caused blood dyscrasias in man, and its cyanimino-containing analogue cimetidine which did not show similar adverse effects.

8.9

Chloroquinolines

Chloroquinolines are reactive groupings due to electron-deficient carbon to which the halogen is attached. This carbon is electron-deficient due to the combined electron-withdrawing effects of the chlorine substituent and the quinoline nitrogen. The electrophilic carbon is thus able to react readily with nucleophiles present in the body. The impact of this grouping on a molecule is illustrated by 6-chloro-4-oxo-10-propyl-4*H*-pyrano[3,2-*g*]quinoline-2,8-dicarboxylate (Figure 8.28). In contrast to many related compounds (chromone-carboxylates) lacking the chloroquinoline, 6-chloro-4-oxo-10-propyl-4*H*-pyrano[3,2-*g*]quinoline-2,8-dicarboxylate is excreted as a

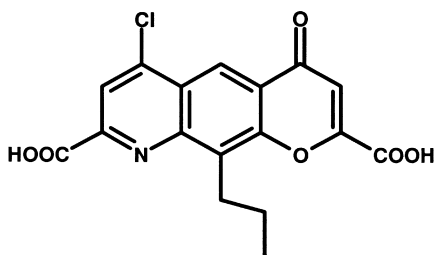


Fig. 8.28 Structure of 6-chloro-4-oxo-10-propyl-4*H*-pyrano[3,2-*g*]quinoline-2,8-dicarboxylate which, in contrast to many related compounds (chromone-carboxylates) lacking the chloroquinoline, is excreted as a glutathione conjugate.

glutathione conjugate [30] formed by nucleophilic attack on the halogen of the chloroquinoline function by the thiol group of glutathione and resultant halogen displacement. Other compounds are excreted as unchanged drug with no evidence of any metabolic breakdown. Moreover the reactivity of the chloroquinoline is illustrated by the observation that the reaction with glutathione occurs without enzyme (glutathione-S-transferase) present *in vitro*, albeit at a slower rate.

8.10

Stratification of Toxicity

Table 8.2 gives a summary of the various toxicities and the stages at which they can occur. Also summarized are the causes for the specificity of the effect. With mutagenicity, certain pre-clinical toxicity, carcinogenicity and late clinical toxicology, the actual structure of the molecule is important and care should be taken to avoid the incorporation of toxicophores into compounds, as outlined about. Direct toxicity is addressed by ensuring the daily dose size is low, the intrinsic selectivity high and the physicochemical properties within reasonable boundaries.

Tab. 8.2 Various expressions of toxicity and their cause relating to the stage of drug development.

Mutagenicity	Metabolites react with nucleic acid	Metabolites sufficiently stable to cross nuclear membrane
Pre-clinical and early clinical	Toxicity directly related to dose size and intrinsic selectivity. Metabolites react with protein and cause cell death	Overstimulation of receptor and others in superfamily. Metabolites not detoxified by glutathione etc.
Carcinogenicity	Metabolites react with nucleic acid or hormonal effects	Metabolites not detoxified by glutathione etc. Effects on thyroxine etc. leads to pituitary tumours
Late clinical	Metabolites react with protein	Protein adduct acts as immunogen; immune response involved in toxicity.

8.11

Toxicity Prediction - Computational Toxicology

With increasing toxicity data of various kinds, more reliable predictions based on structure–toxicity relationships of toxic endpoints can be attempted [31–36]. Even the Internet can be used as a source for toxicity data, albeit with caution [37]. A number of predictive methods have been compared from a regulatory perspective [35]. Often traditional QSAR approaches using multiple linear regression are used [38]. Newer approaches include the use of neural networks in structure–toxicity relationships

[39]. An expert system such as DEREK is yet another approach. Attempts have been made to integrate physiologically-based pharmacokinetic/pharmacodynamic (PBPK/PD) and quantitative structure–activity relationship (QSAR) modelling into toxicity prediction [40]. Most methods need further development [41]. Currently these approaches can serve to give a first alert, rather than being truly predictive. In addition, animal models are not perfect or fully predictive. By comparing animal models to the human data obtained for 131 pharmaceutical agents, an accurate prediction rate for human toxicity of 69 % was observed [42].

New technologies are based on advances in understanding and analysing the effects of chemicals on gene expression or protein expression and processing [43, 44]. More developments can be expected in the coming years.

8.12

Toxicogenomics

A new subdiscipline derived from a combination of the fields of toxicology and genomics is termed toxicogenomics [45]. Using genomic resources, its aim is to study the potential toxic effects of drugs and environmental toxicants. DNA microarrays or “chips” are now available to monitor the expression levels of thousands of genes simultaneously as a marker for toxicity. The complexity of the microarrays yields almost too much data. For instance initial comparisons of the expression patterns for 100 toxic compounds using all the genes on a DNA microarray, failed to discriminate between cytotoxic anti-inflammatory drugs and DNA-damaging agents [46]. A major obstacle encountered in these studies was the lack of reproducible gene responses, presumably due to biological variability and technological limitations. Thus multiple replicate observations for the prototypical DNA-damaging agent, cisplatin, and the non-steroidal anti-inflammatory drugs (NSAIDs), diflunisal and flufenamic acid, were made and a subset of genes yielding reproducible inductions/repressions was selected for comparison. Many of the “fingerprint genes” identified in these studies were consistent with previous observations reported in the literature (e. g. the well-characterized induction by cisplatin of p53-regulated transcripts such as p21waf1/cip1 and PCNA (proliferating cell nuclear antigen)). These gene subsets not only discriminated among the three compounds in the learning set, but also showed predictive value for the rest of the database (approximately 100 compounds with various toxic mechanisms). Further refinement of the clustering strategy, yielded even better results and demonstrated that genes which ultimately best discriminated between DNA damage and NSAIDs were involved in such diverse processes as DNA repair, xenobiotic metabolism, transcriptional activation, structural maintenance, cell cycle control, signal transduction, and apoptosis. The genes span the cycle a cell will go through from initial insult to repair response, and a more detailed understanding of these cycles will not only lead to the development of very sensitive assays for toxicants, but also to a greater understanding of the molecular events of toxicity.

An even more focused direction of this work is to explore the pathway resulting from oxidative stress. Exposure of cells to toxic chemicals can result in reduced glu-

tathione (GSH) depletion, generation of free radicals, and binding to critical cell constituents. This binding and resultant chemical stress is usually followed by a concerted cellular response aimed at restoring homeostasis, although the precise initial stimulus for the response is unclear. One component of this stress response is the upregulation of γ -glutamylcysteine synthetase (γ -GCS) and the preceding molecular events involved in its regulation. C-jun and c-fos mRNA (mRNA) levels and activator protein 1 [AP-1] have been found to be sensitive markers for a number of toxicants [47].

8.13

Enzyme Induction (CYP3A4) and Drug Design

Although largely an adaptive response and not a toxicity enzyme induction, the interaction of cytochrome P450 in particular, with a drug is undesirable, as it may affect the efficacy of the drug or co-administered drugs. The number of clinically used drugs which induce P450 enzymes is, in fact, quite limited. However, in certain disease areas (AIDS, epilepsy) many of the drugs used, whether for primary or secondary indications, have the potential for enzyme induction. Induction is often seen pre-clinically, due to the elevated dose levels used, but this potential rarely transfers to the clinical situation [46].

No clear SAR emerges for induction, nor are any particular groups or functions implicated as shown by the diverse structures of the known CYP3A4 inducers (Figure 8.29). Structures are diverse but most are lipophilic as defined by a positive calculated log *P* value.

A critical factor in P450 induction in the clinic, based on drugs known to induce P450, is the question of dose size. The major inducible form of P450 in man is CYP3A4. The drugs that induce CYP3A4 are given in high doses, often around 500–1000 mg day⁻¹ (Table 8.3). These result in total drug concentrations in the

Tab. 8.3 Dose, total and free plasma concentrations for clinical CYP3A4 inducers.

	Dose (mg day ⁻¹)	C _p (μ M)	C _p free (μ M)
Carbamazepine	400–1200	12	3.6
Phenytoin	350–1000	54	5
Rifampicin	450–600	12	4
Phenobarbitone	70–400	64	32
Troglitazone	200–600	7	0.01
Efavirenz	600	29	0.3
Nevirapine	400	31	12
Moricizine	100–400	3	0.5
Probenicid	1000–2000	350	35
Felbamate	1200–3600	125	95

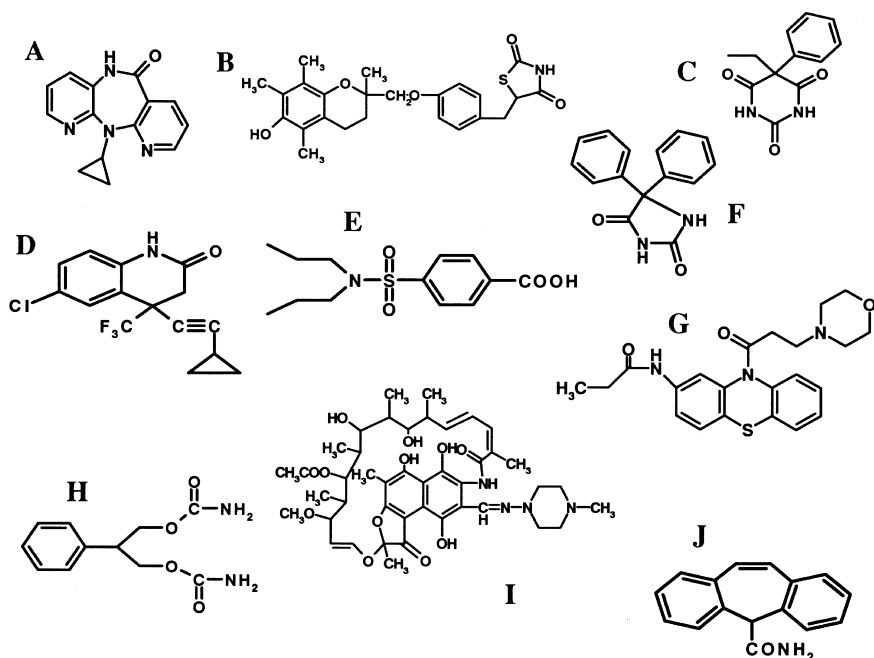


Fig. 8.29 Structures of known clinical CYP3A4 inducers: nevirapine (A), troglitazone (B), phenobarbitone (C), efavirenz (D), probenecid (E), phenytoin (F), moricizine (G), felbamate (H), rifampicin (I) and carbamazepine (J).

10–100 μM range or approximately an order of magnitude lower than that expressed as a free drug concentration (Table 8.3). The concentrations equate closely to the therapeutic plasma concentrations presented in Table 8.3. These data both reflect the relatively weak affinity of the inducing agents and the need for high concentrations or doses. The high clinical concentrations reflect the weak potency of the drugs. For instance the Na^+ channel blockers have affinities of 3, 9 and 25 μM (moricizine, phenytoin and carbamazepine, respectively). With the anti-infectives there is the need to dose to the IC_{95} level or greater. Thus, although efavirenz is a potent inhibitor of wild-type RT HIV ($K_i = 3 \text{ nM}$), there is a need to go to higher concentrations to reach the IC_{95} for the virus and also to treat for possible mutants.

In contrast to these concentrations many clinically-used drugs, which are non-inducers are effective at doses up to two orders of magnitude lower. The need for high doses has other undesirable complications. As outlined above dose size is important in toxicity and enzyme inducers show a high level of adverse drug reactions affecting such organs and tissues as the liver, blood and skin (Table 8.4).

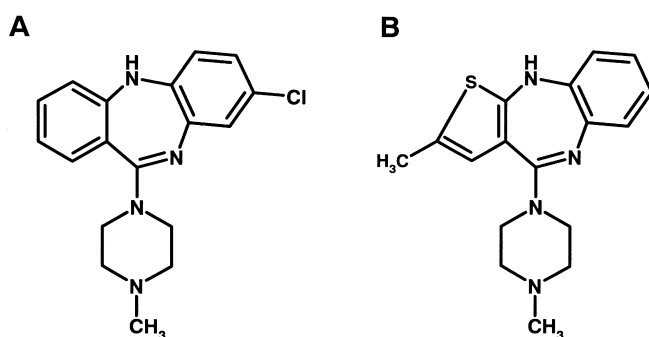
This statement is somewhat at odds with the conventional view that idiosyncratic toxicology is dose-size independent. Idiosyncratic reactions are thought to result from an immune-mediated cell injury triggered by previous contact with the drug. The toxicity may appear after several asymptomatic administrations of the com-

Tab. 8.4 Clinical toxicities and side-effects of P4503A4 inducers.

Carbamazepine	Aplastic anaemia, agranulocytosis, skin rash, hepatitis
Phenytoin	Agranulocytosis, skin rash, hepatitis
Rifampicin	Shock, haemolytic anaemia, renal failure
Phenobarbitone	Aplastic anaemia, agranulocytosis, skin rash
Troglitazone	Hepatic toxicity
Efavirenz	Hepatitis, skin rash
Nevirapine	Hepatitis, skin rash
Moricizine	Prodysrhythmia
Probenicid	Aplastic anaemia, hepatic necrosis
Felbamate	Aplastic anaemia

bound (sensitization period) and is not perceived as dose dependent. For instance when the relationship between the occurrence of adverse side-effects and the use of anti-epileptic drugs was examined, there was no definite dose- or serum concentration-dependent increase in the incidence of side-effects. In fact on closer examination idiosyncratic toxicology and dose size seem firmly linked. Not in the terms of a single drug used over its clinical dose range as above, but that adverse reactions occur more often with high dose drugs. Aside from the examples above an excellent example is clozapine and its close structural analogue olanzapine (Figure 8.30). Clozapine is used clinically over the dose range of 150–450 mg and its use is associated with agranulocytosis. Olanzapine is used clinically at 5–10 mg and is associated with a negligible risk of agranulocytosis. As outlined in Section 8.4 both compounds could potentially be activated to form reactive intermediates such as nitrenium ions.

The impact of reducing dose size by either intrinsic potency increases or optimizing pharmacokinetics is also critical in avoiding P450 induction. An example of this is the anti-diabetic compound troglitazone (Figure 8.31). This is used at a relatively high clinical dose (Table 8.3) and its use is associated with enzyme induction. For instance troglitazone lowers the plasma concentrations of known CYP3A4 substrates such as cyclosporine, terfenadine, atorvastatin, and ethinylestradiol. In contrast, the structurally related rosiglitazone (Figure 8.31) is administered at a lower dose and shows no evidence of enzyme induction. Concomitant administration of rosiglita-

**Fig. 8.30** Structures of clozapine (A) and olanzapine (B).

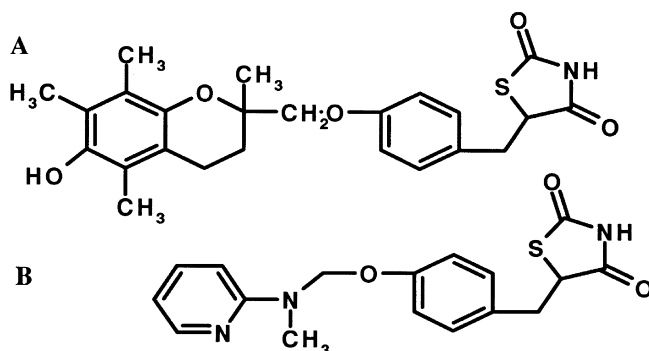


Fig. 8.31 Structures of troglitazone (A) and rosiglitazone (B).

zone (8 mg) did not effect the pharmacokinetics of the CYP3A4 substrates, nifedipine or ethinylestradiol. The clinical dose used closely relates to the receptor potency of these agents. For instance the EC_{50} values for troglitazone and rosiglitazone for affinity against the peroxisome proliferator-activated receptor γ (PPAR- γ) ligand binding domain, are 322 and 36 nM, respectively. Corresponding figures for elevation of P2 mRNA levels as a result of peroxisome proliferator-activated receptor γ agonism are 690 and 80 nM, respectively. This increase in potency is even more marked in intact human adipocytes with affinities for PPAR- γ of 1050 and 40 nM. Examination of these figures illustrates that troglitazone can be classed as a drug of weak affinity, similar to the Na^+ channel blockers.

As a first rule for drug discovery/development programmes it seems prudent to obey the “Golden Rules” of drug design: “Ensure moderate daily dose size by having chosen a viable mechanism and then optimizing potency against the target whilst optimizing pharmacokinetics”. This approach should result in a low dose as exemplified by the anti-diabetic compound troglitazone, a clinical CYP3A4 inducer which has a clinical dose of 200–600 mg and, rosiglitazone a more potent analogue requiring lower dose levels (2–12 mg), which is devoid of CYP3A4 induction in the clinic. This drive for a low dose also minimizes the chances of other potential toxicities

References

- 1 Ikeda K, Oshima T, Hidaka H, Takasaka T, *Hearing Res.* **1997**, *107*, 1–8.
- 2 Kenyon B, Browne F, D'Amato RJ, *Exp. Eye Res.* **1997**, *64*, 971–978.
- 3 Falik R, Flores BT, Shaw L, Gibson GA, Josephson ME, Marchlinski FE, *Amer. J. Med.* **1987**, *82*, 1102–1108.
- 4 Harris L, McKenna WJ, Rowland E, Holt DW, Storey GCA, Krikler DM, *Circulation* **1983**, *67*, 45–51.
- 5 Smith DA, Brown K, Neale MG, *Drug Metab. Rev.* **1985–86**, *16*, 365–388.
- 6 Nelson SD, *J. Med. Chem.* **1982**, *25*, 753–761.
- 7 Hinson JA, Roberts DW, *Ann. Rev. Pharmacol. Toxicol.* **1992**, *32*, 471–510.
- 8 Cary RD, Binnie CD, *Clin. Pharmacokinet.* **1996**, *30*, 403–415.
- 9 Riley RJ, Kitteringham NR, Park BK, *Br. J. Clin. Pharmacol.* **28**, 482–487 (1989).
- 10 Bennett GD, Amore BM, Finnell RH, Włodarczyk B, Kalhorn TF, Skiles GL, Nelson SD, Slattey JT, *J. Pharmacol. Exp. Ther.* **1996**, *278*, 1237–1242.
- 11 Tingle MD, Jewell H, Maggs JL, O'Neill PM, Park BK, *Biochem. Pharmacol.* **1995**, *50*, 1113–1119.
- 12 Miyamoto G, Zahid N, Uetrecht JP, *Can. Chem. Res. Toxicol.* **1997**, *10*, 414–419.
- 13 Spaldin V, Madden S, Pool WF, Woolf TF, Park BK, *Br. J. Clin. Pharmacol.* **1994**, *38*, 15–22.
- 14 Ju C, Uetrecht JP, *Drug Metab. Dispos.* **1998**, *26*, 676–680.
- 15 Stonier PD, *Pharmacoepidemiol. Drug Safe.* **1992**, *1*, 177–185.
- 16 Roden DM, In: *The Pharmacological Basis for Therapeutics* (Eds Goodman LS, Gillman A), pp. 839–874. McGraw-Hill, New York, **1995**.
- 17 Chao Z, Liu C, Uetrecht JP, *J. Pharmacol. Exp. Ther.* **1995**, *275*, 1476–1483.
- 18 Maggs JL, Williams D, Pirmohamed M, Park BK, *J. Pharmacol. Exp. Ther.* **1995**, *275*, 1463–1475.
- 19 Uetrecht J, Zahid N, Tehim A, Fu JM, Rakhit S, *Chemico–Biol. Interact.* **1997**, *104*, 117–129.
- 20 Roberts P, Kitteringham NR, Park BK, *J. Pharm. Pharmacol.* **1993**, *45*, 663–665.
- 21 Cribb AE, Spielberg SP, *Drug Metab. Dispos.* **1990**, *18*, 784–787.
- 22 Coleman MD, *Gen. Pharmacol.* **1995**, *26*, 1461–1467.
- 23 Treiber A, Dansette PM, Amri HE, Girault JP, Giderow D, Mornon J-P, Mansy D, *J. Amer. Chem. Soc.* **1997**, *119*, 1565–1571.
- 24 Mansuy D, *J. Hepatol.* **1997**, *26* (Suppl. 2), 22–25.
- 25 Wolfe SM, *New Engl. J. Med.* **1987**, *316*, 1025.
- 26 Desager JP, *Clin. Pharmacokinet.* **1994**, *26*, 347–355.
- 27 Liu ZC, Uetrecht JP, *Drug Metab. Dispos.* **2000**, *28*, 726–730.
- 28 Hepatic monitoring for tenidap in *Scrip World Pharmaceutical News*, **1995**, *21*, 2073.
- 29 Durant GJ, Emmett JC, Ganellin CR, Miles PD, Parsons ME, Prain HD, White GR, *J. Med. Chem.* **1977**, *20*, 901–906.
- 30 Smith DA, Johnson M, Wilkinson DJ, *Xenobiotica* **1985**, *15*, 437–444.
- 31 Nakadate M, *Toxicol. Lett.* **1998**, *102–103*, 627–629.
- 32 Begnini R, Guiliani A, In: *Computer-Assisted Lead Finding and Optimization*. (Eds Van de Waterbeemd H, Testa B, Folkers G), pp. 291–312. Wiley-VCH, Basel, **1997**.
- 33 Begnini R, Richard AM, *Methods Enzymol.* **1998**, *14*, 264–276.
- 34 Barratt MD, *Toxicol. Lett.* **1998**, *102–103*, 617–621.
- 35 Richard AM, *Toxicol. Lett.* **1998**, *102–103*, 611–616.
- 36 Barratt MD, *Cell Biol. Toxicol.* **2000**, *16*, 1–13.
- 37 Hall AH, *Toxicol. Lett.* **1998**, *102–103*, 623–626.
- 38 Maran U, Karelson M, Katritzky AR, *Quant. Struct. Activity Rel.* **1999**, *18*, 3–10.
- 39 Vracko M, Novic M, Zupan J, *Anal. Chim. Acta* **1999**, *384*, 319–332.
- 40 Yang RSH, Thomas RS, Gustafson DL, Campaign J, Benjamin SA, Verhaar HJM, Mumtaz MM, *Environ. Health Perspect.* **1998**, *106* (Suppl.), 1385–1393.

- 41 Cronin MTD, *Pharm. Pharmacol. Commun.* **1998**, *4*, 157–163.
- 42 Olson H, Betton G, Stritar J, Robinsin D, *Toxicol. Lett.* **1998**, *102–103*, 535–538.
- 43 Sina JF, *Ann. Rep. Med. Chem.* **1998**, *33*, 283–291.
- 44 Todd MD, Ulrich RG, *Curr. Opin. Drug Discov. Dev.* **1999**, *2*, 58–68.
- 45 Nuwaysir EF, Bittner M, Barrett JC, Afshari CA, *Mol. Carcinogen.* **1999**, *24*, 153–159.
- 46 Kitteringham NR, Powell H, Clement YN, Dodd CC, Tettey JNA, Pirmohamed M, Smith DA, McLellan LI, Park BK, *Hepatology* **2000**, *32*, 321–333.
- 46 Burczynski ME, McMillian M, Ciervo J, Li L, Parker JB, Dunn RT, Hicken S, Farr S, Johnson MD, *Toxicol. Sci.* **2000**, *58*, 399–415.
- 47 Smith DA, *Eur. J. Pharm. Sci.* **2000**, *11*, 185–189.

9

Inter-Species Scaling**Abbreviations**

BW	Body weight
CYP2C9	Cytochrome P450 2C9 enzyme
GFR	Glomerular filtration rate
i.v.	Intravenous
MLP	Maximum life span potential
P450	Cytochrome P450
TxRAs	Thromboxane receptor antagonists

Symbols

C_{\max}	Maximum plasma concentration observed
Cl	Clearance
Cl_i	Intrinsic clearance
Cl_{iu}	Intrinsic clearance of unbound (free) drug
Cl_{ou}	Oral unbound clearance (i.e. oral clearance correct for free fraction)
Cl_s	Systemic clearance
f_b	Fraction of plasma-bound drug
f_u	Fraction of drug unbound (to plasma proteins)
f_{ut}	Fraction of unbound drug in tissues
ln	Natural logarithm
Q	Organ blood flow
R	Ratio of binding proteins in extracellular fluid (except plasma) to binding proteins in plasma
r^2	Correlation coefficient
$t_{1/2}$	Elimination half-life
V_d	Volume of distribution
V_e	Volume of extracellular fluid
V_p	Volume of plasma
V_r	Volume of remaining fluid

9.1

Objectives of Inter-Species Scaling

Within the drug discovery setting, one of the principal aims of pharmacokinetic studies is to be able to estimate the likely pharmacokinetic behaviour of a new chemical entity in man. Only by doing this is it possible to establish whether a realistic dosing regimen may be achieved, in terms of both size and frequency of administration. Ultimately these factors will contribute to whether or not the compound can be used practically in the clinical setting and can thus be a successful drug. It is therefore important that pharmacokinetic data derived from laboratory animals can be extrapolated to man. Such extrapolations are at best only an estimate, but can provide valuable information to guide drug discovery programmes. Understanding the physiological processes which underlie the pharmacokinetic behaviour of a molecule will allow a more rational estimation of the profile in man.

When considering the likely pharmacokinetic profile of a novel compound in man, it is important to recognize the variability that may be encountered in the clinical setting. Animal pharmacokinetic studies are generally conducted in inbred animal colonies that tend to show minimal inter-subject variability. The human population contains a diverse genetic mix, without the additional variability introduced by age, disease states, environmental factors and co-medications. Hence any estimate of pharmacokinetic behaviour in man must be tempered by the expected inherent variability. For compounds with high metabolic clearance (e. g. midazolam), inter-individual variability in metabolic clearance can lead to greater than 10-fold variation in oral clearance and hence systemic exposure [1].

9.2

Allometric Scaling

Much of the inter-species variation in pharmacokinetic properties can be explained as a consequence of body size (allometry). Consequently it is possible to scale pharmacokinetic parameters to the organism's individual anatomy, biochemistry and/or physiology in such a manner that differences between species are nullified. Several excellent reviews on allometric scaling are available in the literature [2–7]. Allometric relationships can be described by an equation of the general form:

$$\text{Pharmacokinetic parameter} = A \cdot BW^a \quad (9.1)$$

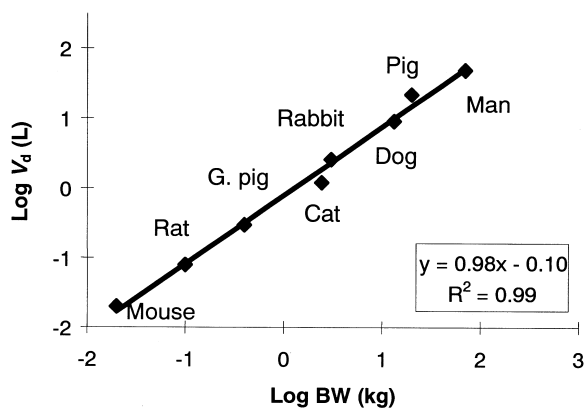
Where A is the coefficient (i.e. the intercept on the y -axis of logarithmically transformed data), BW is the body weight and a is the power function (slope of the line).

9.2.1

Volume of Distribution

When considering volume of distribution, an allometric relationship is not surprising as this value will be dependent upon the relative affinity for tissue compared to

Fig. 9.1 Allometric relationship between body weight and volume of distribution of fluconazole.



plasma and as the make-up of tissues is similar across species the ratio will remain relatively constant. Any species-specific differences in plasma protein binding can be overcome by considering volume of distribution of unbound drug. Due to its unique dependence amongst pharmacokinetic parameters, on body weight, the allometric exponent (a in Eq. 9.1) for volume of distribution is generally around 0.9 to 1.0 [8]. The antifungal agent, fluconazole provides an excellent example of the allometric relationship between body weight and volume of distribution [9]. This compound has low plasma protein binding capacity (12%) across species and therefore this does not need to be considered in the comparison. As can be seen from Figure 9.1 when values for volume of distribution (not weight normalized) are plotted against body weight (BW) on a log–log axis a linear relationship with high correlation is observed ($r^2 = 0.99$).

The value of 0.98 for the allometric exponent is so close to unity as to make the volume of distribution directly proportional to body weight, i.e. weight normalized volume is an invariant parameter (see Table 9.1). The mean value for the volume of distribution in the eight species is $0.82 \pm 0.21 \text{ L kg}^{-1}$.

In cases where plasma protein binding varies across the species, allometric scaling should be based upon the volume of distribution of unbound drug. The considerably

Tab. 9.1 Comparison of absolute and weight normalised values for the volume of distribution of fluconazole in various species.

Species	V_d (L)	V_d (L kg ⁻¹)
Mouse	0.02	1.00
Rat	0.08	0.80
Guinea pig	0.3	0.75
Cat	1.2	0.50
Rabbit	2.6	0.87
Dog	9.1	0.69
Pig	22	1.10
Man	49	0.70

lower free fraction (10- to 20-fold) of zamifenacin in human compared to animal plasma results in decreased volume (weight normalized) of total drug, although the volume of unbound drug remains constant. This is a major factor in the markedly higher C_{\max} (of total drug) value after oral dosing in man compared to animal species [10]. This is not always the case for acidic drugs which are restricted to the blood compartment (typically with a volume of distribution of less than 0.1 L kg^{-1}) as changes in protein binding will not alter the volume of distribution of total drug.

An extensive retrospective analysis [11] examined various scaling approaches to the prediction of clinical pharmacokinetic parameters. In this analysis the most successful predictions of volume of distribution were achieved by calculating unbound fraction in tissues (f_{ut}) of animals and assuming this would be similar in man. Volume of distribution was then calculated using measured plasma protein binding values and standard values for physiological parameters such as extracellular fluid and plasma volumes. The equation used was as follows:

$$V_{\text{d(human)}} = V_{\text{p}} + (f_{\text{u(human)}} \cdot V_{\text{e}}) + (f_{\text{b(human)}} \cdot R \cdot V_{\text{p}}) + V_{\text{r}} \cdot (f_{\text{u(human)}}/f_{\text{ut}}) \quad (9.2)$$

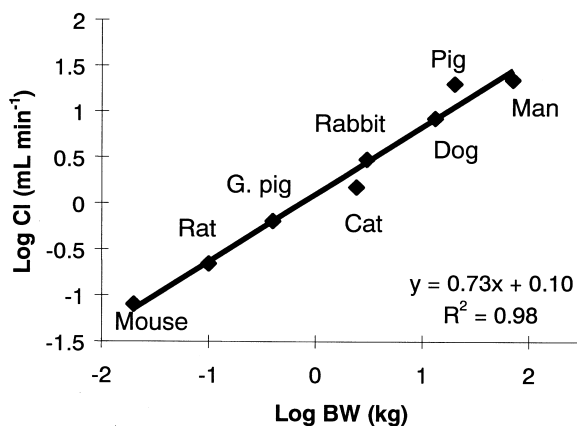
This incorporates volumes of the various fluid compartments, plasma (V_{p}), extracellular fluid (V_{e}), and remainder (V_{r}) in addition to extracellular protein-bound drug determined by the ratio of binding proteins in extracellular fluid relative to plasma (R). The predicted volume of distribution calculated by this method had an average-fold error of 1.56, with 88 % of compounds ($n = 16$) predicted within two-fold of the actual value. This method was slightly more reliable than allometric scaling of the volume of distribution of unbound drug which provided an average-fold error of 1.83, with 77 % of compounds ($n = 13$) predicted within two-fold of the actual value. Both methods were significantly better than allometric scaled values without consideration of protein binding differences which only predicted 53 % of compounds ($n = 15$) within two-fold of the actual value (average-fold error = 2.78).

9.2.2

Clearance

An allometric relationship for clearance is less obvious. However, in many cases the clearance process will be of similar affinity across species, this is particularly so for renal clearance where the processes of filtration and tubular reabsorption are common. In such instances the allometric relationship will be dependent upon organ blood flow. In general when clearance is expressed in units of volume per unit time per unit of body weight (e.g. $\text{mL min}^{-1} \text{ kg}^{-1}$), other mammalian species appear to eliminate drugs more rapidly than man. This is largely a result of the organs of elimination representing a smaller proportion of the body weight as the overall size of the mammal increases. For example the liver of a rat represents approximately 4.5 % total body weight, compared to approximately 2 % for man. The blood flowing to the organ (in this case the liver) is thus reduced when expressed as flow per unit of total body weight from about $100 \text{ mL min}^{-1} \text{ kg}^{-1}$ in the rat to about $25 \text{ mL min}^{-1} \text{ kg}^{-1}$ in man. When considered another way this means each microlitre of blood in the rat passes through the liver every minute, whereas the equivalent time in man is 2.5 min.

Fig. 9.2 Allometric relationship between body weight and systemic clearance of fluconazole.



Thus everything occurs more rapidly in the rat than in man and “physiological time” is shorter (on a chronological scale) the smaller the species. Hence physiological processes that are dependent upon time become disproportionately more rapid in smaller species. This is illustrated by the allometric analysis of creatinine clearance (a measure of glomerular filtration rate) which shows an allometric exponent of 0.69. A similar allometric exponent is obtained for the clearance of fluconazole (Figure 9.2), a compound that is almost exclusively cleared by the kidneys. Hence whilst weight normalized clearance may decrease from $4 \text{ mL min}^{-1} \text{ kg}^{-1}$ in mouse to $0.3 \text{ mL min}^{-1} \text{ kg}^{-1}$ in man, an allometric relationship is observed across the different species with an exponent of 0.73. This value for the exponent is in keeping with the general observation for small organic molecules where successful predictions are associated with an exponent value of about 0.75 [8]. Thus clearance of fluconazole remains relatively constant across species with respect to “physiological time”, as renal clearance remains a constant fraction of the glomerular filtration rate (GFR) at about 20% [9].

As with the allometric relationship with volume of distribution, fluconazole exhibits only low plasma protein binding and for compounds which exhibit variation in protein binding across species, allometry should be based upon clearance of unbound drug. Amongst other drugs cleared by the kidneys which show an allometric relationship, the α_1 -adrenoceptor antagonist, metazosin, is notable in that the allometric exponent for clearance is 0.28 [12]. Together with the unusual allometric exponent of 0.6 for volume of distribution this clearly suggests some abnormality in the disposition of this compound which has not yet been explained.

When clearance is dependent upon metabolism, species-specific differences in the enzymes of metabolism can clearly prevent any such allometric relationship. An example of this is the absence of a close homologue of the human CYP2C9 enzyme in the dog, hence its inability to hydroxylate drugs such as tolbutamide and tienilic acid [13]. This said, many compounds cleared by metabolism do exhibit allometric relationships (e.g. *N*-nitrosodimethylamine, [14]). In an extensive analysis of the allometric relationship between clearance in the rat and man for 54 extensively cleared

drugs, the mean allometric exponent value was 0.66 [15]. This analysis also confirmed the improved correlation when unbound plasma clearance was considered.

9.3

Species Scaling: Adjusting for Maximum Life Span Potential

Allometric scaling of clearance is least successful for metabolically cleared drugs with low extraction. This is perhaps hardly surprising, as these compounds will be most sensitive to the subtle differences in the affinities of species-specific homologues of the enzymes of metabolism. In these cases the clearance in man is generally lower than would be predicted by straightforward allometry. By including a factor, which reflects the reduced rate of maturation in man, these differences can be corrected. Such factors have included maximum life span potential (MLP) and brain weight [16].

Compounds which are substrates for mixed function oxidase enzymes, including P450s, tend to show lower than expected clearance in man based upon the simple allometric scaling incorporating body weight alone. This may be correlated with the enhanced longevity of man compared to most animals, since the faster the pace of life, the shorter it is. Hence slowing the metabolic rate, including that of the mixed function oxidases, allows the MLP to be extended. This reflects a major evolutionary advantage of man over other animal species. Therefore incorporation of MLP into the allometric extrapolation provides a more accurate assessment of physiological time than body weight alone. One additional potential advantage of reduced activity of the mixed function oxidases is decreased activation of pro-carcinogens and decreased free radical formation, hence prolonging life span.

The consideration of clearance in units of volume per maximum life span potential, instead of the traditional volume per weight, provides an allometric relationship for drugs such as antipyrine and phenytoin [17]. Both of these drugs are essentially low clearance compounds, cleared by P450 metabolism. Ultimately, the successful utility of such factors may be purely serendipitous as they simply exploit unique features of man as a species.

9.4

Species Scaling: Incorporating Differences in Metabolic Clearance

An alternative approach to relying simply upon allometric approaches for metabolically-cleared compounds is to take into consideration their relative stability *in vitro*. Clearance by P450 enzymes observed in hepatic microsomes from different species provides a measure of the relative intrinsic clearance in different species. Using the equation for the well-stirred model:

$$Cl_s = Cl_i \cdot Q / (Cl_i + Q) \quad (9.3)$$

The equation can be solved for intrinsic clearance (Cl_i) based upon systemic clearance (Cl_s) obtained after i.v. administration and hepatic blood flow (Q) in the test species. Intrinsic clearance in man can then be estimated based upon relative *in vitro* microsomal stability and the equation solved to provide an estimate for human systemic clearance. Hence this approach combines allometry (by considering differences in organ blood flow) and species-specific differences in metabolic clearance.

The incorporation of *in vitro* metabolism data into allometric scaling of compounds cleared by hepatic metabolism has been extensively evaluated [18] and shown to accurately predict human clearance. In this review it is suggested that the utility of such methods are most appropriately applied in drug candidate selection, to confirm early estimates and to support early clinical studies.

The inclusion of relative metabolic stability in animal and human hepatocytes in allometric scaling for 10 metabolically cleared compounds has been detailed [19]. In this study, the correction for species differences in metabolic rate resulted in extrapolated human clearance values within two-fold of those observed. In contrast extrapolations based on simple allometry or incorporating a correction for brain weight gave up to 10-fold errors on the extrapolated values. Again in these approaches to scaling, differences in plasma protein binding can be incorporated using the equation:

$$Cl_i = Cl_{iu} \cdot f_u \quad (9.4)$$

where f_u is the fraction unbound in plasma of the relevant species. Extrapolation based on unbound drug clearance is generally the approach of choice for estimating metabolic clearance in man prior to progressing a compound into clinical trials [20].

A comparison of various inter-species scaling methods was conducted for the endothelin antagonist, bosentan [21]. This compound is eliminated mainly through metabolism. Simple, direct allometric scaling based on five animal species provided a relatively poor correlation coefficient (r^2) of 0.525. Whilst the r^2 value was greatly improved (0.895) by correcting for brain weight, this gave a relatively poor prediction of human clearance of 44 mL min⁻¹ versus an actual value of 140 mL min⁻¹. The best r^2 value (0.976) was obtained by correcting for rates of metabolism in liver hepatocytes from the various species and this also provided a relatively good prediction of human clearance at 100 mL min⁻¹. Whilst the correlation coefficient was inferior when incorporating metabolic stability in liver microsomes (0.725) instead of hepatocytes, this also provided a good estimate of human clearance at 126 mL min⁻¹. In this example no account was taken of plasma protein binding differences between species.

9.5

Inter-Species Scaling for Clearance by Hepatic Uptake

When transporter proteins are involved in the rate-determining step of compound clearance, there is clearly the potential for species differences to exist which are not related to allometry. Given the large (and growing) number of transporter proteins

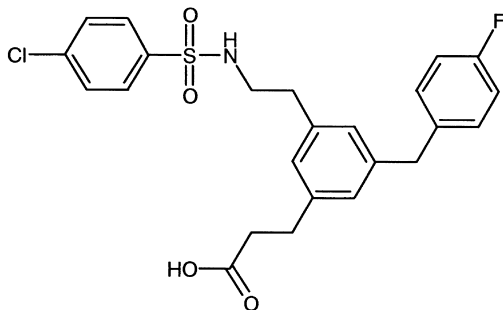


Fig. 9.3 Structure of the thromboxane receptor antagonist, UK-147,535.

implicated in the removal of drugs from the systemic circulation (see Chapter 5) there exists the possibility for divergent substrate specificity in the various laboratory animal species and man.

Organic anions have frequently been implicated as substrates for transporters in the sinusoidal membrane of the liver. This was illustrated for a series of TxRAs, where hepatic uptake was identified as the rate-determining step in the clearance process [22]. A representative compound from this series, UK-147,535 (Figure 9.3), was progressed to clinical trials [23]. It is thus possible to contrast clearance of this compound between a number of species including man (Figure 9.4).

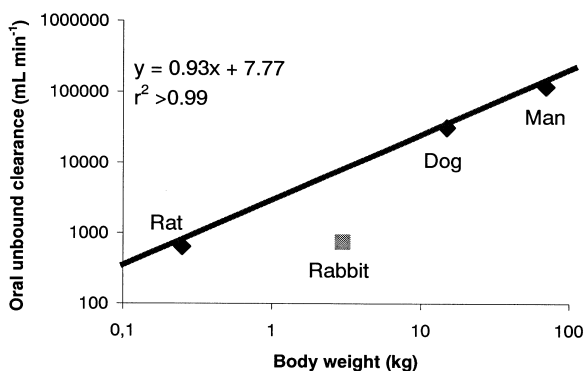
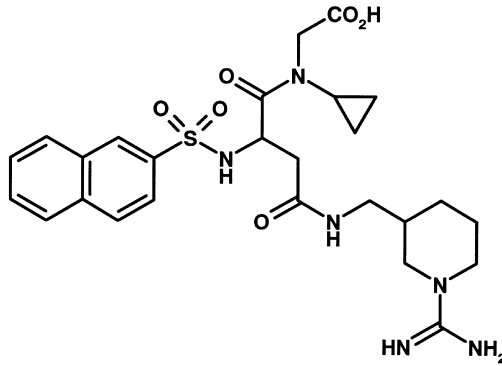


Fig. 9.4 Allometric relationship for clearance of UK-147,535 in various species.

As observed in Figure 9.4 the intrinsic clearance (as represented by oral unbound clearance Cl_{ou}) of UK-147,535 shows an allometric relationship between the rat, dog and man. This would indicate that the transporter protein involved is conserved across these species and has similar affinity. However, marked reduction in clearance in the rabbit suggests the absence, or marked alteration, of the responsible protein in the hepatic sinusoidal membrane of this species. This finding may explain the common observation of reduced biliary excretion of acidic compounds in rabbits compared to other species [24, 25].

It remains to be established whether other transporter proteins for other drug classes (e. g. cations) are conserved between species. Active transport processes are believed to be involved in the renal and hepatic clearance of the zwitterionic throm-

Fig. 9.5 Structure of the thrombin inhibitor, napsagatran.



bin inhibitor, napsagatran (Figure 9.5). Allometric scaling based on pharmacokinetic data from the rat, rabbit, monkey and dog overestimated total clearance, non-renal clearance and volume of distribution in man by 3-, 7- and 2-fold respectively. As napsagatran is not metabolized *in vitro* or *in vivo*, this would suggest that species differences in the transport proteins involved in the clearance of napsagatran, especially the protein responsible for hepatic uptake across the sinusoidal membrane, compromise the kinetic extrapolations from animals to man. Notably, amongst the individual species investigated, the monkey was most predictive of human clearance and volume of distribution [26].

9.6

Elimination Half-life

The relationship between elimination half-life ($t_{1/2}$) and body weight across species results in poor correlation, most probably because of the hybrid nature of this parameter [27]. A better approach may be to estimate volume of distribution and clearance by the most appropriate method and then estimate half-life indirectly from the relationship:

$$t_{1/2} = (0.693 \cdot V_d) / Cl_s \quad (9.5)$$

References

- 1 Wandel C, Bocker RH, Bohrer H, deVries JX, Hofmann W, Walter K, Klingeist B, Neff S, Ding R, Walter-Sack I, Martin E, *Drug Metab. Dispos.* **1998**, *26*, 110–114.
- 2 Boxenbaum H, *J. Pharmacokinet. Biopharm.* **1981**, *10*, 201–227.
- 3 Boxenbaum H, D'Souza R, *NATO ASI Series, Ser. A* **1988**, *145*, Harma. Meth. Stat. App. PG.
- 4 Hayton WL, *Health Phy.* **1989**, *57*, 159–164.
- 5 Paxton JW, *Clin. Exp. Pharm. Physiol.* **1995**, *22*, 851–854.
- 6 Mahmood I, Balian JD, *Life Sci.* **1996**, *59*, 579–585.
- 7 Ritschel WA, Vachharajani NN, Johnson RD, Hussain AS, *Comp. Biochem. Physiol.* **1992**, *103C*, 249–253.
- 8 Mordenti J, *J. Pharm. Sci.* **1986**, *75*, 1028–1040.
- 9 Jezequel SG, *J. Pharm. Pharmacol.* **1994**, *46*, 196–199.
- 10 Beaumont KC, Causey AG, Coates PE, Smith DA, *Xenobiotica* **1996**, *26*, 459–471.
- 11 Obach RS, Baxter JG, Liston TE, Silber M, Jones BC, MacIntyre F, Rance DJ, Wastall P, *J. Pharm. Exp. Ther.* **1997**, *283*, 48–58.
- 12 Lapka R, Rejholec V, Sechser T, Peterkova M, Smid M, *Biopharm. Drug Dispos.* **1989**, *10*, 581–589.
- 13 Smith DA, *Drug Metab. Rev.* **1991**, *23*, 355–373.
- 14 Gombar CT, Harrington GW, Pylypiw HM, Anderson LM, Palmer AE, Rice JM, Magee PN, Burak ES, *Cancer Res.* **1990**, *50*, 4366–4370.
- 15 Chou WL, Robbie G, Chung SM, Wu T-C, Ma C, *Pharm. Res.* **1998**, *15*, 1474–1479.
- 16 Ings RMJ, *Xenobiotica* **1990**, *20*, 1201–1231.
- 17 Campbell DB, Ings RMJ, *Hum. Toxicol.* **1988**, *7*, 469–479.
- 18 Lave T, Coassolo P, Reigner B, *Clin. Pharmacokinet.* **1999**, *36*, 211–231.
- 19 Lave T, Dupin S, Schmitt C, Chou RC, Jaeck D, Coassolo P, *J. Pharm. Sci.* **1997**, *86*, 584–590.
- 20 Smith DA, Jones BC, Walker DK, *Med. Res. Rev.* **1996**, *16*, 243–266.
- 21 Lave T, Coassolo P, Ubeaud G, Bradndt R, Schmitt C, Dupin S, Jaeck D, Chou RC, *Pharm. Res.* **1996**, *13*, 97–101.
- 22 Gardner IB, Walker DK, Lennard MS, Smith DA, Tucker GT, *Xenobiotica* **1995**, *25*, 185–197.
- 23 Dack KN, Dickinson RP, Long CJ, Steele J, *Bioorg. Med. Chem. Lett.* **1998**, *8*, 2061–2066.
- 24 Simons PJ, Cockshott ID, Douglas EJ, Gordon EA, Knott S, Ruane RJ, *Xenobiotica* **1991**, *21*, 1243–1256.
- 25 Illing HPA, Fromson JM, *Drug Metab. Dispos.* **1978**, *6*, 510–517.
- 26 Lave T, Portmann R, Schenker G, Gianni A, Guenzi A, Girometta M-A, Schmitt M, *J. Pharm. Pharmacol.* **1999**, *51*, 85–91.
- 27 Mahmood I, *J. Pharm. Pharmacol.* **1998**, *50*, 493–499.

10

High(er) Throughput ADME Studies

Abbreviations

ADME	Absorption, distribution, metabolism, excretion
CYP3A4	Cytochrome P450 3A4
DMPK	Drug metabolism and pharmacokinetics
HTS	High throughput screening
MTS	Medium throughput screening
P-gp	P-glycoprotein
PK	Pharmacokinetics
UHTS	Ultra-high throughput screening

10.1

The HTS Trend

New approaches to medicinal chemistry such as parallel synthesis and combinatorial chemistry strategies [1] and refinement of high throughput screening in biology place Drug Discovery at a crossroads. Will traditional rationale medicinal chemistry continue as the cornerstone of how we discover drugs or will sheer numbers of compounds be the winning formula. High compound numbers are essential whatever the eventual scenario to ensure that early lead matter is available. The size of compound files of the future, millions of compounds, means informatics and automation are key ingredients for a successful drug discovery organization [2]. How much drug metabolism needs to adapt is part of the question. Clearly many of the *in vitro* approaches can be automated and thus increase efficiencies. These systems are equally adaptable to screening a file or providing fast turnaround on newly synthesized products of a rationale discovery programme. Both approaches are being pursued. This chapter discusses the place of ADME screens and describes some of the recent developments which give insight into how medicinal chemistry, in a not too far future, may benefit.

10.2

Drug Metabolism and Discovery Screening Sequences

The development of higher throughput approaches in ADME studies is driven by the advances in high-speed chemistry and pharmacological screening [3], a view of the future where many more compounds would need to be screened, and the availability of the technology. Departments of Drug Metabolism and Pharmacokinetics in the pharmaceutical industry are organizing themselves for the rapid evaluation of large numbers of compounds [4–8]. Higher throughput can move a screening approach up the traditional sequence, provide more comprehensive data on a single compound, or just screen more compounds or even files. The pre-ADME days of Discovery had screening sequences based on an *in vitro* functional response often followed by an oral rodent pharmacodynamic model. The advent of ADME, cloned receptors etc., has led to the hierarchical sequence shown in Figure 10.1. Higher throughput could allow a parallel process, which collects large amounts of *in vitro* pharmacology and ADME data as the primary stage.

The hierarchical model is closest to the traditional approach and meets the needs of a focused, disciplined approach, where molecules are drug-like, with a real possibility of passing some of the ADME criteria. The horizontal model is optimum for looking for exceptions to drug-like property rules and can build SAR streams much

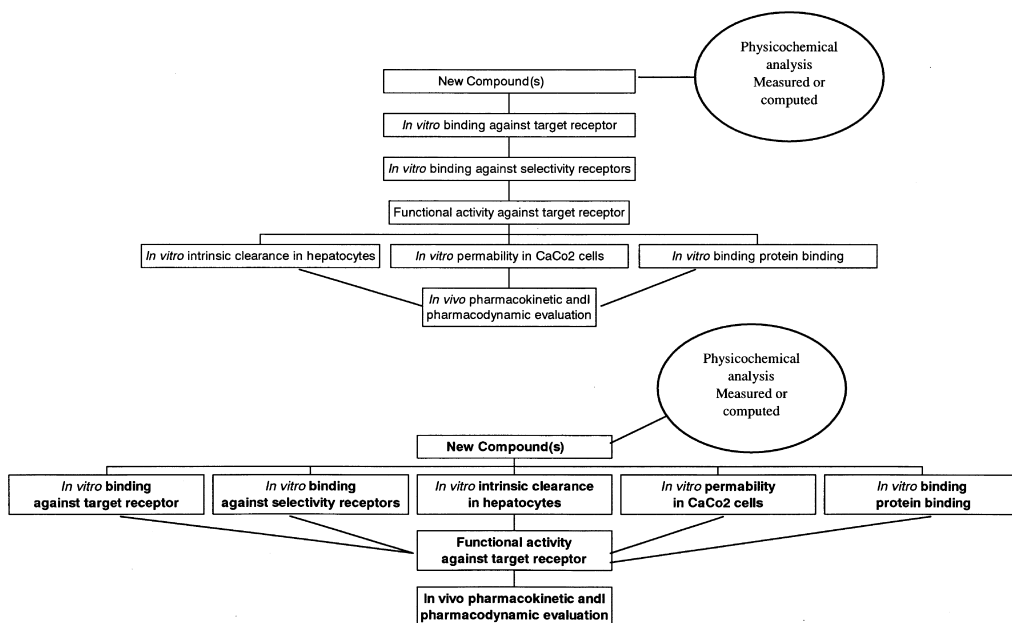


Fig. 10.1 Hierarchical and horizontal *in vitro* screening sequences. In each phase only compounds possessing certain criteria would move to the next phase. In the hierarchical model

(top) ADME data is collected only on compounds with adequate potency and selectivity. In the horizontal model (bottom) ADME data is collected on all compounds synthesized.

more rapidly so allowing very comprehensive real-time SAR of the type normally reserved for retrospective analysis. These two models indicate a divergence of how the data is handled. The hierarchical model means that full data is available on a few compounds, can be manipulated on a spreadsheet and is within the understanding of a medicinal chemist. This relates to the data being unimportant and the information being retained to drive the process. The horizontal model could result in more than 5000 data points to collate as SAR. This immediately requires computational systems and complex analysis to process and optimize. Some progress has been made in methods used in early ADME evaluation [6] with *in silico* and higher throughput physicochemical methods being linked to appropriate *in vitro* models [7]. The next sections give an inventory of some of these approaches.

10.3 Physicochemistry

The importance of physicochemistry to drug disposition and ADME is summarized in tabular form in Table 10.1.

Tab. 10.1 Physicochemical properties and the relationship to key disposition processes.

	Lipophilicity	Molecular size	Hydrogen bonding	Ionization	Melting point, crystal packing
Dissolution	√√√ ↓			√√	√√√ ↓
Membrane permeation, lipoidal	√√√ ↑	√√	√√	√	
Membrane permeation, aqueous		√√√ ↓			
Non-specific binding to proteins and phospholipids	√√√ ↑			√√√	
Carrier transport					
Metabolism	√√√ ↑			√	
Renal clearance	√√√ ↓				

Number of ticks indicate relative importance and the arrows indicates how an increase in the physicochemical property affects the ADME property, e. g. dissolution is decreased by increasing lipophilicity.

10.3.1

Solubility

Solubility is a key parameter for dissolution of compounds following oral administration (Section 3.1). The process depends on the surface area of the dissolving solid and the solubility of the drug at the surface of the dissolving solid. Solubility is inversely proportional to the number and type of lipophilic functions within the molecule and the tightness of the crystal packing of the molecule. Rapid, robust methods reliant on turbidimetry to measure solubility have been developed [10, 11], which can handle large numbers of compounds. Since ionization can also govern solubility, approaches for the rapid measurement of pK_a values of sparingly soluble drug compounds have also been developed [12]. Ideally only soluble compounds would be synthesized in a Discovery programme which is where predictive solubility methods using neural networks [13, 14], would be such an advantage.

10.3.2

Lipophilicity

Lipophilicity is the key physicochemical parameter linking membrane permeability, and hence drug absorption and distribution with route of clearance (metabolic or renal). Measured or calculated lipophilicity of a compound is readily amenable to automation. Many of these calculation approaches rely on fragment values, but simple methods based on molecular size to calculate $\log P$ values have been demonstrated to be extremely versatile [15]. A combination of measured and fragmental approaches allow extremely accurate prediction of new compound properties. For actual measurement rather than prediction, investigations in using alternatives to octanol/water partitioning include applications of immobilized artificial membranes (IAM) [16] and liposome/water partitioning [17, 18]. The IAM method offers speed of measurement as an advantage over the classical octanol/water system. Liposome binding may possibly be transferred to a higher throughput system and could provide a “volume of distribution” screen when linked with other properties. Hydrogen bonding capacity of a drug solute is now recognized as an important constituent of the concept of lipophilicity. Initially $\Delta\log P$, the difference between octanol/water and alkane/water partitioning was used as a measure for solute H-bonding but this technique is limited by the poor solubility of many compounds in the alkane phase. Computational approaches to this range through simple heteroatom counts (O and N), division into acceptors and donors, and more sophisticated measures such as free energy factors (used in program Hybot) and polar surface area.

10.4

Absorption / Permeability

When a compound is crossing a membrane by purely passive diffusion, a reasonable permeability estimate can be made using single molecular properties such as $\log D$

or hydrogen bonding (see Chapters 1 and 3). Currently *in vitro* methods such as Caco-2 monolayers are widely used to make absorption estimates (see Chapter 3). The trend is to move to 24- and 96-well plates, but this is possibly the limit for this screen in its current form. New technologies need to be explored. Artificial membranes have been suggested for high throughput permeability assessment [19–23]. However, besides the purely physicochemical component contributing to membrane transport, many compounds are affected by biological events including the influence of transporters and metabolism. Many drugs appear to be substrates for transporter proteins, which either promote or are detrimental to permeability. Currently no theoretical SAR basis exists to account for these effects. Ultimately the fastest method is to make absorption estimates *in silico* (see Chapter 3) [24, 25]. Experience in the use of all the above approaches needs to be gathered before these systems can be considered to be reliable and truly predictive.

10.5

Pharmacokinetics

Important progress in terms of higher throughput in ADME/PK work was realized recently by wider use of liquid chromatography/mass spectrometry (LC/MS), which has now become a standard analytical tool [26]. Flow NMR spectroscopy has become a routine method to resolve and identify mixtures of compounds and has found applications in drug metabolism and toxicology studies [27].

Mixture dosing (N-in-One dosing, or cocktail dosing, or cassette dosing) has been explored as a means of achieving higher throughput [28–30]. Efficient groupings may consist of 10–25 compounds. In order to avoid potential interactions the dose should be kept as low as possible. Another approach is the analysis of pooled plasma samples and the use of an abbreviated standard curve per compound [31]. From an estimated AUC a ranking of compounds offers early PK information.

A rapid spectrofluorimetric technique for determining drug–serum protein binding in high throughput mode has been described [32].

P-glycoprotein-mediated efflux is a potential source of peculiarities in drug pharmacokinetics, such as non-linearity. This includes dose-dependent absorption, drug–drug interactions, intestinal secretion and limited access to the brain. Assays are in development to quantify the interaction between transporters and drugs. One of the first is a 96-well plate assay for P-gp binding [33, 34] and an MDR1 ATPase test [35].

10.6

Metabolism

The balance between renal clearance and metabolism is readily predicted by physicochemical properties [36]. Rate of metabolism and formation of metabolic products can be screened for, using liver microsomal systems and mass spectrometry. The

utility of pulsed ultrafiltration–mass spectrometry, where microsomal fractions are entrapped in stirred ultrafiltration chambers and the output of the chamber is introduced directly into an electrospray mass spectrometer shows particular promise [37].

Higher throughput screening with human cytochrome P450 to study P450-mediated metabolism is now available [38–40]. Similarly, rapid microtitre plate assays to conduct for example, P450 enzyme inhibition studies have been developed, using individually expressed CYP enzymes (Supersomes) [41].

10.7

Computational Approaches in PK and Metabolism

A number of approaches are available or under development to predict metabolism, including expert systems such as MetabolExpert (Compudrug), Meteor (Lhasa), MetaFore [42] and the databases Metabolite (MDL) and Metabolism (Synopsis) [43]. Ultimately such programs may be linked to computer-aided toxicity prediction based on quantitative structure–toxicity relationships and expert systems for toxicity evaluation such as DEREK (Lhasa) (see also Chapter 8) [44].

QSAR and neural network approaches in combination with physiologically-based pharmacokinetic (PBPK) modelling hold promise in becoming a powerful tool in drug discovery [45]. Below we briefly discuss some of these studies.

10.7.1

QSPR and QSMR

As a possible alternative to *in vitro* metabolism studies, QSAR and molecular modelling may play an increasing role. Quantitative structure–pharmacokinetic relationships (QSPR) have been studied for nearly three decades [42, 45–52]. These are often based on classical QSAR approaches based on multiple linear regression. In its most simple form, the relationship between PK properties and lipophilicity has been discussed by various workers in the field [36, 49, 50].

Similarly, quantitative structure–metabolism relationships (QSMR) have been studied [42]. QSAR tools, such as pattern recognition analysis, have been used to e. g. predict phase II conjugation of substituted benzoic acids in the rat [53].

10.7.2

PK Predictions Using QSAR and Neural Networks

Neural networks are a relatively new tool in data modelling in the field of pharmacokinetics [54–56]. Using this approach, non-linear relationships to predicted properties are better taken into account than by multiple linear regression [45]. Human hepatic drug clearance was best predicted from human hepatocyte data, followed by rat hepatocyte data, while in the studied data set animal *in vivo* data did not significantly contribute to the predictions [56].

10.7.3

Physiologically-Based Pharmacokinetic (PBPK) Modelling

There are several approaches to pharmacokinetic modelling. These include empirical, compartmental, clearance-based and physiological models. In the latter full physiological models of blood flow to and from all major organs and tissues in the body are considered. Such models can be used to study concentration–time profiles in the individual organs and e. g. in the plasma [57–60]. Further progress in this area may result in better PK predictions in humans [61]

10.8**Outlook**

Ultimately rapid methods are needed to obtain data adequate at each stage of drug discovery. At candidate selection level the extrapolation from animals to man, through the integration of pharmacokinetics and pharmacodynamics (PK/PD), becomes crucial for success [62, 63]. Such HT methods are currently being implemented and further developed in the pharmaceutical and biotechnology industry.

References

- 1 Antel J, *Curr. Opin. Drug Discov. Dev.* **1999**, *2*, 224–233.
- 2 Calvert S, Stewart FP, Swarna K, Wiserman JS, *Curr. Opin. Drug Disc. Dev.* **1999**, *2*, 234–238.
- 3 Tarbit MH, Berman J, *Curr. Opin. Chem. Biol.* **1998**, *2*, 411–416.
- 4 Rodrigues AD, *Pharm. Res.* **1997**, *14*, 1504–1510.
- 5 Rodrigues AD, *Med. Chem. Rev.* **1998**, *8*, 422–433.
- 6 Smith DA, *Biomed. Health Res.* **1998**, *25*, 137–143.
- 7 Eddershaw PJ, Beresford AP, Bayliss MK, *Drug Discov. Today* **2000**, *5*, 409–414.
- 8 White RE, *Ann. Rev. Pharmacol. Toxicol.* **2000**, *40*, 133–157.
- 9 Smith DA, Van de Waterbeemd H, *Curr. Opin. Chem. Biol.* **1999**, *3*, 373–378.
- 10 Avdeef A, *Pharm. Pharmacol. Commun.* **1998**, *4*, 165–178.
- 11 Lipinski CA, Lombardo F, Dominy BW, Feeney PJ, *Adv. Drug Del. Rev.* **1997**, *23*, 3–25.
- 12 Allan RI, Box KJ, Coomer JEA, Peake C, Tam KY, *J. Pharm. Biomed. Anal.* **1998**, *17*, 699–710.
- 13 Huuskonen J, Salo M, Taskinen J, *J. Chem. Inform. Comput. Sci.* **1998**, *38*, 450–456.
- 14 Huuskonen J, Salo M, Taskinen J, *J. Pharm. Sci.* **1997**, *86*, 450–454.
- 15 Buchwald P, Bodor N, *Curr. Med. Chem.* **1998**, *5*, 353–380.
- 16 Ong S, Liu H, Pidgeon C, *J. Chromatogr. A.* **1996**, *728*, 113–128.
- 17 Ottiger C, Wunderli-Allenspach H, *Eur. J. Pharm. Sci.* **1997**, *5*, 223–231.
- 18 Balon K, Riebesehl BU, Muller BW, *J. Pharm. Sci.* **1999**, *88*, 802–806.
- 19 Kansy M, Kratzat K, Parrilla I, Senner F, Wagner B, In: *Molecular Modelling and Prediction of Bioreactivity* (Eds Gundertofte K, Jorgensen F), pp. 237–243. Plenum Press, New York, **2000**.
- 20 Kansy M, Senner F, Gubernator K, *J. Med. Chem.* **1998**, *41*, 1007–1010.
- 21 Kansy M, In: *Pharmacokinetic Optimization in Drug Research: Biological, Physicochemical and Computational Strategies* (Eds Testa B, Van de Waterbeemd H, Folkers G, Guy R). Wiley-HCA, Zurich, **2001** pp. 447–464.
- 22 Avdeef A, In: *Pharmacokinetic Optimization in Drug Research: Biological, Physicochemical and Computational Strategies* (Eds Testa B, Van de Waterbeemd H, Folkers G, Guy R). Wiley-HCA, Zurich, **2001** pp. 305–349.
- 23 Faller B, Wohnsland F, In: *Pharmacokinetic Optimization in Drug Research: Biological, Physicochemical and Computational Strategies* (Eds Testa B, Van de Waterbeemd H, Folkers G, Guy R). Wiley-HCA, Zurich, **2001** pp. 257–273.
- 24 Van de Waterbeemd H, In: *Pharmacokinetic Optimization in Drug Research: Biological, Physicochemical and Computational Strategies* (Eds Testa B, Van de Waterbeemd H, Folkers G, Guy R). Wiley-HCA, Zurich, **2001** pp. 499–511.
- 25 Krämer SD, *Pharm. Sci. Tech. Today* **1999**, *2*, 373–380.
- 26 Unger SE, *Ann. Rep. Med. Chem.* **1999**, *34*, 307–318.
- 27 Stockman BJ, *Curr. Opin. Drug Disc. Dev.* **2000**, *3*, 269–274.
- 28 Adkinson KK, Halm KA, Shaffer JE, Drewry D, Sinhababu AK, Berman J, In: *Integration of Pharmaceutical Discovery and Development* (Eds Borchardt RT, Freidinger RM, Sawyer TK, Smith PL), pp. 423–443. Plenum Press, New York, **1998**.
- 29 Shaffer JE, Adkinson KK, Halm K, Hedeem K, Berman J, *J. Pharm. Sci.* **1999**, *88*, 313–318.
- 30 Bayliss MK, Frick LW, *Curr. Opin. Drug Disc. Dev.* **1999**, *2*, 20–25.
- 31 Cox KA, Dunn-Meynell K, Korfmacher WA, Broske L, Nomeir AA, Lin CC, Cayen MN, Barr WH, *Drug Discov. Today* **1999**, *4*, 232–237.
- 32 Parikh HH, McElwain K, Balasubramanian V, Leung W, Wong D, Morris ME, Ramanathan M, *Pharm. Res.* **2000**, *17*, 632–637.
- 33 Döppenschmitt S, Langguth P, Regardh CG, Andersson TB, Hilgendorf C, Spahn-Langguth H, *J. Pharmacol. Exp. Ther.* **1999**, *288*, 348–357.

- 34 Döppenschmitt S, Spahn-Langguth H, Regardh CG, Langguth P, *Pharm. Res.* **1998**, *15*, 1001–1006.
- 35 Sarkadi B, Price EM, Boucher RC, Germann UA, Scarborough GA, *J. Biol. Chem.* **1992**, *267*, 4854–4858.
- 36 Smith DA, Jones BC, Walker DK, *Med. Res. Rev.* **1996**, *3*, 243–266.
- 37 Van Breemen RB, Nikolic D, Bolton JL, *Drug Metab. Dispos.* **1998**, *26*, 85–90.
- 38 Crespi CL, *Curr. Opin. Drug Discov.* **1999**, *2*, 15–19.
- 39 Crespi CL, Miller VP, Penman BW, *Med. Chem. Res.* **1998**, *8*, 457–471.
- 40 Crespi CL, Miller VP, Penman BW, *Anal. Biochem.* **1997**, *248*, 188–190.
- 41 Palamanda JR, Favreau L, Lin C, Nomeir AA, *Drug Discov. Today* **1998**, *3*, 466–470.
- 42 Testa B, Cruciani G, In: *Pharmacokinetic Optimization in Drug Research: Biological, Physicochemical and Computational Strategies* (Eds Testa B, Van de Waterbeemd H, Folkers G, Guy R). Wiley-HCA, Zurich, **2001** pp. 65–84.
- 43 Ehrhardt PW, (Ed.) *Drug Metabolism Databases and High-Throughput Testing During Drug Design and Development*. IUPAC, Blackwell Science, Malden, MA, **1999**.
- 44 Cronin MTD, *Pharm. Pharmacol. Commun.* **1998**, *4*, 157–163.
- 45 Van der Graaf PH, Nilsson J, Van Schaick EA, Danhof M, *J. Pharm. Sci.* **1999**, *86*, 306–312.
- 46 Hansch C, *Drug Metab. Rev.* **1972**, *1*, 1–14.
- 47 Seydel JK, Schaper KJ, *Pharmacol. Ther.* **1982**, *15*, 131–182.
- 48 Mayer JM, Van de Waterbeemd H, *Environ. Health Perspect.* **1985**, *61*, 295–306.
- 49 Toon S, Rowland M, *J. Pharmacol. Exp. Ther.* **1983**, *225*, 752–763.
- 50 Walther B, Vis P, Taylor A, In: *Lipophilicity in Drug Action and Toxicology* (Eds Pliska V, Testa B, Van de Waterbeemd H), pp. 253–261. VCH, Weinheim, 1996.
- 51 Seydel JK, Trettin D, Cordes HP, Wassermann Malyusz M, *J. Med. Chem.* **1980**, *23*, 607–613.
- 52 Hinderling PH, Schmidlin O, Seydel JK, *J. Pharmacokinet. Biopharm.* **1984**, *12*, 263–287.
- 53 Cupid BC, Holmes E, Wilson ID, Lindon JC, Nicholson JK, *Xenobiotica* **1999**, *29*, 27–42.
- 54 Hussain AS, Johnson RD, Vachharajani NN, Ritschel WA, *Pharm. Res.* **1993**, *10*, 466–469.
- 55 Brier ME, Zurada JM, Aronoff GR, *Pharm. Res.* **1995**, *12*, 406–412.
- 56 Schneider G, Coassolo P, Lavé Th, *J. Med. Chem.* **1999**, *42*, 5072–5076.
- 57 Yoshikawa Y, Sone H, Yoshikawa H, Takada K, *Yakubutsu Dotai* **1999**, *14*, 22–31.
- 58 Iwatsubo T, Hirota N, Ooie T, Suzuki H, Sugiyama Y, *Biopharm. Drug Dispos.* **1996**, *17*, 273–310.
- 59 Kawai R, Mathew D, Tanaka C, Rowland M, *J. Pharmacol. Exp. Ther.* **1998**, *287*, 457–468.
- 60 Poulin P, Theil FP, *J. Pharm. Sci.* **2000**, *89*, 16–35.
- 61 Norris DA, Leesman GD, Sinko PJ, Grass GM, *J. Control. Rel.* **2000**, *65*, 55–62.
- 62 Campbell DB, *Ann. NY Acad. Sci.* **1996**, *801*, 116–135.
- 63 Campbell DB, *Biomed. Health Res.* **1998**, *25*, 144–158.